Politecnico di Milano

School of Industrial and Information Engineering

Department of Energy (DENG)

Master of Science in Energy Engineering

Investigation and Design of Novel Peak Shaving District Heating Systems based on Thermochemical Materials

Pouya Javanmard

ID: 941277

Internal Supervisor:

Prof. Andrea Giostri

External Supervisors:

Dr.Ir. Amir Mahmoudi

Dr. Mina Shahi

External Co-supervisor:

Ir. Chung-Yu Yeh

Academic Year: 2021-2022

This Research Study has been performed in

"Thermal Engineering" Research Group in

Faculty of Engineering Technology (ET) of University of Twente

UNIVERSITY OF TWENTE.

Under the supervision of Dr.Ir. Amir Mahmoudi and Dr. Mina Shahi

And co-supervision of Ir. Chung-Yu Yeh

And by partnership with "TKI Urban Energy", "De Kleijn Energy Consulting", "Ennatuurlijk B.V." and "Twence Holding B.V."

“Ensure access to affordable, reliable,
sustainable and modern energy for all”

- Sustainable Development Goal 7 by United Nations

“Heat, like gravity, penetrates every
substance of the universe,
its rays occupy all parts of space.
The object of our work is to
set forth the mathematical laws
which this element obeys.”

- Joseph Fourier

Contents

List of Figures

List of Tables

Nomenclature

TCHS	Thermochemical Heat Storage
TCM	Thermochemical Material
SHS	Sensible Heat Storage
LHS	Latent Heat Storage
HTF	Heat Transfer Fluid
CFD	Computational Fluid Dynamics
α	Status of Conversion [-]
ε	Bed Porosity [-]
χ	Stoichiometric Coefficient [-]
μ	Dynamic Viscosity [Pa.s]
ρ	density [kg/m^3]
κ	Permeability [m^2]
K	Thermal Conductivity [W/m.K]
A_f	Pre-exponential Factor [1/min]
C_p	Heat Capacity [J/kg.K]
E_a	Activation Energy [J/mol]
R	Gas Constant [J/kg/K]
T	Temperature
P_w	Water Vapor Pressure [Pa]
P_{eq}	Equilibrium Water Vapor Pressure [Pa]
M	Molecular Mass [kg/kmol]
C_F	Forchheimer Parameter [-]
k_B	Boltzmann Constant [-]

Indices:

v	Water Vapor
s	TCM
s_0	Dehydrated TCM

Abstract

Currently, domestic heating for the households is one of the major end uses of fossil fuel. However, the challenge is how to fulfill the peak-load demand without using natural gas which is important for the heating supply reliability. The Netherlands has targeted for removing natural gas as the main heat source for over 7 million households by 2050 and move through sustainable district heating network. One of the technologies which can be developed and utilized is the heat storage technology based on thermochemical materials. This system can be charged during the summer period with green-electricity by renewables and then discharged in the winter to provide the required heat to the households for domestic use. In fact, the exothermic hydration reaction of a salt heats up a heat transfer fluid to provide the desired thermal energy.

This study will investigate the heat storage systems based on potassium carbonate as thermochemical material, then design and optimize two different reactor setups for this application using the COMSOL Multiphysics® software, make evaluations and comparisons to contribute the research for development of these systems.

The two designs will be based on using multi-tube and helical coil heat exchangers, and according to a sensitivity analysis performed during the study, they will be improved mainly in terms of outlet temperature for heat transfer fluid, but also status of conversion for the material to monitor the reaction speed and the energy density of the reactor.

Keywords: Thermochemical Heat Storage, Thermochemical Material, Sustainable District Heating Network

Astratto

Attualmente, il riscaldamento domestico per le famiglie è uno dei principali usi finali dei combustibili fossili. Tuttavia, la sfida è come soddisfare la domanda di carico di punta senza utilizzare gas naturale, che è importante per l'affidabilità della fornitura di riscaldamento. I Paesi Bassi hanno l'obiettivo di rimuovere il gas naturale come principale fonte di calore per oltre 7 milioni di famiglie entro il 2050 e di passare attraverso una rete di teleriscaldamento sostenibile. Una delle tecnologie che possono essere sviluppate e utilizzate è la tecnologia di accumulo di calore basata su materiali termochimici. Questo sistema può essere ricaricato durante il periodo estivo con energia verde da fonti rinnovabili e poi scaricato in inverno per fornire il calore necessario alle famiglie per uso domestico. Infatti, la reazione di idratazione esotermica di un sale riscalda un fluido termovettore per fornire l'energia termica desiderata.

Questo studio indagherà i sistemi di accumulo di calore a base di carbonato di potassio come materiale termochimico, quindi progetterà e ottimizzerà due diverse configurazioni di reattori per questa applicazione utilizzando il software COMSOL Multiphysics®, effettuerà valutazioni e confronti per contribuire alla ricerca per lo sviluppo di questi sistemi.

I due progetti si baseranno sull'utilizzo di scambiatori di calore multitubo e a serpentino elicoidale e, secondo un'analisi parametrica eseguita durante lo studio, saranno migliorati principalmente in termini di temperatura di uscita per fluido termovettore, ma anche stato di conversione per il materiale per monitorare la velocità di reazione e la densità di energia del reattore.

Parole Chiave: Accumulo termochimico, Materiale termochimico, Rete di teleriscaldamento sostenibile

Chapter 1

Introduction

1.1. Statistics

The Energy sector is the source of around three-quarters of greenhouse gas emissions today. The IEA (International Energy Agency) has set a global pathway to net-zero emissions by 2050 which requires all the governments to strengthen and then successfully implement their energy and climate policies. Switching to cleaner renewable energy technologies has a key role in this roadmap [1].

Currently, domestic heating for the households is one of the major end uses of fossil fuel (as figure 1 also suggests). In fact, heat sources like gas boilers or co-generation plants which are largely based on natural gas are widely used for this application. There is a need to derive sustainable heat from alternative sources.

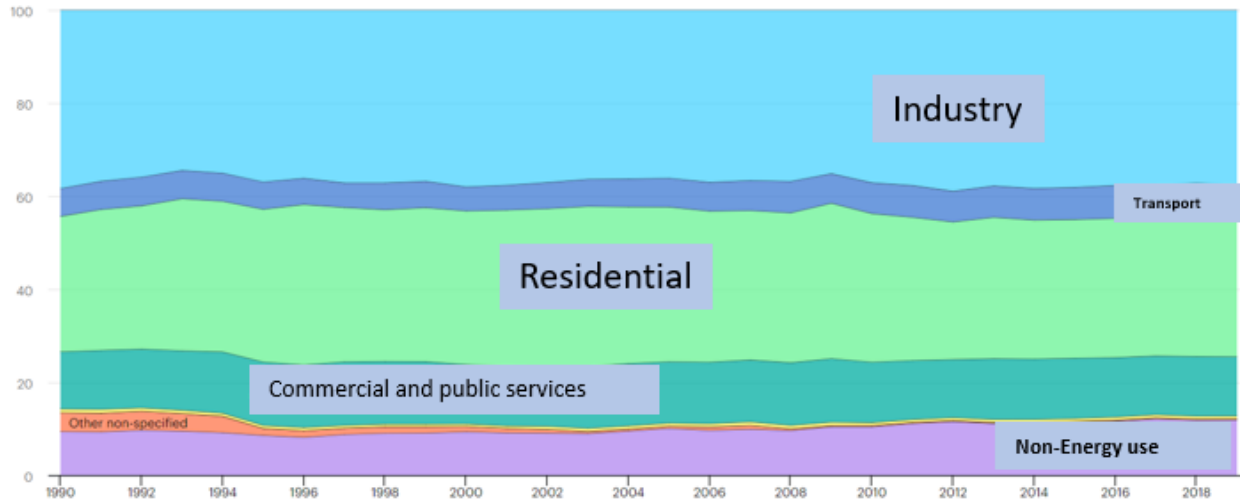

Fig1. World final Natural Gas consumption by sector (in percentage), 1990-2019 [2]

The Netherlands established a National Climate Agreement (*Klimaatakkord*) in 2019, targeting for removing natural gas as the main heat source for over 7 million households by 2050. A new sustainable district heating network will be developed and initially, 1.5 million households must connect to the new heating network by 2030[3]. Also, a new heat plan (*Warmteplan*) was conducted as a regulatory framework [4]. The sustainable district heating system is one of those steps consistent with the country's national climate policy which is to decrease greenhouse gas emission by 49% by 2030 and by 95% by 2050 compared to 1990 levels.

From the data shown on figure 2, it is clearly shown that residential sector is the largest natural gas user in the Netherlands. Furthermore, the declining trend since 2016 could keep on thanks to the new energy technologies for the sustainable district heating network.

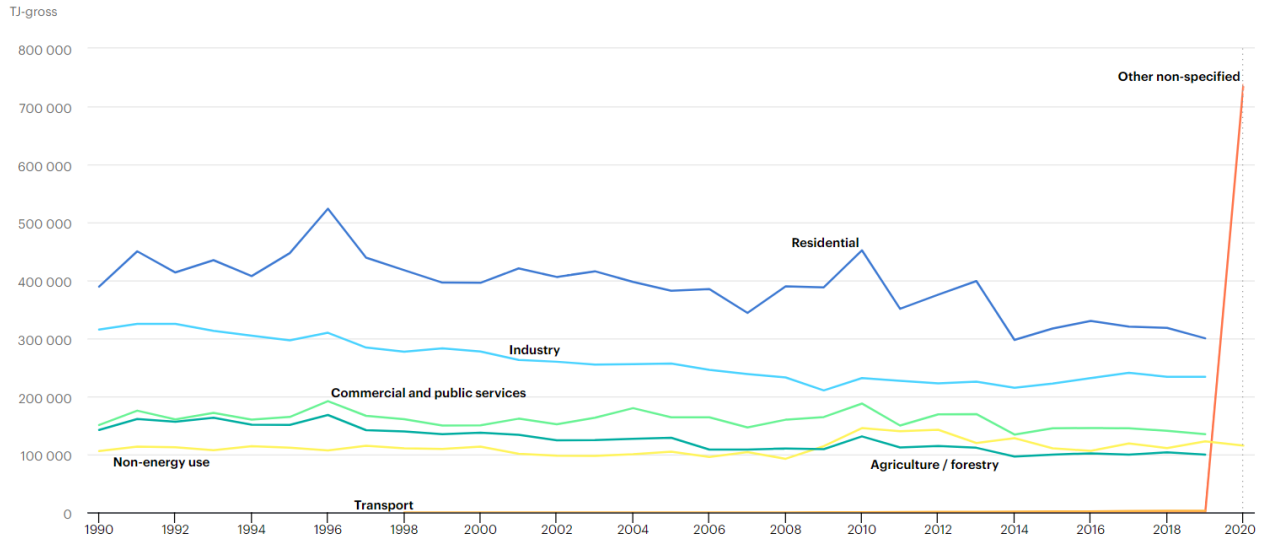

Fig2. Natural Gas Consumption by sector in the Netherlands,1990-2019 [5]

One of the technologies which can be developed and utilized is the heat storage technology based on thermochemical materials. Analyzing thermochemical heat storage technology and designing a practical reactor for this application is the main focus for this study. Different types of heat storage systems and their advantages and drawbacks will be discussed in details in Chapter 2.

1.2. Russia-Ukraine War: Another Trigger

Part of this thesis was done while the Russia-Ukraine war started and many European countries again found out about the importance of reducing their reliance on natural gas as they wanted to reduce imports from Russia. This could be also a trigger and incentive for all the sustainability energy projects in Europe and Netherlands.

Russian share of Dutch gas consumption is low at 15 percent, compared to 34 percent in Europe as a whole. The Netherlands plans to stop using Russian fossil fuels by the end of the year, the government said on 22 April 2022, vowing to spend an estimated 623 million euros ($675 million) on incentives for companies to fill a major gas storage facility. Dutch government said it was focused on making energy savings, greener policies and importing more energy from other countries [6] [7].

The “Nederlandse Vereniging Duurzame Energie” (NVDE), stated that the Netherlands can save almost five billion cubic meters of natural gas in one year and 10 billion cubic meters of gas saving is achievable in 4 years. Currently, Dutch dependence on energy imports is high, but some measures have also been proposed to shift through more sustainable energy [8]. One of them is the speeding up legislation aimed at collective heating facilities and natural gas-free residential districts and making budget so that 1 million homes can connect to this novel heat network before 2030.

1.3. Objective

The baseload demand in a district heating system is usually satisfied by biomass/waste combustion in the Netherlands. However, the challenge is how to fulfill the peak-load demand without using fossil fuels which is important for the heating supply reliability. The proposed research is targeting a novel peak shaving system for the district heating application.

Seasonal heat storage using a thermochemical material (TCM) is a novel heat storage technology which can transform the conventional district heating network to a newer, cleaner and more sustainable network. This system can be charged during the

summer period with renewable sources (e.g. solar) and then discharged in the winter to provide the required heat to the households for domestic use.

The aim of this study is to investigate the TCM based heat storage system, design and optimize a novel reactor for this application using the COMSOL Multiphysics® software.

1.4. Thesis Structure

In Chapter 2, the main points derived from the literature review will be presented. Focus will be on introducing the different configuration types and components for thermochemical heat storage technologies and their comparison.

In Chapter 3, a numerical investigation of the model will be discussed to explain the kinetic modelling and governing equations.

In Chapter 4, a basic 2D model will be designed and sensitivity analysis will be made to figure out the main design parameters controlling this model.

In Chapter 5, based on the studies and the basic modelling, the possible final designs of the reactor will be presented. The results will be processed for each model, together with the related analyzes and explanations. Also, improvement procedure of these models will be discussed and finally, some relevant comparisons will be done.

In Chapter 6, all the main conclusions obtained during the study will be summarized. Furthermore, any relevant recommendations on the designing will be discussed to have a better engineering view for future studies.

Chapter 2

Literature Review

2.1. Energy Storage Systems

Energy Storage systems can contribute significantly to meet society's needs for more efficient, environmentally friendly energy use in building heating and cooling, aerospace power and utility applications. For many energy technologies, storage is a crucial aspect. A variety of energy storage methods have been developed and they can be categorized as figure 3 [9]:

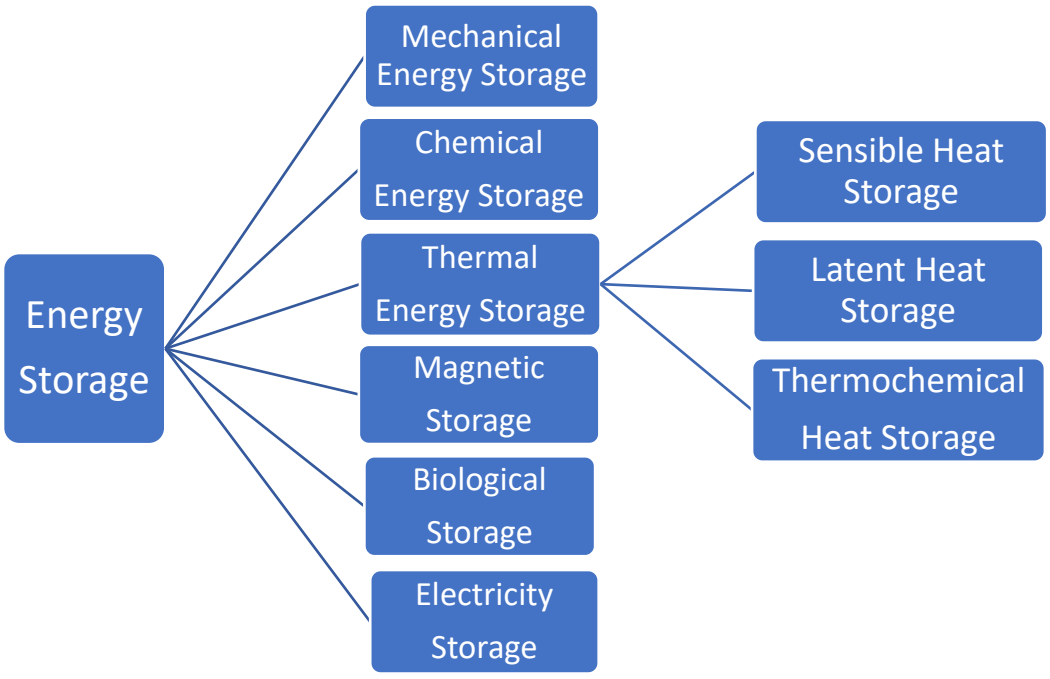

Fig3. Classification of Energy Storage Methods

This study will focus on thermal energy storage.

2.1.1. Thermal Energy Storage

As it is already shown in the Fig3, Thermal energy storage is divided in three main types including Sensible, Latent and Thermochemical heat storage [10].

In Sensible heat storage system, energy (or heat) is stored/released by cooling/heating a liquid or solid storage material through a heat transfer interaction. This heat transfer can be expressed as equation 1:

$$Q = m \times Cp \times \Delta T \qquad (1)$$

Where m and Cp are the mass and the specific heat capacity of the storage material respectively and ΔT is the temperature difference of this material before and after the operation.

Latent heat storage is done thanks to the phase change of a material (e.g., evaporation, melting and crystallization) and the high enthalpy change during this process. If Q donates the stored energy during latent process and m and L are the mass and specific latent heat of the phase change material (PCM), the equation 2 can be applied:

$$Q = m \times L \qquad (2)$$

Thermochemical heat storage actually uses a reversible chemical reaction to store thermal energy. This method has high energy density and allows long-term thermal energy storage [11].

The main principle of thermochemical heat storage is based on a reversible reaction like equation 3:

$$C + heat \leftrightarrows A + B \qquad (3)$$

Where C is the TCM and can absorb energy and convert chemically into A and B. This is the charging process which is endothermic and absorbs energy. After the charging, A and B are stored separately with little or no energy losses. Usually, the materials are stored at ambient temperatures to have no losses. The reversed reaction

which is actually formation of C from combination of A and B is an exothermic discharging reaction and releases energy which also permits the stored energy to be recovered. The heat of this reaction is the storage capacity of the system.

2.1.2. Comparison

Based on studying several literatures in which various types of thermal energy storage have been analyzed, the main advantages and disadvantages of sensible, latent and thermochemical heat storage can be summarized in Table 1 [12][13].

Table 1. Advantages and disadvantages of different types of thermal energy storage

	Sensible	**Latent**	**Thermochemical**
Temperature Range	• Up to 110 °C (Water tanks) • 50 °C (aquifers and ground storage) • 400 °C (Concrete)	• 20-40°C (paraffins) • 30-80°C (salt hydrates) (High temperature PCMs were not included)	• 20-200 °C
Storage Density	• Low (with high temperature interval): 0.2 GJ/m3 (for typical water tanks)	• Moderate (with low temperature interval): 0.3-0.5 GJ/m3	• Normally high: 0.5-3 GJ/m3
Technology Status	• Available commercially	• Available commercially for some temperatures and materials	• Generally not available, but undergoing research and plot project tests
Lifetime	• Long	• Often limited for storage material cycling	• Depends on reactant degradation and side reaction
Advantages	• Low Cost • Reliable • Simple application with available materials	• Medium storage density • Relatively low volume requirements • Short distance transport possibility	• High storage density • Low heat losses (storage at ambient temperatures) • Possibility of charging in

			summer (high solar fraction) • Long storage period • Long distance transport possibility • Highly compact energy storage
Disadvantages	• Significant heat loss over time (depending on level of insulation) • Large volume and space needed • Charging in summer (seasonal storage) increases heat loss • Charging in winter (short term storage) decreases solar fraction.	• Low heat conductivity • Corrosivity of materials • Significant heat losses (depending on level of insulation) • Charging in summer (seasonal storage) increases heat loss • Charging in winter (short term storage) decreases solar fraction.	• High capital costs • Technically complex also because of containing TCM materials

A Schematic comparison of volumetric storage capacities has been shown in Figure 4 [14]. For sensible storage materials, water has been selected as representative. The regions denoting PCMs and TCMs are actually an illustration of the overall trend not the strict limits. Some PCMs and TCMs have been mentioned in this figure, but in fact, there are a lot more of these materials also at higher temperatures.

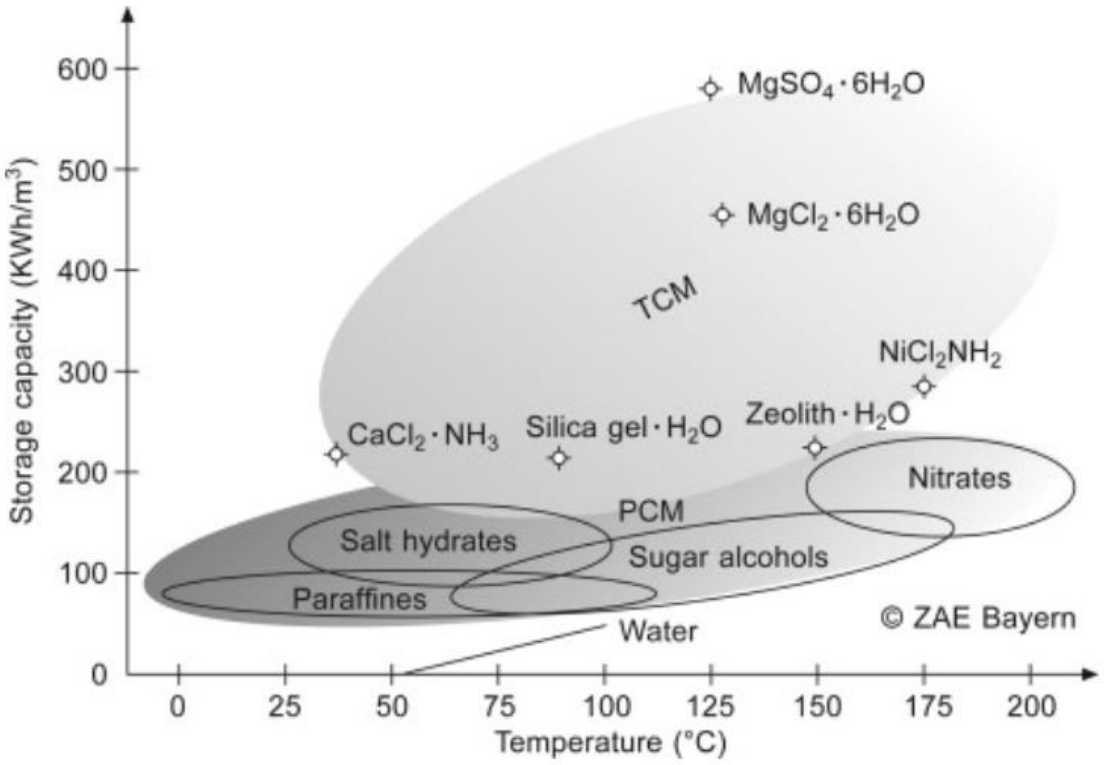

Fig4. Storage capacities of PCM and TCM compared to water

2.2. Thermochemical Heat Storage System – Components

Depending on the different systems to be used in TCHS, they can include reactor, heat exchangers, evaporator/evaporator, vessels, valves and pipes. Discussing on a system level, there are some different types used in this technology which will be explained in the next section.

2.2.1. Thermochemical Heat Storage System – System Types [15]

Systems for solid-gas reactors can be designed either in open or closed system configurations and it is possible to use an integrated, separated or modular reactor. Next, all of these definitions will be explained.

2.2.1.2. Open and closed systems

In an open system concept, there is one vessel which is the reactor. This reactor contains the solid materials and the moist air at atmospheric pressure flows through it.

This system is open to the atmosphere, so the pressure is set to the atmospheric pressure. As a result, high pressure drops across the reactor can take place [16].

No internal heat exchanger and thus no evaporator/condenser are being used in open system, as the heat transfer fluid and the reactive gas are the same in this configuration.

The process, which is also shown in Figure 5, is simply as follows [17][18]:

In charging mode (summer time), ambient air is heated by a heat source (e.g. solar) and moves to the reactor where salt dehydration happens.

In discharging mode (winter time), ambient humid air with low temperature passes through the reactor, salt hydration process happens and heat is released to the house.

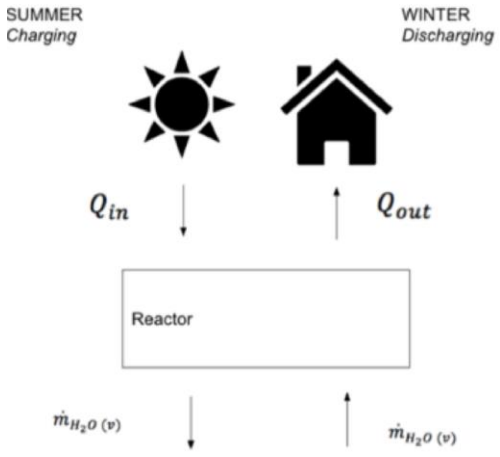

Fig5. An integrated configuration for an open system

In a closed system, there are two vessels, a reactor which contains the material and a condenser/evaporator holding the reactive gas. Unlike open system, in closed system the heat energy is transferred via a heat exchanger. In closed system, material

reacts with a pure gas. In the discharge mode, a heat source is required to vaporize the liquid, so closed system needs higher temperature for the hydration reaction [19].

The process in a closed system, which is also shown in Figure 6, is simply as follows [17][18]:

In the charging mode, dehydration reaction happens in the reactor receiving heat from heat source, and a gas-liquid phase change reaction occurs in the condenser by releasing heat.

In the discharging mode, evaporator produces vapor which passes to the reactor and hydrates the material inside it.

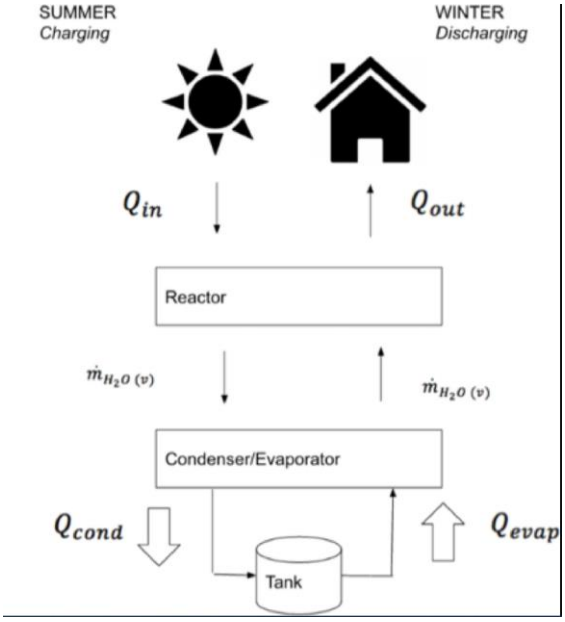

Fig6. An integrated configuration for a closed system

According to a previous study done by Michel et al. [17], it has been concluded that in open systems, mass transfer is a limitation factor, because of the pressure drops across the reactor which causes higher entropy production. On the other hand, in closed systems, heat transfer is a limitation factor, because mass transfer is determined by the total pressure, which can be optimized.

To have a better overview of these two configurations and distinguish their differences, their pros and cons have been reported in the Table 2.

Table2. Advantages and disadvantages of open and closed systems [15][18]

	Advantages	Disadvantages
Open System	• Atmospheric Pressure • Simple Design • High system energy density • No heat exchanger required • Fewer Components than closed system • Heat transfer could be increased by forced circulation	• Low discharging temperature with similar vapor pressure compared to closed system • Fan and humidifier often needed to drive the sorbate flow and provide partial humidification • High gas flow causes pressure drops • Gas and side reactions should be safe because they are released to the atmosphere • Mass transfer limiting
Closed System	• Higher discharging temperature with similar vapor pressure compared to open system • Better control of mass transfer, as there is no mass exchange with environment • Can have a combined use for both cooling and heating • Higher Power density • Possibility of low-pressure state and pressure control	• Complex system • Large heat transfer area required • Periodical evacuation needed because of formation of incondensable gases • Sorbate needs to be stored • Low system energy density due to heat exchangers and storage of reaction components

	• Stability during heat generation	• Heat transfer limiting

2.2.1.3. Integrated, Separated and Modular reactors [15]

In an integrated reactor (Figure 7), total amount of TCM is in the bed; so, after the material is placed inside the reactor, it does not need to be moved. This is more suitable when the reactor material is solid, due to possibility of removing energy consumption for transport [20].

In a separated reactor (Figure 7), the TCM is transported to the reactor when heat is required and stored separately from where the hydration and dehydration reactions take place. This way, only the necessary amount of material is heated at a given time, improving efficiency, decreasing heat transfer surface and sensible heat losses.

In modular reactor (Figure 8), like integrated reactors, TCM is not transported. Within these reactors, material is divided into smaller and insulated modules and each of these modules includes its own heat exchanger. Consequently, each small module can be heated upon request and for any desired application, power output of every module can be optimized.

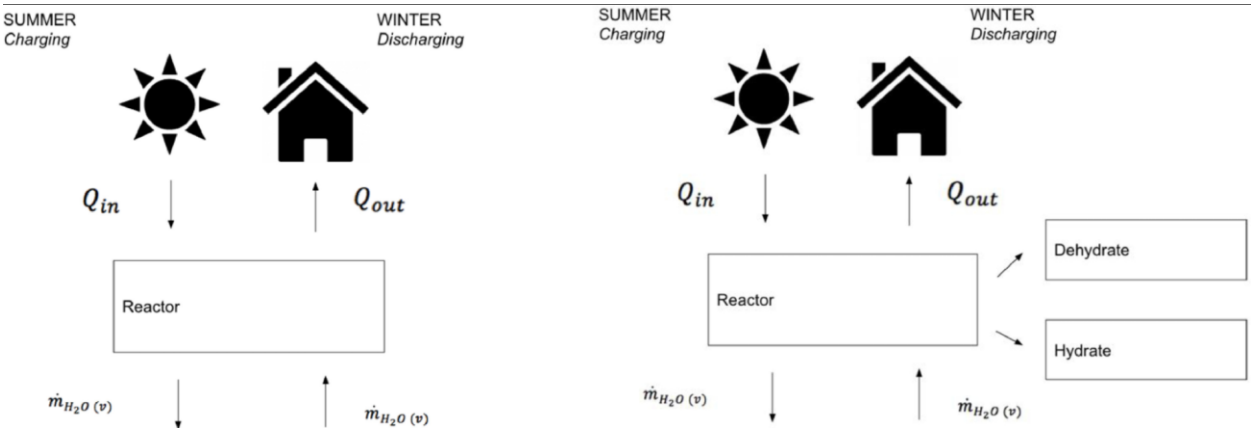

Fig7. Open system reactor with integrated configuration(left) or separated(right)

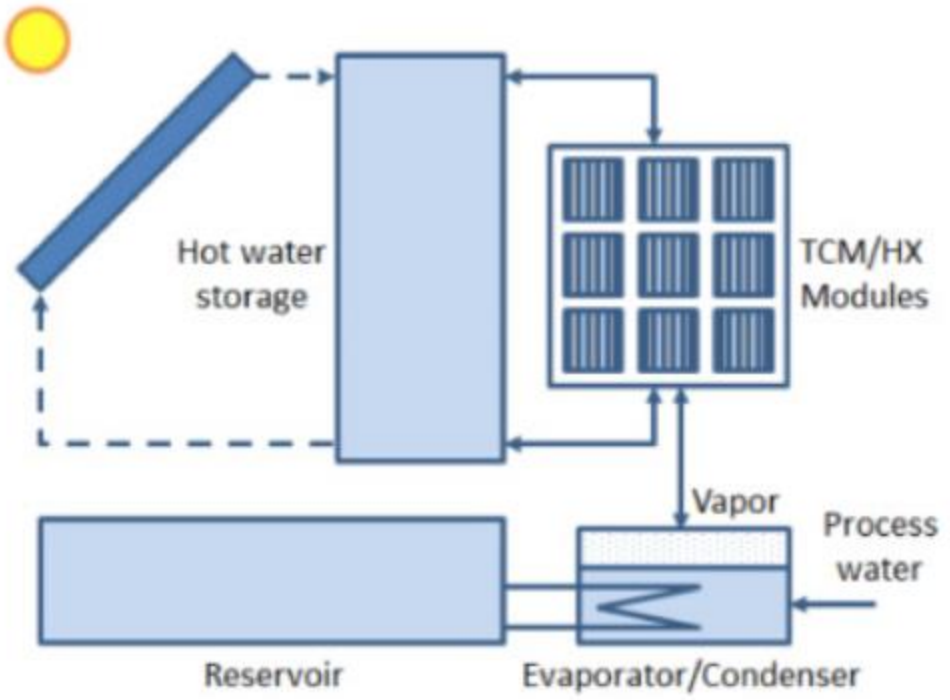

Fig8. Modular reactor bed in a closed system configuration

These three configurations have been discussed in several literatures and some benefits and drawbacks have been concluded for each type which have been summarized in Table3.

Table3. Advantages and Disadvantages of Integrated, Separated and Modular configurations

	Advantages	Disadvantages
Integrated	• No transport of material, thus reducing energy consumption required for material transport [20]	• Larger reactor causes higher sensible heat losses while charging as whole reactor must heat up [21] • Control of reaction is complex as the large reactor must be designed for reaction conditions [18][20]

Separated	• only the necessary amount of material is heated at a given time, improving efficiency, decreasing heat transfer surface and sensible heat losses. [22] • The heat and vapor transfer can be optimized efficiently compared to integrated system • Overall process is more efficient for seasonal storage because only a small volume of material is heated up [21]	• More complex design, more vessels and increased pumping power as the material needs to be transported to the reactor from a storage tank [18][20]
Modular	• Surface area of heat exchange can be optimized and reactor size can increase or decrease accordingly [23] • The entire material does not need to be flushed with the gas flow during operation, which reduces pressure drop [18][24]	• Larger volume due to each module's own heat exchanger leading to high capital costs and lower volumetric energy density [18][24]

2.3. Fixed, Moving and Fluidized bed reactors

Another major categorization should be considered when reactor design for thermochemical heat storage systems based on salt hydrates is being discussed. Reactors could be divided into fixed (packed) bed, moving bed or fluidized bed [15]. Next, a brief description of each of these reactors will be provided and their positive and negative points will be mentioned.

2.3.1. Fixed Bed Reactors

In Fixed bed reactors, the material is stationary inside a vertical vessel (Figure 9). Their simple design and easier modelling have made them widely usable and so suitable for hydration/dehydration reactions due to the solid-gas states. Fixed bed reactors are commonly used but they have several restrictions such as heat and mass transfer limitations and large temperature gradients throughout the bed [25]. This kind of issues should be investigated by the designer of a reactor who wants to utilize fixed bed reactors for thermochemical heat storage applications.

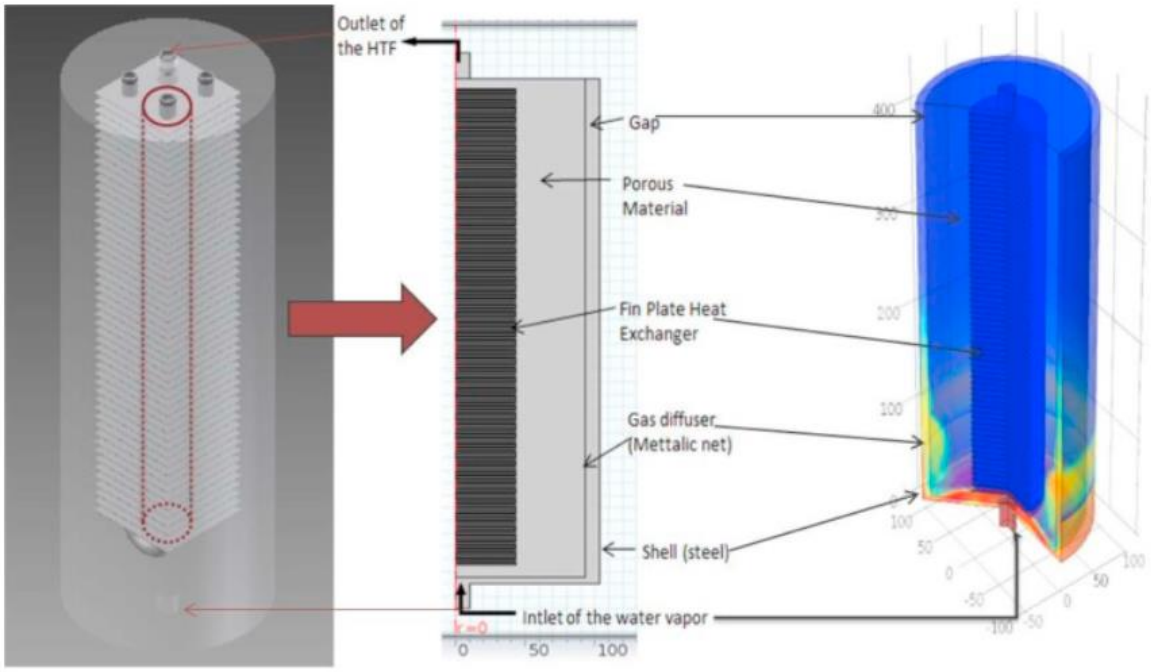

Fig9. An example of a closed fixed bed with an integrated heat exchanger designed by Fopah-lele et al. in [26]

2.3.2. Moving Bed Reactors

In Moving Bed Reactors, salt is moving continuously or in portions (such as stirring) (Figure 10). In other words, in these reactors, bed moves with respect to the vessel. Distribution of fluid flow and vapor sorption are more uniform in the moving bed reactors and the heat transfer coefficient is also higher than the fixed bed reactors. However, correct design of these reactors is a challenge as they have moving parts and more complex than fixed bed reactors which also was also an important criterion in the selection of reactor type in the design phase of this thesis.

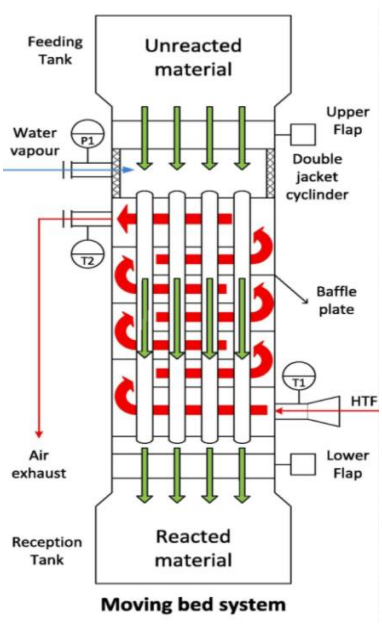

Fig10. A closed moving bed with a heat exchanger designed by Cosquillo Mejia et al. in [27]

2.3.3. Fluidized Bed Reactors

In Fluidized bed reactors (figure 11), the solid is in fine particles which are suspended by the upwards flow of the fluid(gas) [15]. When this upward velocity of the fluid goes higher than a minimum fluidization velocity, the solid particles start moving randomly.

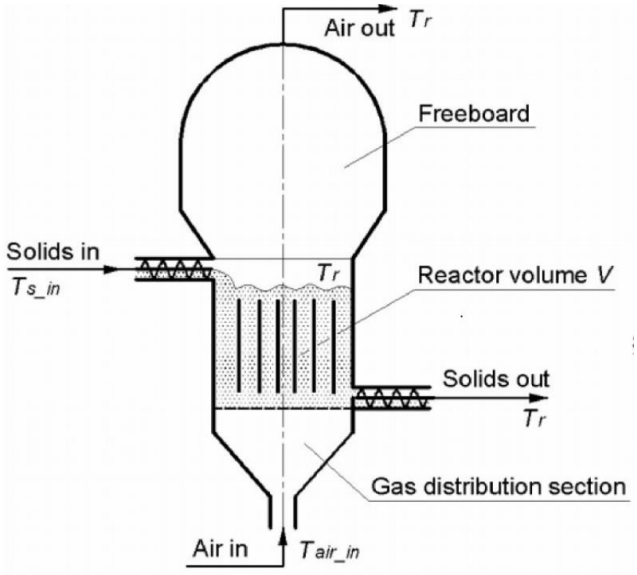

Fig 11. A fluidized bed reactor [28]

There have been many studies done about these reactors. This is the designer's choice to decide which kind of reactor to use according to the application in which it will be used. During the recent years, many experimental and non-experimental studies have been performed to make reasons for the better choice in different situation. One study, for instance, is related to the researchers in TNO ('*Toegepast Natuurwetenschappelijk Onderzoek*'), an independent research organization in the Netherlands which mainly conducts applied science researches.

Zondag et al. prepared a fixed bed hydration/dehydration setup using CaCl2 as the salt in the laboratory [29]. They tried to conduct experiment in the effect of the stirring on the heat transfer. They believed that stirring the material inside the bed optimizes the heat and vapor transport and removing all inert gasses can facilitate the diffusion and overall, these steps can improve the hydration time. To this aim, they used an agitated heat exchanger. Finally, they concluded that stirring the material in an evacuated bed could strongly improve the heat transfer.

In another study, Zondag et al. compared a moving (screw) bed, a fluidized bed and a gravity-assisted bulk flow bed (a type of moving bed) and their performance for domestic heating [28]. They found out that moving bed had a high COP whereas the fan energy needed for fluidization of particles decreased the COP of fluidized bed reactor noticeably. Out of the three, they opted for the moving bed, in particular the screw design, as the most suitable type for the application.

To have a better overview, pros and cons of all these reactors have been collected from articles and reported in Table 4.

Table4. Advantages and Disadvantages of Fixed, Moving and Fluidized bed reactors

	Advantages	Disadvantages
Fixed Bed	• Easier to model [15] • Easier to manufacture [15] • Small Size [15] • Small Capital Cost [15]	• Temperature gradients [15] • Low heat and mass transfer [20] • High pressure drops inside the reactor [20]

Moving Bed	• Direct heat transfer between solid and the gas [20] • Good temperature control [15] • Compared to a fluidized bed, it requires less energy [15] • High heat transfer coefficient	• More difficult to model due to having moving parts [15] • Complex reactor design [15] • Lowest conversion per unit volume [15] • Complex hydrodynamics [18]
Fluidized Bed	• High heat transfer coefficient [20] • Uniform mixing of particles [15] • Risks of hotspots and thermal instability are minimized [15]	• Complex to Model [20] • Complex hydrodynamics [20] • Erosion of internal parts [15] • Increased reactor vessel size [15] • Pumping Energy Requirements [15]

2.4. TCM Material

The TCM is the material which involves in hydration/dehydration reactions in the reactor and gives heat to the HTF which can be finally used for space heating and hot tap water application. Therefore, selection of a suitable TCM for the TCHS application should be based on some thermodynamical, economical but also safety considerations.

Donkers et al. [30] collected thermodynamic data for 262 salts, investigated 563 reactions, introduced several filters to come up with the best possible salts for the application. They targeted an energy density of 2 GJ/m^3 on material level (without considering water storage, open system configuration) because energy density on system level is always lower than material (salt) level as in the whole system, not all the volume contains TCM. Also, the TCM should provide temperatures of domestic hot water (DHW) (T > 65 °C) and space heating (HW) (T > 40 °C) within one heating step. This temperature should be reached with a corresponding vapor pressure of 12 mbar, which is equal to an equilibrium vapor pressure of a water source at 10 °C. The second filter was introduced as a compromise between the strict boundary conditions for an ideal salt hydrate and achievable boundary conditions acknowledged to available salt hydrates. The energy density is lowered to a value of 1.3 GJ/m^3 on material level, which results in approximately 1 GJ/m^3 in a closed system. The hydration/dehydration temperatures are increased/decreased respectively. This filter will definitely impact system level design, e.g., higher dehydration temperatures and additional heating to reach hot tap water temperatures.

Finally, they came up with a table of 25 most suitable hydrate reactions and reported their characteristics in a table. In this section, some of the salts have been chosen to be discussed in table 5.

Table5. Characteristics of some potential TCM salts [30]

	Energy density open system (GJ/m^3)	Energy density closed system (GJ/m^3)	$T_{Hydration}$ (°C) with p_w =12 mbar in reaction	$T_{Dehydration}$ (°C) with p_w = 20 mbar	Price (euro/kg)	**Point of Concern**
$GdCl_3$	2.70	1.56	90	98	R	Rare Earth
LiCl	2.08	1.36	66	72	37	Price
$Ca(ClO_4)_2$	1.75	1.17	92	100		Explosive
RbF	1.57	1.10	84	91	>10	Price
$CaCl_2$	1.54	1.06	63	111	0.29	Deliquescence and higher hydrates

$Mg(NO_3)_2$	1.53	1.04	61	68		Instable
$LaCl_3$	1.48	1.03	66	73	R	Rare Earth
K_2CO_3	1.30	0.96	59	65	1	
$MgCl_2$	1.93	1.24	61	104	0.18	HCl formation - Instable
Na_2S	1.60	1.14	75	82	0.65	H_2S formation- Safety/Instable

2.4.1. TCM Material – Our Choice

The TCM selected for this study is Potassium Carbonate. Generally, for selecting a suitable TCM, factors like higher energy density, Lower Price, Cyclability, being non-toxic, non-flammable and non-corrosive should be taken into account.

K2CO3 has some advantages. It is highly available, chemically robust, safe, cheap and not so much corrosive. However, the energy density of K2CO3 is 1.28 GJ/m3 for an open system and 0.95 GJ/m3 for a closed system which is relatively a low number if we compare with other TCM materials and is also evident from Table 5. [30] One other point is the low discharge temperature (22-45) which is of course enough for space heating.

2.5. Heat Exchanger

Another key component which is used in the closed system configuration is the heat exchanger. This component is used for transferring heat between the section with TCM material and the section with heat transfer fluid. For this application, an indirect contact heat exchanger (ICHX) is desired.

In an ICHX, a wall separates the TCM and HTF section and heat transfer happens continuously through this wall.

There are quite a lot of heat exchanger designs and configurations, each with its own benefits and drawbacks and choosing the heat exchanger configurations is actually another decision which should be made by the designers. Based on literature review,

some of the practical heat exchangers types have been introduced briefly in this section.

2.5.1. Shell and plate heat exchangers

This configuration consists of an outer shell which has some plates placed in parallel with each other. TCM particles, for instance, can enter and flow past the plates and transfer heat to them. Then, one could design tubes containing the HTF, which run through the shell and are attached to the plates. This way, the heat of TCM reaction can transfer from the plates to the HTF. An example of this concept is shown in Fig 12. Note that this is only one way of this design and other possible designs can be also implemented.

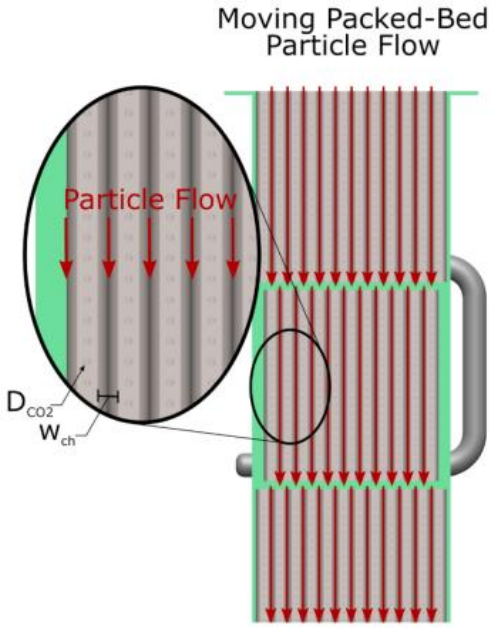

Fig12. A shell and plate heat exchanger [31]

Some main advantages of this design are the possibility of large heat exchange surface area and thus high heat transfer performance. On the other hand, cleaning may be an issue for this design [32].

2.5.2. Shell and tube heat exchangers

This configuration consists of several tubes which are inside a cylindrical shell. One of the fluids can move inside the tubes and one of them can be chosen to move inside the shell and heat transfer takes places between them. Sometimes a component called “baffle” can also be used to control the flow of the shell fluid.

Shell and tube heat exchangers are easy to repair and maintenance, have flexible design and can also withstand some severe conditions. On the other hand, they may have a large footprint and also their performance at low temperatures can be low [33].

Figure 13 demonstrates an example of a shell and tube heat exchanger.

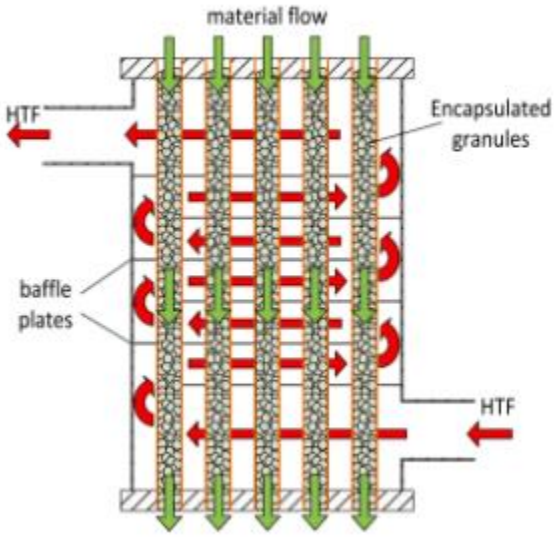

Fig 13. A shell and tube heat exchanger [27]

2.5.3. Spiral Plate Heat Exchanger

A spiral heat exchanger (figure 14) consists of two long flat plates wrapped around a mandrel or center tube, creating two concentric spiral channels.

These heat exchangers can handle viscous liquids and fouling liquids better due to having single passage, they are more compact and have less footprint compared to

shell and tube heat exchanger. Of course, limited maximum size and maximum pressure and field repair difficulty can be their noticeable disadvantages [34].

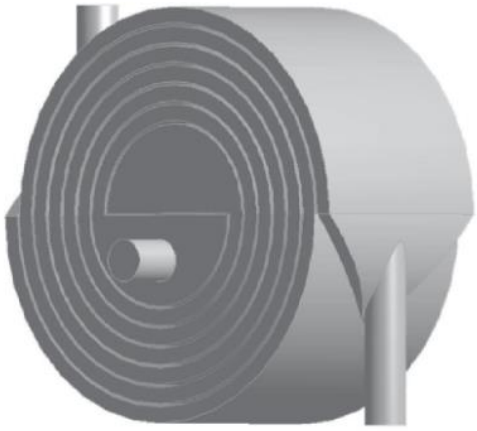

Fig 14. A Spiral Plate heat exchanger

2.5.4. Helical Coil Heat Exchangers

Helical Coil Heat Exchanger or HCHE (figure 15) is a type of heat exchanger which has a shell called annulus and inside it, there is a helical coil. It occupies less space and provides more surface area for effective heat transfer as compared to shell and tube heat exchanger [35].

Increasing number of turns of the heat exchanger would slightly increase the effectiveness. There is an optimum value for number of turns of the helical coil corresponding to a maximum effectiveness [36].

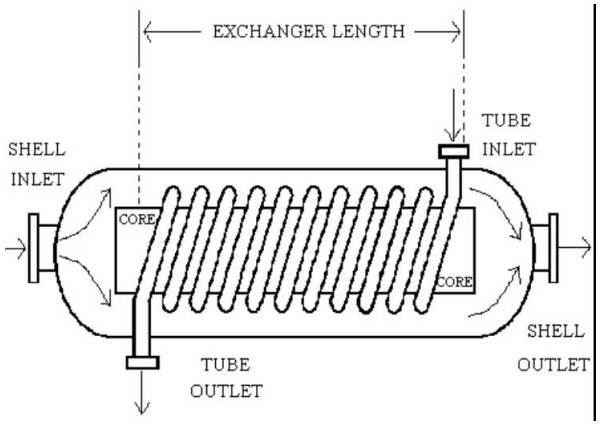

Fig 15. Schematics of a Helical Coil Heat Exchanger

HCHE has the advantages like efficient use of space, compatibility with low flowrates or laminar flow cases and also compatibility with cases in which there is low pressure in one of the fluids [37]. In applications where one of the fluids has components in multiple phases, HCHE also may have small-tube plugging problems and the cleaning may be also difficult, however compared to shell and tube heat exchangers, they tend to require less cleaning [38].

2.6. Heat Transfer Fluid

The heat transfer fluid is another important factor in a reactor which is used to extract heat from the heat exchanger. There are several deciding criteria to choose a suitable heat transfer fluid including high heat conductivity, low viscosity, large heat capacity, high working temperature range, nontoxicity, non-explosivity, easy replacement and cleaning and price [39]. Thermal Oils are too expensive for widespread use. Liquid metals and molten salts have high melting point problem.

Air and water can be concluded as two better options as they are both cheap and easy to model. Between them, water is preferred due to better heat transfer properties.

2.7. Final Design Choices

Figure 16 is a summary of the final design choices in the study.

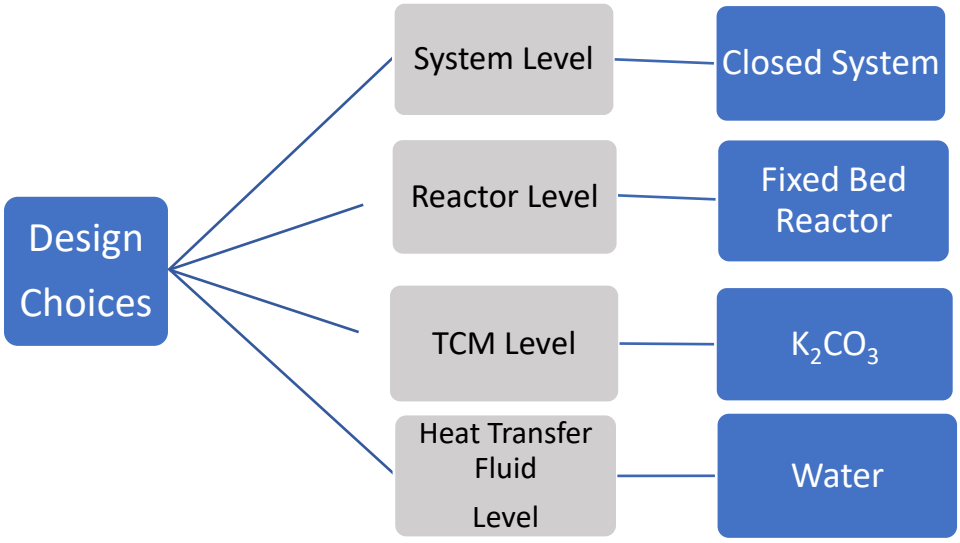

Fig 16. Final Design Choices

Chapter 3

Theoretical Investigation and Basic Modelling

3.1. Introduction

Literature review gave a wide and valuable understanding on the thermochemical storage systems theory, their different types, benefits and limitations and based on all these studies, decision on designing a closed system fixed bed reactor based on potassium carbonate as TCM and water as HTF was made.

In this chapter, the main governing equations and reaction kinetics for this type of application will be discussed. To have a better understanding, a simple 2D model will be also defined in COMSOL Multiphysics®. Full boundary and initial conditions will be explained in this model which will be also be used as a theoretical fundamental for the final reactor design. Sensitivity analysis will be done on the simple model to give a nice overview of which controlling parameters there are in this model which will give the design knowledge to facilitate the final reactor design.

3.2. Basic Modelling

First, a simple 2D design have been brought first on paper and then into COMSOL Multiphysics®. This simple model (figure 17) together with all the conditions and the assumptions will be discussed in this part.

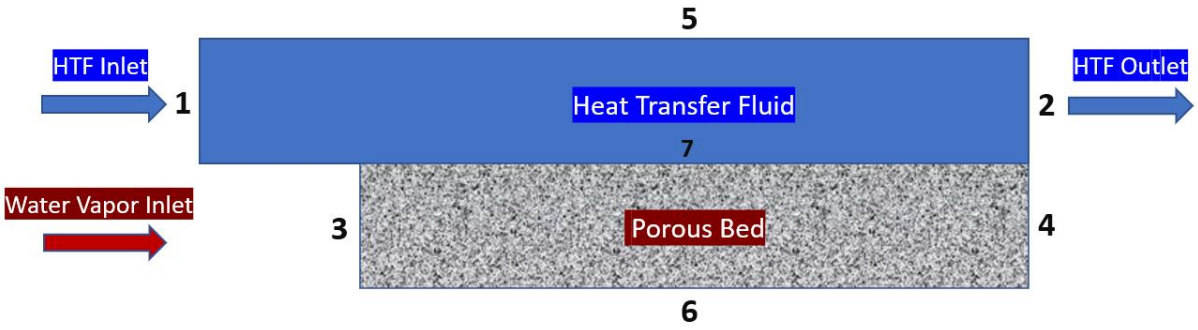

Fig17. Basic 2D Model in COMSOL

Figure 17 depicts the basic two-dimensional model which have been used from the beginning of this study to facilitate understanding the physics of the thermochemical heat storage reactor. This basic model consists of a porous bed which contains the TCM salt and water vapor from the evaporator enter this bed. Above bed, the heat transfer fluid has been considered. Each boundary is marked with a number and the boundary conditions have been presented in the Table 6.

Table6. Boundary Conditions of the Basic 2D Model

Boundary	Type	Boundary Conditions
1	Mass Flow Rate Inlet	$\dot{m}$ = 0.01 kg/s T = const = 30°C $\partial c/\partial x = 0$
2	Pressure Outlet	P = 0 Pa
3	Pressure Inlet	P = 1200 Pa T = 10 °C c = const = 0.5 [mol/m3]
4	No Flow Thermal Insulation	$q \cdot n = 0$ $\rho u \cdot n = 0$

5	Wall	No slip wall $u = 0$ $q \cdot n = 0$
6	Symmetry	$q \cdot n = 0$ $\rho u \cdot n = 0$
7	Wall	No slip wall $u = 0$

As for Initial Conditions, the initial Heat Transfer Fluid temperature, initial TCM temperature, the extent of conversion (alpha), the initial TCM pressure have been set to 30°C, 30°C, 0.1 and 130 Pa.

3.3. Assumptions

In order to simplify the problem, like every heat and mass transfer problems, several assumptions have been made. These must be relevant and considered in a way that prevent the high complexity of the calculations in COMSOL. The main assumptions of this model are as below:

1. The Material bed is a homogenous porous medium and has constant properties such as heat capacity and thermal conductivity.

2. The TCM Particles are stationary (They do not move).
3. Permeability and Bed Porosity are constant over time (porosity is set to 0.7)

4. Local Temperature Equilibrium ($Ts \approx Tv \equiv T$) is considered in the porous media, with this assumption, one single equation is solved for two phases (solid and gas) using effective material properties.

5. Because of the low temperature range, any heat transfer by radiation in the porous media is neglected.

6. Inlet Mass Flow Rate of heat transfer fluid is constant (is set to 0.01 kg/s).

3.4. Reaction Kinetics

Reaction kinetics provide a measurement of reaction rates, factors that affect the speed of a chemical reaction and insight into reaction mechanisms. Understanding the kinetics of a reaction is critical for being able to control a reaction and direct the desired outcome of the reaction.

In this application, a reversible reaction of hydration of potassium carbonate (exothermic) and its dehydration (endothermic) takes place as equation 4:

$$K_2CO_3 + (1.5)\, H_2O(s) + \Delta H \Leftrightarrow K_2CO_3(s) + 1.5H_2O(g) \qquad (4)$$

A dependent variable called α (alpha) is defined as the status of conversion. This variable ranges shows how much the conversion process of the solid material has been completed and it can range from 0 to 1. In hydration process, if α reaches to 1, this means that the TCM material (potassium carbonate) is fully hydrated. Analyzing this variable in the reactor model shows the speed of the reaction and the cycle time of the reactor. In other words, the faster alpha reaches to 1, the sooner the reactor completes one cycle of hydration reaction.

The rate of reaction of the reaction is defined as the variation of α over time and is denoted by $\frac{d\alpha}{dt}$.

Generally, the rate of reaction is assumed to be formulated in terms of temperature *T*, partial pressure *P* and the status of conversion α[40]. Therefore, the reaction rate is generally formulated as equation 5:

$$\frac{d\alpha}{dt} = K(T) \cdot f(\alpha) \cdot \ h(P, P_{eq}) \qquad (5)$$

where K defines the rate coefficient, $h(P, P_{eq})$ defines the pressure dependence and the function $f(\alpha)$ describes the reaction mechanism. The status of conversion α must be defined in a way that satisfies the equation 6: [40]

$$\acute{m} = \rho_s \,.\, \frac{d\alpha}{dt} \qquad (6)$$

where $\acute{m}$ is water vapor consumption (kg/m^{3}s) and ρ_s is the solid density. The unit of $\frac{d\alpha}{dt}$ is 1/s from this equation. Equation 6 actually demonstrates the vapor mass change.

Mahmoudi et al. [40] performed TGA (Thermogravimetric Analysis) measurements for a thermochemical heat storage system based on potassium carbonate to evaluate the kinetics of K_2CO_3. After their experiments, they concluded that the equation 5 can be rewritten as equation 7:

$$\frac{d\alpha}{dt} = A_f \cdot e^{\frac{-E_a}{RT}} \cdot (1-\alpha)^q \cdot (1-\frac{P_{eq}}{P}) \qquad (7)$$

Which shows the temperature as an Arrhenius function and:

- A_f is the pre-exponential factor in 1/s,
- E_a is the activation energy in J/mol
- R is the universal gas constant in J/kg/K
- T is the temperature in K
- α is the status of conversion
- P_{eq} is the equilibrium water vapor pressure in Pa
- P is the water vapor pressure in Pa

The values derived in the aforementioned study which has been done in University of Twente in 2021, have been also used for the modelling of this study. These Values are as Table 7 [40]:

Table 7. Constant Values for kinetics equation

	A_f (1/s)	E_a (J/mol)	q
Hydration	2.7×10^{-9}	-34828	0.7
Dehydration	225	43382	0.8

Next, the equilibrium water vapor pressure should be defined. The phase diagram of K_2CO_3 (figure 18) is constructed based on the Clausius-Clapeyron equation (equation 8) and used to define the equilibrium water vapor pressure [41]. This pressure is actually like an upper limit for the reaction. In other words, if this pressure is equal to water vapor pressure, the reaction will stop. Otherwise, the difference between these two pressures is the driving force for the reaction to proceed.

$$\frac{d\ \ln(P_{eq})}{d(\frac{1}{T})} = \frac{\Delta h}{R} \qquad (8)$$

where P_{eq} [Pa] is the equilibrium water vapor pressure between the two hydrate phases, T[K] is the corresponding temperature, R [J/kg/K] is the gas constant and Δh [J/mol] is the reaction enthalpy per mole of H_2O.

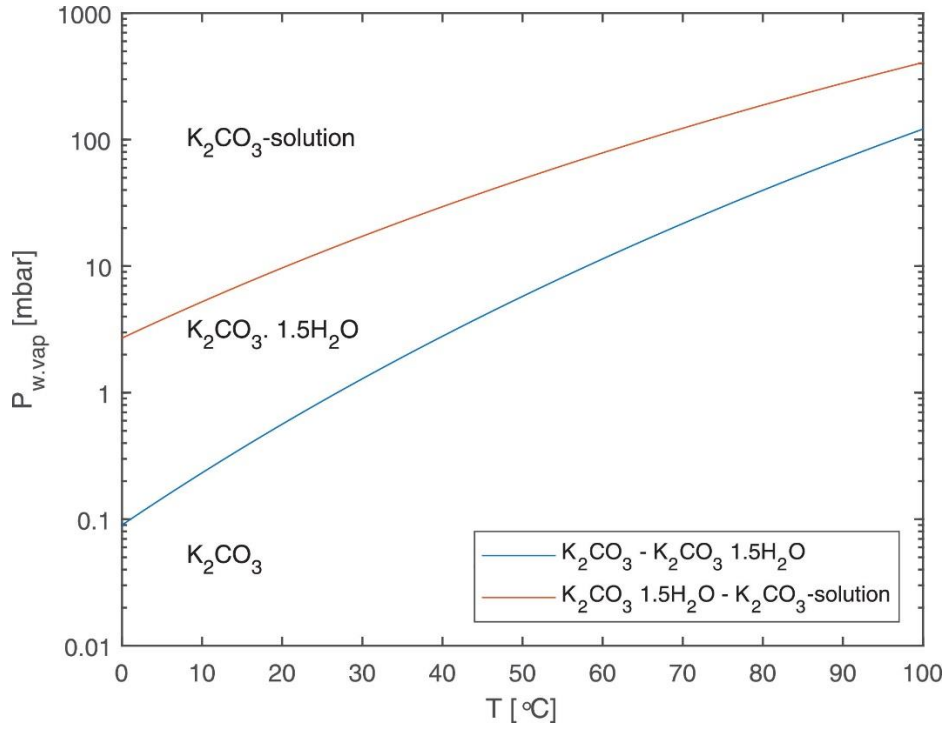

Fig 18. Phase diagram of K_2CO_3 based on Clausius-Clapeyron Equation [41]

The blue line in the Fig 18 shows the equilibrium line between the two states of hydration of potassium carbonate. The equilibrium pressure from this phase diagram can be fitted by the equation 9 [41]:

$$P_{eq} = 4.228 \times 10^{12}\, e^{-\frac{7337}{T}} \qquad (9)$$

Where T is the temperature in K.

Therefore, the model could compute the equilibrium water pressure from equation 9 and put it in the equation 7.

An important parameter in this study is the pressure ratio which is the ratio between water vapor pressure and water vapor equilibrium pressure (P_w/P_{eq}) and as it has been explained before, reaction will continue until this ratio reaches to 1, as the difference between these two pressures is the driving force of the reaction.

It is also worth to mention that the brown line in the Fig 18 demonstrates the deliquescence (liquefaction) phenomenon. This takes place after a certain state of hydration of potassium carbonate, due to the depression of the melting point upon water uptake as the material is highly hygroscopic [41]. This actually leads to formation of an aqueous solution instead of a solid-state material.

This will be problematic as the dehydration process of this overhydrated solution can produce an agglomerated bulk of solid material, instead of the initial powdery porous form. Agglomeration is an undesirable phenomenon, because it prevents or decelerates the subsequent water uptake process [42].

Considering this effect, the operation condition should be chosen such that overhydration does not happen. By controlling the conditions in an experiment, as well as in a storage system, it becomes possible to stay below the deliquescence line [41].

3.5. Energy Balance in Porous Media

Considering the porous media, hydration reaction is exothermic and releases heat. This heat is removed from the porous media by two heat transfer methods: Conduction and Convection. As already has been mentioned in the assumptions made on the model, heat transfer by radiation is neglected. Thus, Energy Balance in Porous media can be written as below:

Heat Accumulation = Heat Conduction + Heat Convection + Heat Source Term

And can be formulated as equation 10:

$$\left(C_{p,s}\,(1-\varepsilon)\rho_s + C_{p,v}\,\varepsilon\rho_v\right)\frac{\partial T}{\partial t} = \nabla\cdot\left(K_{eff}\nabla T\right) - \rho_v C_{p,v}\left(\vec{u}_{fd}\cdot\nabla T\right) + (1-\varepsilon)\frac{\rho_{s0}}{M_{s0}}\frac{\partial \alpha}{\partial t}\Delta H_r \quad (10)$$

Where:

- ε is the bed porosity
- $C_{p,s}$ is the specific heat capacity at constant pressure of the TCM in J/kg.K

- $C_{p,v}$ is the specific heat capacity at constant pressure of the water vapor in J/kg.K
- ρ_s is the density of the TCM in kg/m^3
- ρ_v is the density of the water vapour in kg/m^3
- u_{fd} is the velocity field of water vapor through the TCM in m/s
- M_s is the molar mass of TCM in kg/kmol
- ΔH_r is the reaction enthalpy of the TCM in J/mol
- K_{eff} is the effective thermal conductivity of the porous bed in W/(m.K)

There are several ways to compute the effective thermal conductivity of porous bed. For this case, a volume average method is being used, including the term related to the solid phase and the term related to the gas phase as equation 11:

$$K_{eff} = (1-\varepsilon)\lambda_s + \varepsilon\lambda_v \qquad (11)$$

3.6. Mass Balance in Porous Media

As it has been mentioned already, the system is closed system. This means that there is no mass exchange between the system and the surroundings and thus increasing the mass density of TCM will decrease the mass density of the water vapor and the dehydrated TCM. Mass balance can be written both for TCM and water vapor as equations 12 and 13:

Water Vapor: $$\varepsilon\frac{\partial\rho_v}{\partial t} = -\nabla\cdot\left(\rho_v.\vec{u}_{fd}\right) + D_v.\Delta\rho_v - (1-\varepsilon)\cdot\chi\cdot\rho_{s0}\cdot\frac{\partial\alpha}{\partial t}.\frac{M_v}{M_{s0}} \qquad (12)$$

TCM: $$\frac{\partial\rho_{s1}}{\partial t} = -\frac{\partial\rho_{s0}}{\partial t} = \rho_{s0}.\frac{\partial\alpha}{\partial t} \qquad (13)$$

Where:

- D_v is the effective gas diffusivity in the porous bed in m^2/s
- χ is the stoichiometric coefficient of water in the reaction (=1.5)
- M_{s0} is the molar mass of the dehydrated TCM in g/mol
- M_v is the molar mass of water vapor in g/mol

Analyzing in details, in equation 12, from left to right, first term refers to the change of water vapor mass concentration in the porous bed, second term refers to convection (change of water vapor mass concentration due to the flow, third term refers to the diffusion (change of water vapor mass concentration due to the diffusion from outside) and the last term is the mass sink term or the reaction rate, accounting for the hydration of TCM. It is also worth to mention that this equation includes the process of transfer of water vapor or diffusion within the porous bulk, not within the particles of TCM itself. The latter is derived experimentally when obtaining the reaction kinetics of the TCM.

Equation 13 states that the change in the mass concentration of the hydrated/dehydrated porous bed equals to mass concentration of the dehydrated porous bed being hydrated owing to the reaction.

3.7. Diffusion

Diffusion is an omnipresent natural phenomenon. Basically, there are two distinct approaches to model diffusion, one focusing on dynamics of an individual particle while other focusing on the collective motion of many particles. [43] Going through the studies which had obtained the formulations for diffusion coefficient, the so-called "Stokes-Einstein" relation (equation 14) can be used. This equation does not depend on the particle mass and the only particle property included is the particle diameter (d_p) [43]:

$$D_v = \frac{k_B \cdot T}{6\pi\mu(\frac{d_p}{2})} \qquad (14)$$

Where:

- k_B is the Boltzmann constant (=1.38064852)
- μ is the dynamic viscosity of the water vapor in Pa.s
- d_p is the diameter of TCM particles in m

Due to the forced flow, it is expected that the effect of the diffusivity becomes negligible.

3.8. Porosity

This is one of the most fundamental parameters in porous media. A porous media is a solid matrix which is partially filled with interconnected pores (void) that can convey fluid under applied pressure gradient [44].

Porosity of a porous medium (equation 15) is defined as the void volume (in m^3) divided by the total bulk volume of the medium (in m^3). The effective porosity, which can be more practical (equation 16), can be defined as the fraction of the interconnected pore volume to the bulk volume of the porous body [44]:

$$\varepsilon_a = \frac{V_{pore}}{V_{bulk}} \qquad (15)$$

$$\varepsilon_{eff} = \frac{V_{int.pore}}{V_{bulk}} \qquad (16)$$

In this study, the porosity, which will be given a constant value and undergo parameter analysis to find a suitable value, is denoted by ε.

3.9. Permeability

Permeability is another fundamental parameter in the porous media which correlates to the porosity. Higher porosity which means higher void fractions, leads to higher permeability but lower thermal conductivity of the bed. Permeability is a description of the shape and orientation of the pores.

Establishing a suitable permeability model is an important step as there are several equations for this depending on the flow through the porous media to be darcian or non-darcian. Distinguishing whether the flow is darcian can be concluded through the Reynolds Number. Therefore, before selecting the permeability equation, Reynolds number and Darcy law should be discussed.

3.10. Flow Model

Determination of the type of the flow in every heat and mass transfer model is a crucial step as it can determines the governing equation to be used for different flow types. One common non-dimensional number which is widely used in these cases is the Reynolds Number.

Reynolds Number, is the ratio of the inertial forces to viscous forces within a fluid which is subjected to relative internal movement due to different fluid velocities. The formulation of Reynolds Number can be written in different ways depending on the application where it is used. Reynolds Number for a porous media can be derived from equation 17 [45]:

$$Re = \frac{v_\varepsilon \sqrt{\kappa} \rho}{1750 \mu \varepsilon^{1.5}} \qquad (17)$$

Where:

- v_ε is the real flow velocity in cm/s (and is obtained from v/ε)
- κ is the permeability in μm^2
- ρ is the density of the water vapor in g/cm^3
- μ is the viscosity of the water vapor in mPa.s

In case Re<10, the flow is darcian, meaning that it follows Darcy's law, where the pressure gradient is a linear function of the flow velocity. The calculated Reynolds number based on equation 17 with porosity of 0.7 is 4.8 which means that the flow is darcian.

3.11. Darcy's Law

In a porous medium, the global transport of momentum by shear stresses in the fluid is often negligible, because the pore walls impede momentum transport to the fluid outside the individual pores. A detailed description, down to the resolution of every pore, is not practical in most applications. A homogenization of the porous and fluid media into a single medium is a common alternative approach. Darcy's law together with the continuity equation and equation of state for the pore fluid (or gas) provide a complete mathematical model suitable for a wide variety of applications involving porous media flows, for which the pressure gradient is the major driving force [46].

Darcy's law (equation 18) states that the velocity field is determined by the pressure gradient, the fluid viscosity, and the structure of the porous medium:

$$u = -\frac{\kappa}{\mu} \nabla p \qquad (18)$$

Where u is the Darcy's velocity or specific discharge vector in m/s. κ is the permeability of the porous medium in m^2 and can be defined either directly or by predefined permeability models.

Equation 18 is the linear Darcy's law as it shows a linear relation between the velocity field and the pressure. This equation is only valid for very low velocities or at low Reynolds Numbers (Re<10) [46][47].

If the flow is relatively fast (Re > 10), Darcy's linear relation between velocity and pressure drop is no longer valid. Therefore, different permeability models have been introduced to capture these effects. A quadratic drag must be added to the Darcy's law using Forchheimer's equation. A general form of the nonlinear relationship of pressure gradient to velocity can be written as equation 19:

$$-\nabla p = \frac{\mu}{\kappa} u + \beta \rho u|u| \qquad (19)$$

Where β is the inertial resistance coefficient ($-\beta = \frac{C_F}{\sqrt{\kappa}}$). Here C_F is called "Forchheimer parameter" and is derived by: $C_F = \frac{1.75}{\sqrt{150{\varepsilon_p}^3}}$.

Based on the textbooks, Flows with Re<10 are Darcian Flows and they can be described by the "Kozeny-Carman" equation, for the transitional regime, 10<Re<1000, flow can be better described by the non-Darcian "Ergun" equation, and for Re>1000, "Burke-Plummer" equation can be used for turbulent flows [46][47].

In this step, due to the low Reynolds Number that is estimated in the basic model, the Kozeny-Carman equation has been chosen to obtain the permeability (equation 20)[48].

$$\kappa = \frac{{d_p}^2}{180} \frac{{\varepsilon_p}^3}{(1-{\varepsilon_p}^2)} \qquad (20)$$

Where d_p is the average particle diameter and ε_p is the porosity.

Darcy's law interface in COMSOL combines the Darcy's law with the continuity equation (equation 21):

$$\frac{\partial}{\partial t}(\rho \varepsilon_p) + \nabla \cdot (\rho u) = Q_m \qquad (21)$$

Where Q_m is the mass source term (in kg/(m^3.s)). This mass source is similar to the mass sink term in the equation 12 in the model.

3.12. Energy Balance for the Heat transfer Fluid

Focusing on the HTF section of the model, the no slip condition for the walls has been assumed as already mentioned. From heat and mass transfer knowledge, it can be stated that near the wall between TCM and HTF, where the velocity is zero, heat transfer by conduction is dominant. However, the more distance the fluid gets from this wall, heat transfer by convection becomes more important. According to the Energy balance (equation 22), the heat accumulation in HTF section should be equal to the sum of the heat transfer by the two mentioned methods to the HTF:

$$Heat\ Accumulation = Heat\ Conduction + Heat\ Convection$$

$$C_{p,htf}\rho_{htf}\frac{\partial T}{\partial t} = \nabla \cdot \left(\lambda_{htf}\nabla T\right) - \rho_{htf}C_{p,htf}(u_{fd,htf} \cdot \nabla T) \qquad (22)$$

Where:

- $C_{p,htf}$ is the specific heat capacity of the HTF in J/(kg.K)
- P_{htf} is the density of the HTF in kg/m^3
- λ_{htf} is the thermal conductivity of the plate in W/(m.K)
- $u_{fd,htf}$ is the velocity field of the HTF in m/s

Note that in the basic model, no heat exchanger has been added to the geometry for simplicity of the initial studies, but in the final designs, the heat exchanger will be one crucial part of the reactor.

3.13. Flow Model for HTF – "Laminar Flow" Interface

Previous Fluids Dynamics studies state that a flow remains laminar as long as the Reynolds number is below a certain critical value. At higher Reynolds numbers, disturbances have a tendency to grow and cause transition to turbulence. This critical Reynolds number depends on the model, but a classical example is pipe flow, where the critical Reynolds number is known to be approximately 2000.

Reynolds Number for a flow in duct can be obtained by equations 23 and 24:

$$Re = \frac{VD_h}{\nu} \qquad (23)$$

$$D_h = \frac{4A}{P} \qquad (24)$$

Where:

ρ is the density of the fluid (in kg/m^3), V is the velocity (m/s), ν is the kinematic viscosity (in m^2/s), D_h is the hydraulic diameter in which A is the cross-section and the P is the wetted perimeter of the duct. For the basic model, a relatively low Reynolds number equal to 1320 was computed considering a velocity of 0.002 m/s, inlet height of 0.01m, length of 0.12 and an assumed inlet area of 0.02m, which clearly states that the flow is in laminar regime (the geometric numbers are for 2D basic model) Thus, Laminar Flow interface of the COMSOL was added to describe the HTF.

The Laminar Flow (spf) interface [49] is used to compute the velocity and pressure fields for the flow of a single-phase fluid in the laminar flow regime. A flow remains laminar as long as the Reynolds number is below a certain critical value. At higher Reynolds numbers, disturbances have a tendency to grow and cause transition to turbulence. This critical Reynolds number depends on the model, but a classical example is pipe flow, where the critical Reynolds number is known to be approximately 2000.

The physics interface supports incompressible flow, weakly compressible flow (the density depends on temperature but not on pressure), and compressible flow at low Mach numbers (typically less than 0.3). It also supports flow of non-Newtonian fluids. For this study, the flow has been assumed to be incompressible flow.

The equations solved by the Laminar Flow interface are the Navier–Stokes equations for conservation of momentum and the continuity equation for conservation of mass(equation 25 and 26):

$$\rho \frac{\partial u}{\partial t} + \rho(u \cdot \nabla)u = \nabla \cdot [-pI + K] + F \qquad (25)$$

$$\rho \nabla \cdot u = 0 \qquad (26)$$

Equations 25 and 26 are actually formulation of Navier-Stokes equations for incompressible flow and so the density is a constant value. K demonstrates the viscous stress tensor (in Pa) and F is the volume force vector (in N/m^3) [49].

3.14. TCM Mass and Energy Density

TCM Mass is the amount of TCM that can be stored in a porous bed and it can be derived by equation 27:

$$TCM\ Mass = \rho_s \cdot V \cdot (1 - \varepsilon) \qquad (27)$$

Where:

- ρ_s is the density of the TCM in kg/m^3
- V is the bed volume in m^3
- ε is the porosity

Energy Density is the amount of energy that can be stored in a given system, substance or piece of space [50]. It can be calculated in volumetric or gravimetric terms. However, Volumetric is more common and in the porous media, it can be calculated as equation 28:

$$Energy\ Density = \frac{TCM\ Mass \cdot Hr}{Total\ Volume} \qquad (28)$$

Where:

- Hr is the heat of reaction in kJ/kg

3.15. Meshing

Base of every Computational Fluids Dynamics (CFD) computation software is the meshing. In COMSOL Multiphysics, after designing the geometry of the model, setting up the equations in the related modules and defining all the parameters and variables, the meshing node is added to configured before moving to the computation.

There are different kinds of meshing methods for every 2D and 3D surface. Meshes can be either structured or non-structured [51]. The interior mesh vertices in a structured mesh are adjacent to the same number of elements. Figure 19 shows two different structured meshes, the left one is “mapped mesh” with quadrilateral elements, and the right one is a structured triangular mesh.

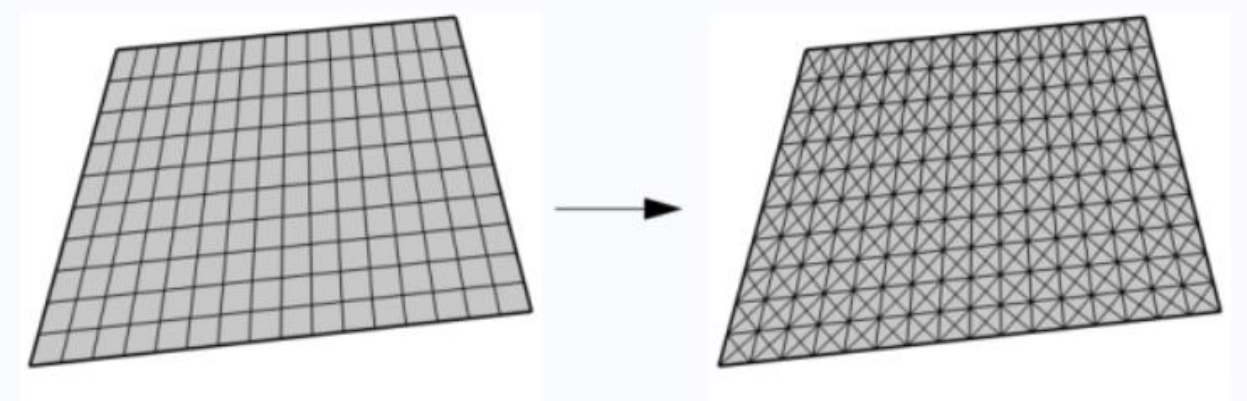

Fig 19. A structured Mapped Mesh (left) and a structured triangular mesh (right)

On the other hand, unstructured mesh can be defined for all types of geometries, regardless of space dimensions, topology or shape. When the tetrahedral, triangle, or quad mesh are used, the number of mesh elements is determined by the shape of the geometry and various mesh parameters.

There are nine predefined sizes to choose in COMSOL, ranging from Extremely fine to Extremely coarse [51]. The sizes of the generated mesh elements are determined by absolute mesh size parameters that can be viewed and edited for a user-controlled mesh. The meshing could be done either with these predefined element size or with custom element size. In a custom mode, five controlling parameters, which determine the mesh characteristics, can be set manually by the designers. These five are as below:

- **Maximum element size**: This parameter is used to limit the allowed element size. By using a parametric sweep to vary the maximum element size, model can be solved using meshes with different mesh density to study how it affects the solution.
- **Minimum element size**: This parameter is used to specify the minimum allowed element size. For example, it can prevent the generation of many elements around small curved parts of the geometry.
- **Maximum element growth rate**: This parameter is used to determine the maximum rate at which the element size can grow from a region with small elements to a region with larger elements. For example, with a maximum element growth rate of 1.5, the element size can grow by at most 50% (approximately) from one element to another. The value must be greater or equal to one.

- **Curvature factor**. This parameter is used to determine the size of boundary elements compared to the curvature of the geometric boundary (that is, the ratio between the boundary element size and the curvature radius). The curvature radius multiplied by the *curvature factor*, which must be a positive scalar, gives the maximum allowed element size along the boundary. A smaller curvature factor gives a finer mesh along curved boundaries.
- **Resolution of narrow regions**: This parameter is used to control the number of layers of elements that are created in narrow regions (approximately). The value must be a nonnegative scalar. A higher value gives a finer mesh in narrow regions.

For the basic 2D Model used in the initial parameter studies, “Free triangular” meshes were selected for the whole domains as figure 20 and element size was set to a “Extra Fine” accuracy. There is not a single way to discuss about the quality of Mesh but a parameter sweep can be done. The main result of this model is the outlet temperature of the heat transfer fluid. So, a comparison of this results using different sizes was performed in figure 21.

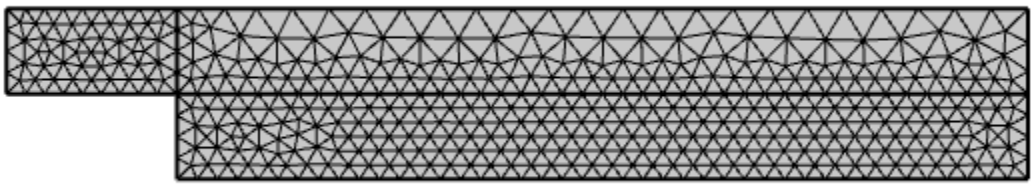

Fig 20. The “Free Triangular” unstructured mesh used for the basic model

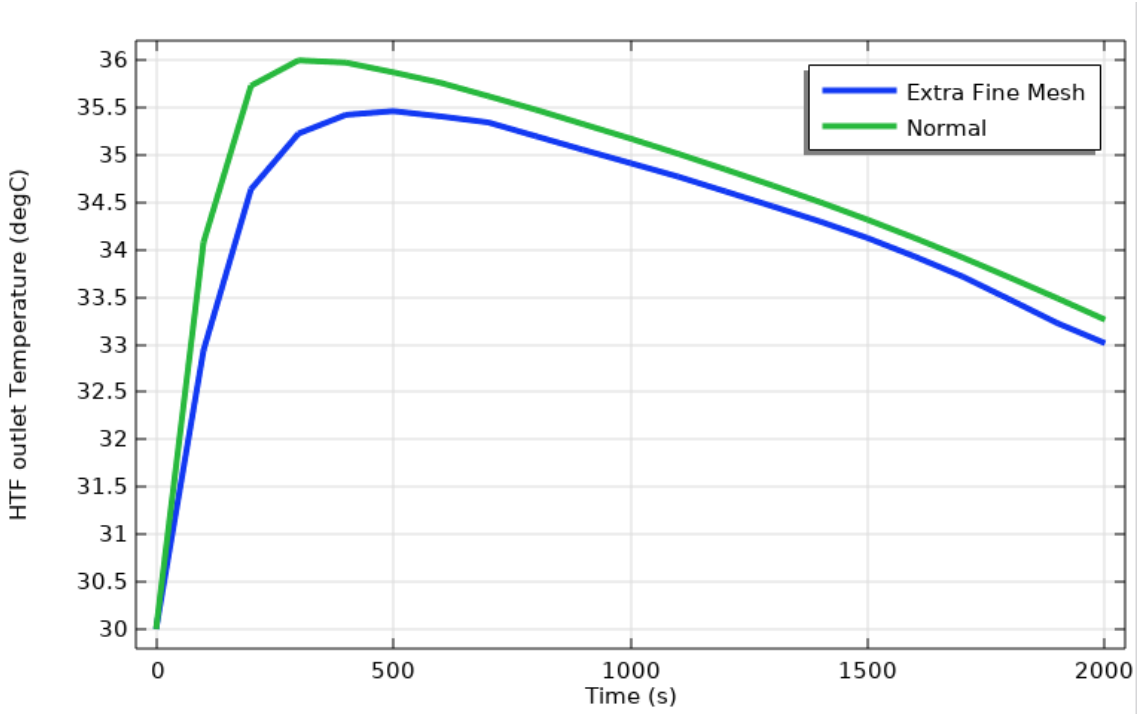

Fig 21. Sensitivity Analysis of the model to Normal and Extra Fine Meshes

Figure 21 shows the sensitivity analysis being made to show the effect of Meshing (Mesh Independency Test). “Extra Fine” Mesh has smaller element sizes and smaller curvature factor compared to a normal mesh in general, leading to more nodes to compute in the geometry. So, it is expected that the outlet temperature of heat transfer fluid in this basic model resulting from ‘Extra Fine” mesh should be more accurate and therefore mesh settings have been set to “Extra Fine” as a conclusion.

3.16. Modules

COMSOL Multiphysics®, as its name suggests, comprises different kinds of modules which are used to study different physical phenomena. While discussing the numerical theories of the model in this chapter, some of the used modules for this study have been mentioned, but it may be also better to sum them up in this section.

1. “The heat transfer in porous media (ht)” has been added and used to describe heat transfer by convection and conduction in porous media. The solid-gas porous media in the reactor bed can be totally described by this module.

2. “Darcy Law (dl)” has been added and used to simulate fluid flow through interstices in a porous medium. Darcy law equations have been explained in this chapter. Velocity and pressure of the vapor in this study are calculated by darcy law.
3. “Laminar flow (spf)” has been added and used to describe the velocity and pressure fields for the flow of a single-phase fluid in a laminar regime, which is the heat transfer fluid domain in this study.
4. “Domain ODEs and DAEs (dode)” has been added and used to solve distributed ODEs and DAE in domains, on boundaries and edges, and at points. In this study, equation 3 has been defined as a source term to be solved and values of α to be obtained. The initial α value for the equation has been set to 0.1.

3.17. Solver

Last step before moving to the computation and postprocessing, is setting up the correct solver. For this study, a “Time-Dependent” solver will be used. Time-Dependent Solver is used for computing the solution over time. This study type is also used for optimization problems that are constrained with a time-dependent PDE. Study steps and the time range can be set in this section. For the base model, the usual range that has been used to plot the required results is $0<t<2000$s. This range has been selected since in first simulation experiences, the peak value for HTF outlet temperature and the complete conversion of material were both in this time range and the longer time is avoided for quick computations by the software.

Chapter 4

Sensitivity Analysis

4.1. Goal

In Chapter 3, a basic 2D model was designed in COMSOL Multiphysics®, aiming to help the designer understand the physics and theories of a thermochemical heat storage reactor based on the process of hydration/dehydration of K_2CO_3.

To have a better understanding of the main controlling parameters in this model, a sensitivity analysis study was done, aiming to know which parameters can be more controlling and deciding on the results of this application, especially the main result which is the HTF outlet temperature, and to get a nice approach on the improvement of the final model in the future.

One benefit of this approach for the final model will be saving of time, as doing sensitivity studies and making computations for the final 3D model will take much longer than the basic 2D one in COMSOL Multiphysics®.

4.2. Approach

First, some constant parameters of the study will be indicated with their corresponding values. Second, some parameters which have been expected to have a noticeable effect on the HTF outlet temperature theoretically, will be investigated in a parametric study and their effects will be experimented by COMSOL and verified. Note that in all the studies, hydration reaction will be analyzed.

4.3. Constant Parameters

There are some constant parameters in the equations of the model which should be defined. The values related to the kinetics parameters in this section are for the hydration reaction. The pre-exponential factor and the activation energy values have

been obtained from a recent study in University of Twente [40]. The main constant parameters of the model have been mentioned in Table 8:

Table 8. Constant Parameters of the model

A_f :Pre-exponential Factor (1/s)	2.7E-9
E_a: Activation Energy (J/mol)	-34828
Hr: Heat of Reaction (kJ/mol)	-91.32
D_p: particle diameter (mm)	1
$C_{p,K2CO3}$: K_2CO_3 Specific Heat Capacity (J/(g.K)	0.86527
ρ_{K2CO3}: K_2CO_3 density (kg/m^3)	2290
K_{K2CO3}: K_2CO_3 Thermal Conductivity (W/m.K)	0.8
Mm_{K2CO3}: Molar Mass of K_2CO_3 (g/mol)	138
C_p,wv: Water vapor Specific Heat Capacity (J/(g.K)	1.878
ρ_{wv}: Water Vapor density (kg/m^3)	0.0094
K_{wv}: Water Vapor Thermal Conductivity (W/m.K)	0.02
Mm_{wv}: Molar Mass of Water Vapor (g/mol)	18

4.4. Sensitivity Analysis

In CFD, for the improvement of a system and have a nice overview of its effect, one can change a single variable while keeping others constant and plot an output result to see the variations and evaluate the behavior of the system.

In the current model, the main goal has been increasing the HTF outlet temperature, so the main focus should be the effect of the controlling parameters on the variation of the HTF outlet temperature. However, the parameter α which shows the status of conversion, has also been chosen as an indicator to be analyzed in case of variation over time, as it shows the speed of the reaction. Variation of this extra indicator together with the HTF outlet temperature can give a better conclusion for the sensitivity analysis. Note that no economical calculations will be made in this study as it is beyond the planned scope of this phase of research. However, some comments will be made about cost aspects which can be used for the researchers in the economical phase.

Design variables can be divided into geometry variables like the bed length and thicknesses of TCM and HTF layers, and operation variables like Porosity, HTF mass flow rate and the evaporator pressure.

First, based on the knowledge about the physics and equations, several parameters have been chosen as the ones which are expected to affect the performance of the model and results significantly. Second, the sensitivity analysis has been done and conclusions have been made where necessary in this section.

4.4.1. Bed Length

Having the basic model in mind, one possible improvement is to increase the bed length, meaning that both TCM Bed and HTF layer in this model can be extended in length. It has been expected that this change should increase the HTF outlet temperature, as it increases the heat transfer surface between TCM and HTF. Figure 22 demonstrates this sensitivity analysis.

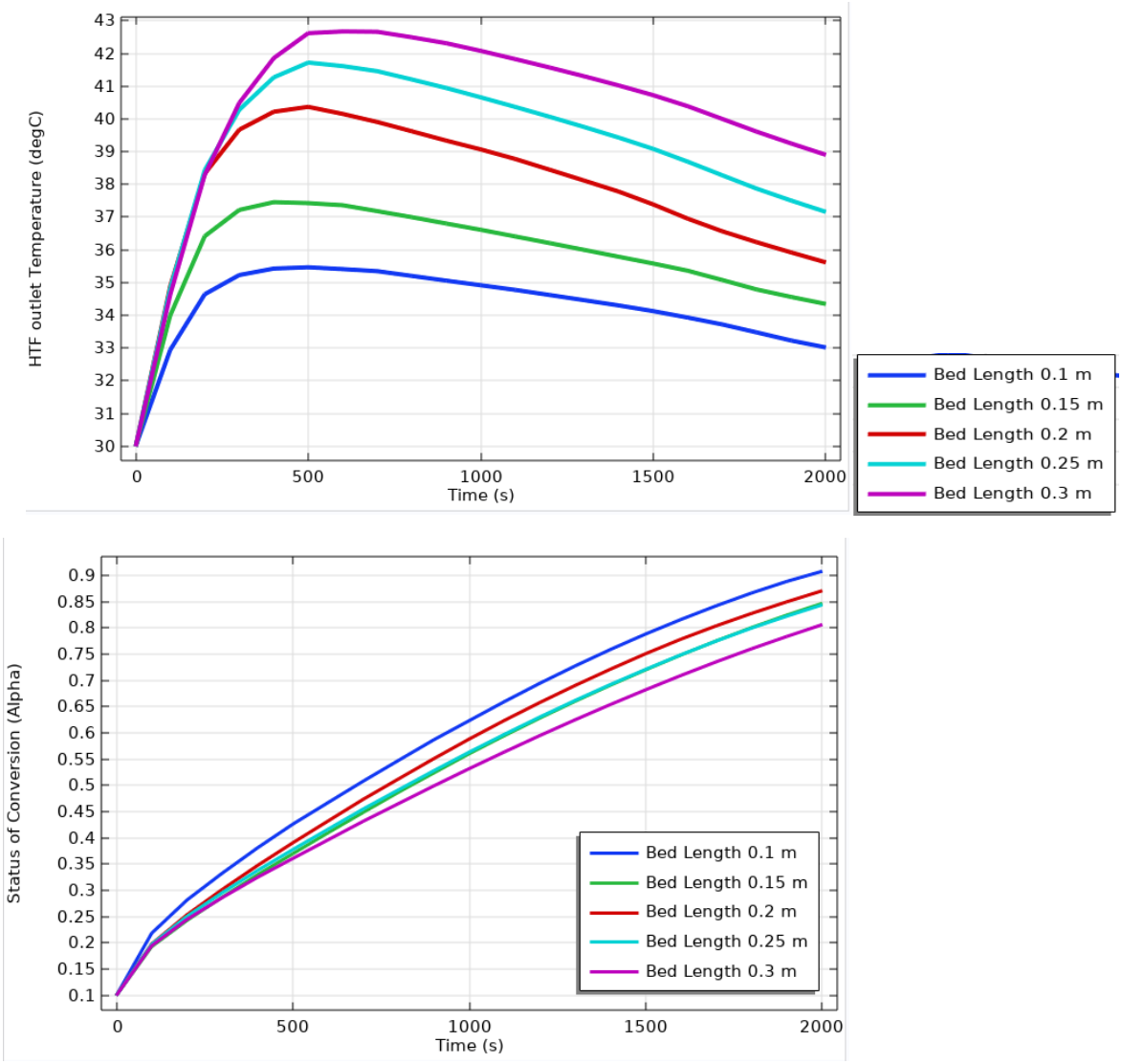

Fig22. Plots for “Bed Length” parameter analysis

According to the plots in Figure 22, it has been observed that constructing a longer reactor bed can increase the HTF outlet temperature, because there is more heat exchange surface. But on the other hand, the longer the bed, the lower the status of conversion and slower reaction. This also looks reasonable, as in the longer bed, there is more TCM material which should be converted. From this observation, it can be concluded that in also in the final design, reactor bed length can be a good improvement target, but it should not be increased very much, as the longer reactor will be also more costly and fail in economic analysis.

4.4.2. TCM Layer thickness

Another geometric option that was expected to have the possible influence (figure 23), is the thickness of the TCM layer. In this part, only the thickness of the TCM layer has been changed, without any change in HTF layer geometry.

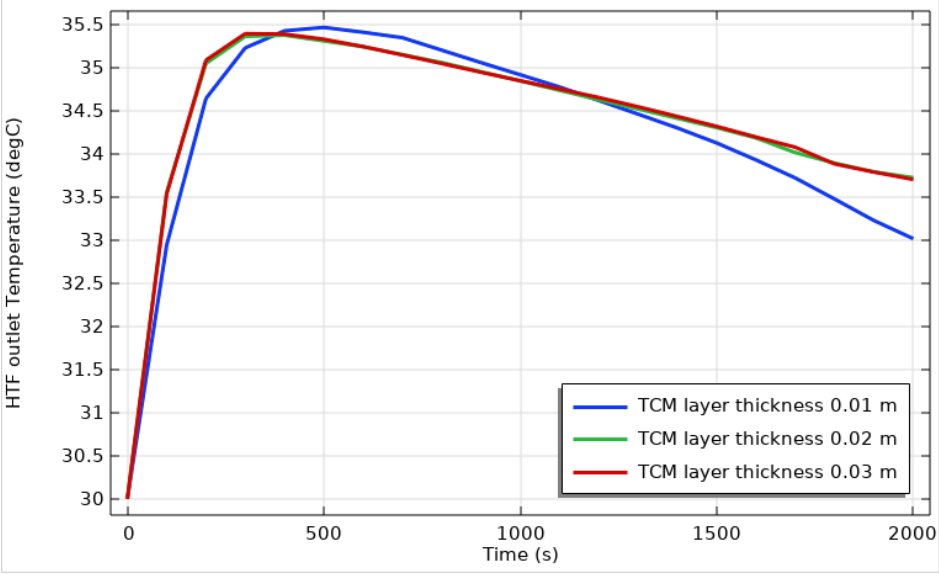

Fig 23. The HTF outlet temperature plot for “TCM layer thickness” parameter study

It was clearly observed that increasing only the TCM layer thickness is not a good option. In Figure 22, the plots for 0.02m and 0.03m were relatively similar and by

checking for higher thicknesses, the results were also the same. This can be justified by plotting the status of conversion in figure 24, showing that the reaction speed is becoming lower as TCM layer thickness grows, simply because there is more TCM material with the same amount of heat transfer fluid and heat transfer will not be efficient and the system will not have a good energy density.

However, figure 23 also shows that for thicker TCM layer, temperature reaches to the peak earlier and also it remains at descends more slowly than the thinner TCM. So, it can be concluded that in the final design, TCM layer can be produced relatively wide but the trade-off between this layer and the HTF layer should be taken into account to have a system with a suitable energy density.

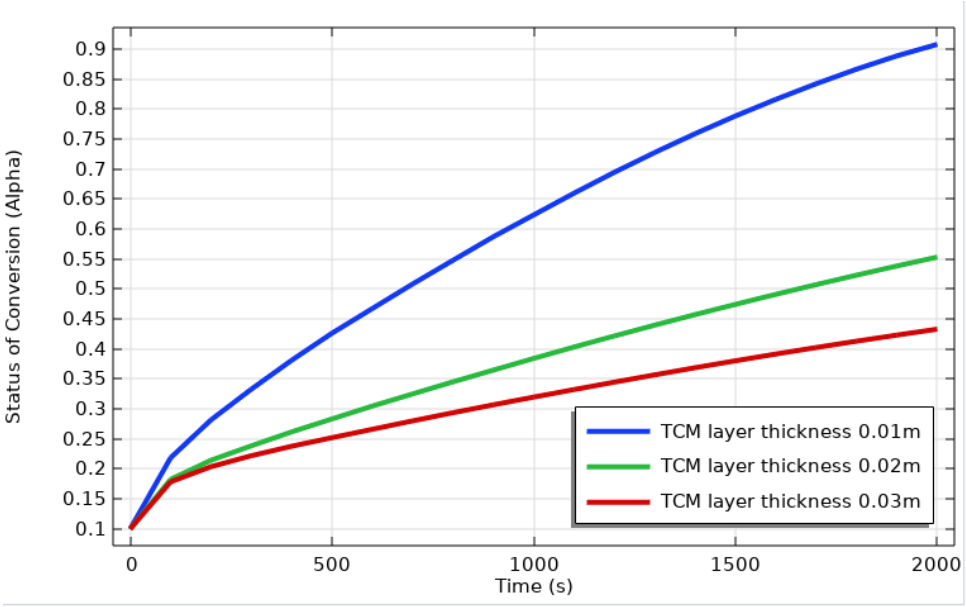

Fig 24. Status of Conversion trends for different TCM layer thickness

4.4.3. HTF layer thickness

Last geometric parameter which has been decided to be investigated is the HTF layer thickness. For the base model, it was expected that decreasing this layer can increase HTF outlet temperature. Because, assuming a constant mass flow rate for the HTF, when HTF width is decreased, the cross-sectional area is decreased, leading to higher HTF velocity. As a result, the fluid has less time to have contact with the hot bed and the temperature decrease of outlet is lower, keeping it in a higher value. Plots in

Figure 25 along with other comments give a better understanding of this improvement.

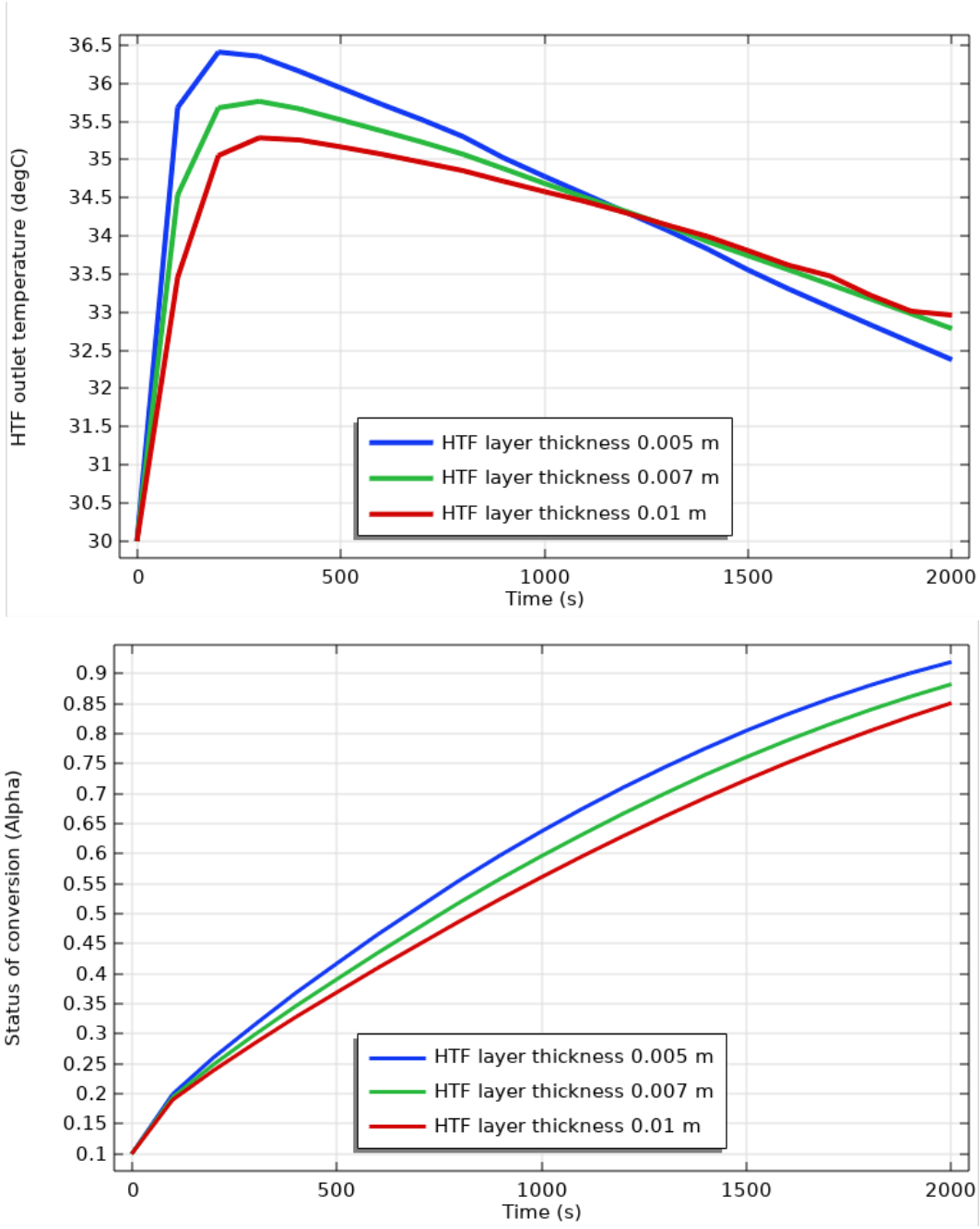

Fig 25. Plots for "HTF layer thickness" parameter study

Looking at the plots, thinner HTF layer has faster conversion and higher outlet peak temperature due to the mentioned reason. But again, this has to be taken into account here, TCM layer thickness remains constant and temperature plot of the thinner HTF layer descends faster. Therefore, also here it is concluded that this geometric parameter can be a good improvement target for the final design but the change of HTF layer and TCM layer thicknesses should be considered in a trade-off way so that the energy density of an improved reactor becomes higher than a base design.

4.4.4. Porosity

Porosity is one of the most important parameters to be defined in the porous media. Theoretically, lower porosity means lower permeability in the porous media which leads to restrictions in the moving of the flow in the bed. As a result, it is expected that lower porosity should impede the reaction rate, increase the inside pressure and decrease the status of conversion but increase the HTF outlet temperature due to less material to heat up the heat transfer fluid.

Figures 26 and 27 show the sensitivity analyzes on porosity. Note that porosity of 0.7, for instance, means there is 70% vapor and 30% solid.

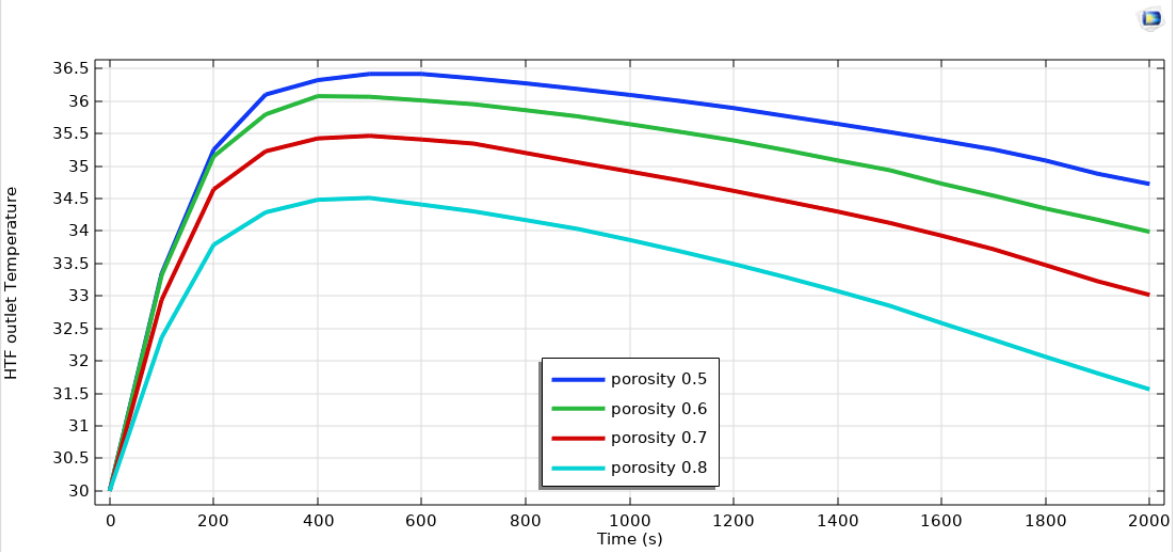

Fig 26. HTF outlet temperature variation in different porosities

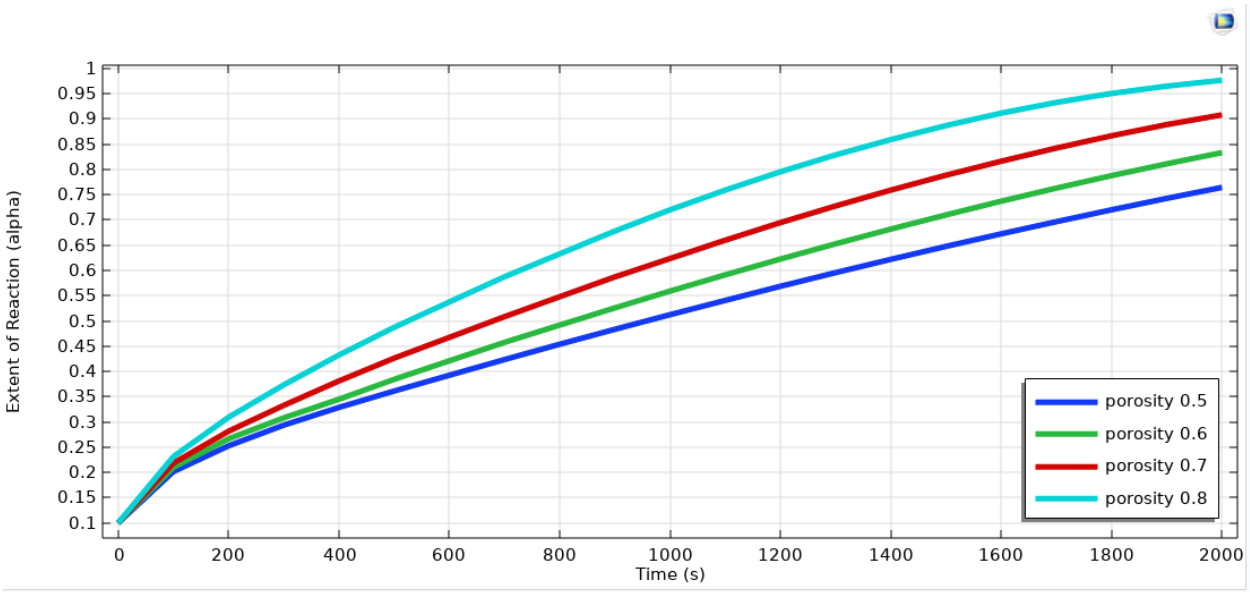

Fig 27. Status of Conversion variations in different porosities

From the figures 26 and 27, it can be concluded that a value like 0.7 for the porosity is a reasonable choice in this case. Later, on the final designs, it was also considered that 0.7 can be chosen as a reasonable value for porosity not only to have a good status of conversion but also to have a suitable HTF outlet temperature. Note that 0.8 is not an appropriate option for a porous bed, as there is not enough material to heat up the heat transfer fluid (there is only 20% solid).

4.4.5. Evaporator Pressure

Previously, it has been discussed that in a closed system reactor, there is an evaporator mounted in the configuration. The water evaporates there and water vapor enters the bed. It has been expected that a higher evaporator pressure can be a good improvement target, since pressure difference inside the reactor increases, which is actually the reaction potential of the system, leading to the increase of the status of conversion. On the other hand, more reaction in the same reactor can lead to higher temperatures for HTF. To Verify this, corresponding plots have been processed as figure 28:

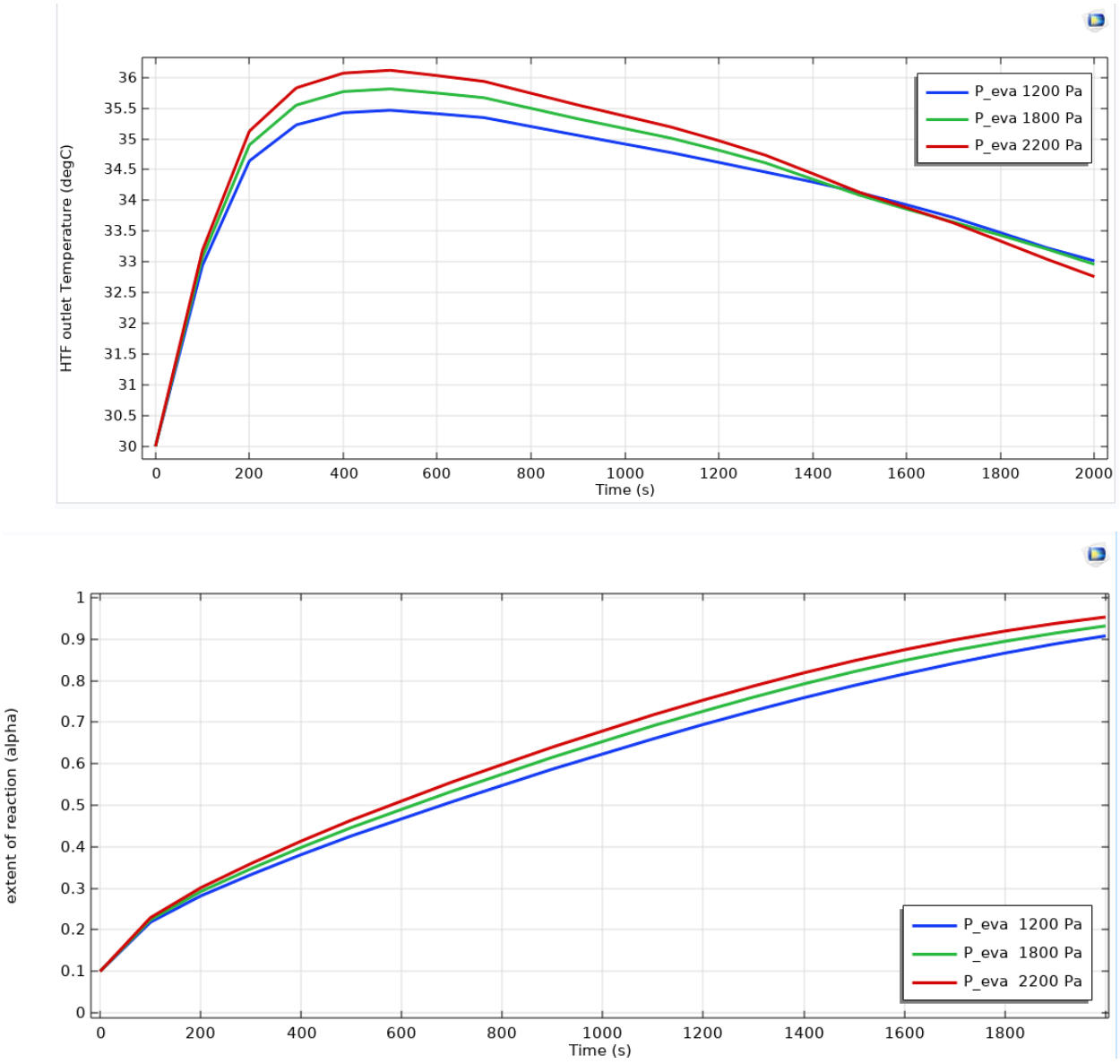

Fig 28. Plots for the "evaporator pressure" parameter analysis

The above plots have completely met expectations. It is concluded that evaporator pressure is also another controlling parameter of the reactor design.

4.4.6. Inlet Mass Flow Rate

In this study, the boundary condition of constant mass flow rate has been chosen for the heat transfer fluid. Theoretically, it is expected that as mass flow rate corresponds to density, velocity and the area of the HTF (also the equation mass flow rate = density × Velocity × Area, also suggests), increasing this parameter, while density and area are constant, should increase the velocity. Fluid with higher velocity has a lower heat exchange time, thus having lower temperature which is not desirable. Figure 29 shows the sensitivity analysis on mass flow rate.

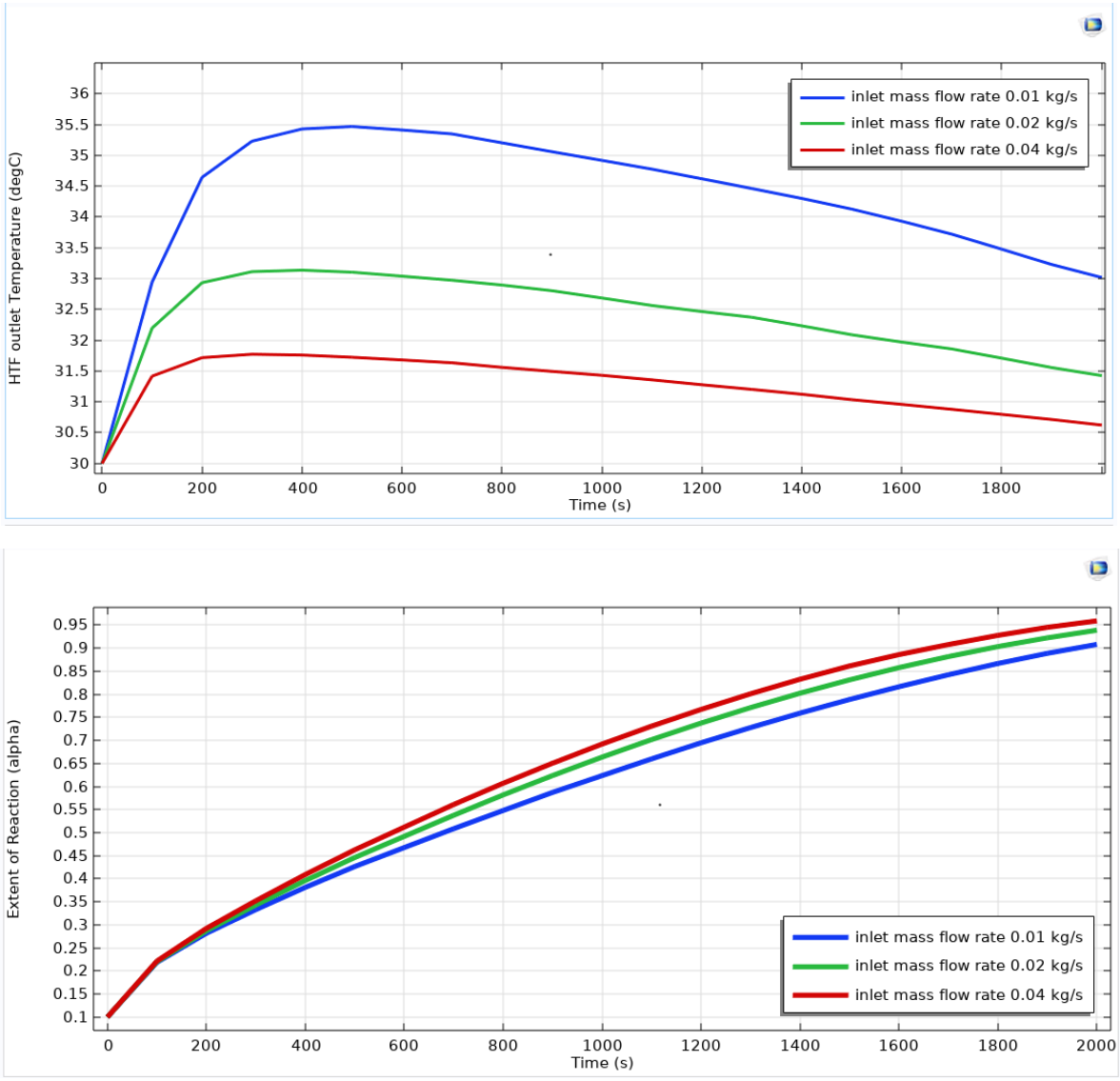

Fig 29. Plots for "inlet mass flow rate" parameter analysis

According to the above plots, it can be concluded that a smaller mass flow rate (in this case 0.01 kg/s) is better, as it has clearly higher HTF outlet temperature and still an acceptable status of conversion. The better status of conversion for the higher values of mass flow rate could probably be justified by more amount of HTF mass in time unit, thus higher heat transfer and higher reaction speed.

4.5. Summary

A sensitivity analysis was done for the basic 2D model which has been introduced in the previous chapter. Study was done on two groups of parameters, some of them were geometric and some others related to the operations of the reactor. Theoretical expectations were compared with the results in the software and the plots to find out some design parameters for the reactor. Indicator plots included the HTF outlet temperature together with the status of the conversion, and they were all explained.

These analyzes can give a good overview for the design and improvement of a final reactor in the next chapter, also because doing sensitivity analysis for a 3D model will be more time-consuming.

Chapter 5

Final Designs Proposals

5.1. Introduction

The basic 2D Model which has been introduced in the previous chapter, helped the designer to have a better knowledge of the application and the sensitivity analysis determined some main design parameters of the reactor.

In this chapter, based on the information and experience obtained both from theory and the basic model, a concept design of a 3D closed system fixed bed reactor model will be designed, some important results will be generated and remarkable comments will be made in order to see the capabilities of such designs for the desired application and also make inspirations for the future researchers who will try to work and develop their proposed models to satisfy the required demand.

During the design phase, two different models have been designed and an improvement process has also been performed for each of them. These two configurations will be introduced in details and their performance results will be proposed in this chapter.

5.2. Ideas

Prior to the design of the reactor, several related articles were studied in which different reactors with different type of heat exchanger were used. First idea was using a fin-plate heat exchanger inspired by a study from Fopah-Lele et al [26].

The Figure 30 shows the fin-plate heat exchanger idea for their similar application. Large heat transfer, Ability to withstand high pressures and light weight were the main advantages of this type whereas difficulty to clean the narrow pathways and the possibility of clogging were some of the disadvantages.

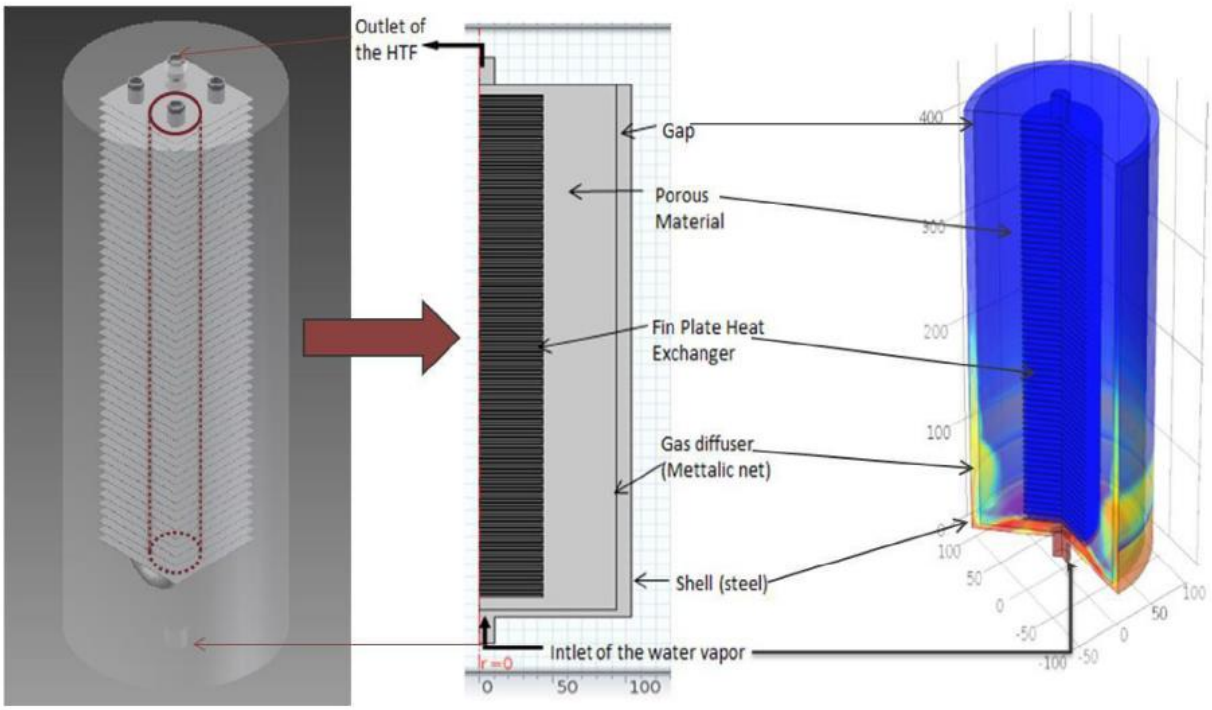

Fig 30. Finned-plate heat exchanger design by Fopah-Lele et al [26]

Second idea was to design a multi-tube heat exchanger which is type of shell and tube heat exchangers which had also been discovered in another study (figure 31) [27]. Shell and tube heat exchanger have been introduced more in the Chapter 2.

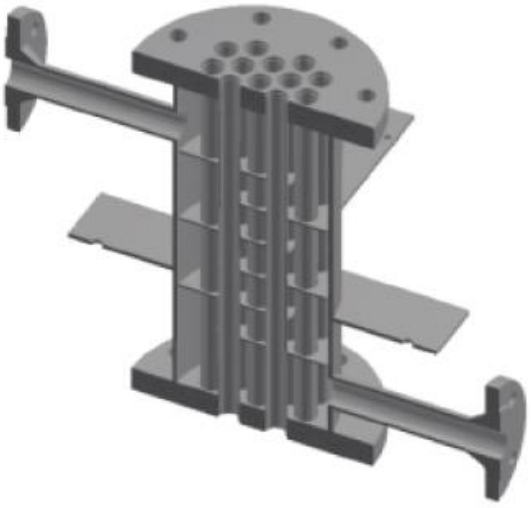

Fig 31. A Sample of a reactor with multi tube design [27]

The third idea after studying relevant studies (also from Fopah-Lele in another study [51]) was a reactor based on Spiral or Helical heat exchangers which have been also introduced in Chapter 2. Figure 32 shows their sample.

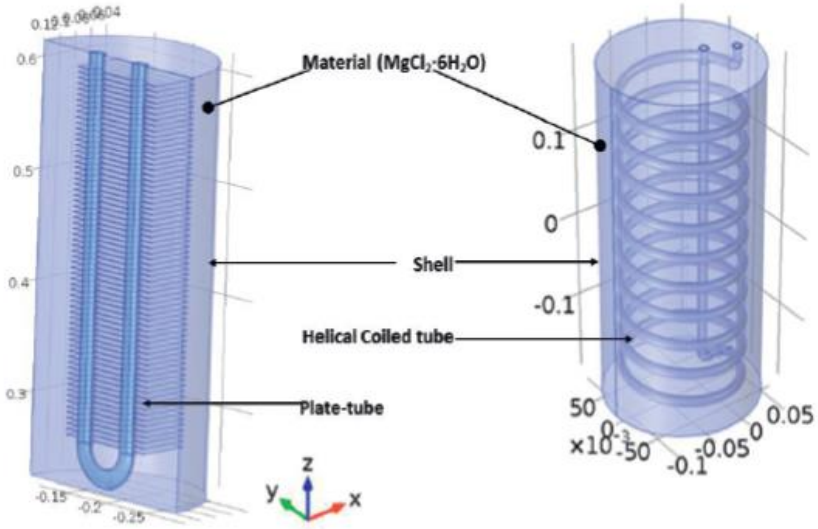

Fig 32. A sample of a reactor with helical heat exchanger [51]

The Final decision for the design phase after investigating the benefits, drawbacks and design complexity of the ideas has been to keep on with the multi-tube and helical heat exchangers, design and improve two different reactors based on them and make a final comparison and draw the results.

5.3. Multi-Tube Design – Concept

The first design has been a multi-tube or shell and tube configuration as figure 33. The working mechanism is such that the TCM particles have been defined inside the tubes and water vapor enters this TCM tubes from an inlet section. On the other hand, the liquid water as the heat transfer fluid enters the shell and moves with 90 degrees beside the tubes and through the shell, taking the heat of hydration reaction of the salt, increasing its temperature and flows to the HTF outlet inlet.

The schematic of the model design with the main boundary conditions and initial conditions which have form the base design, have been illustrated in the figure below:

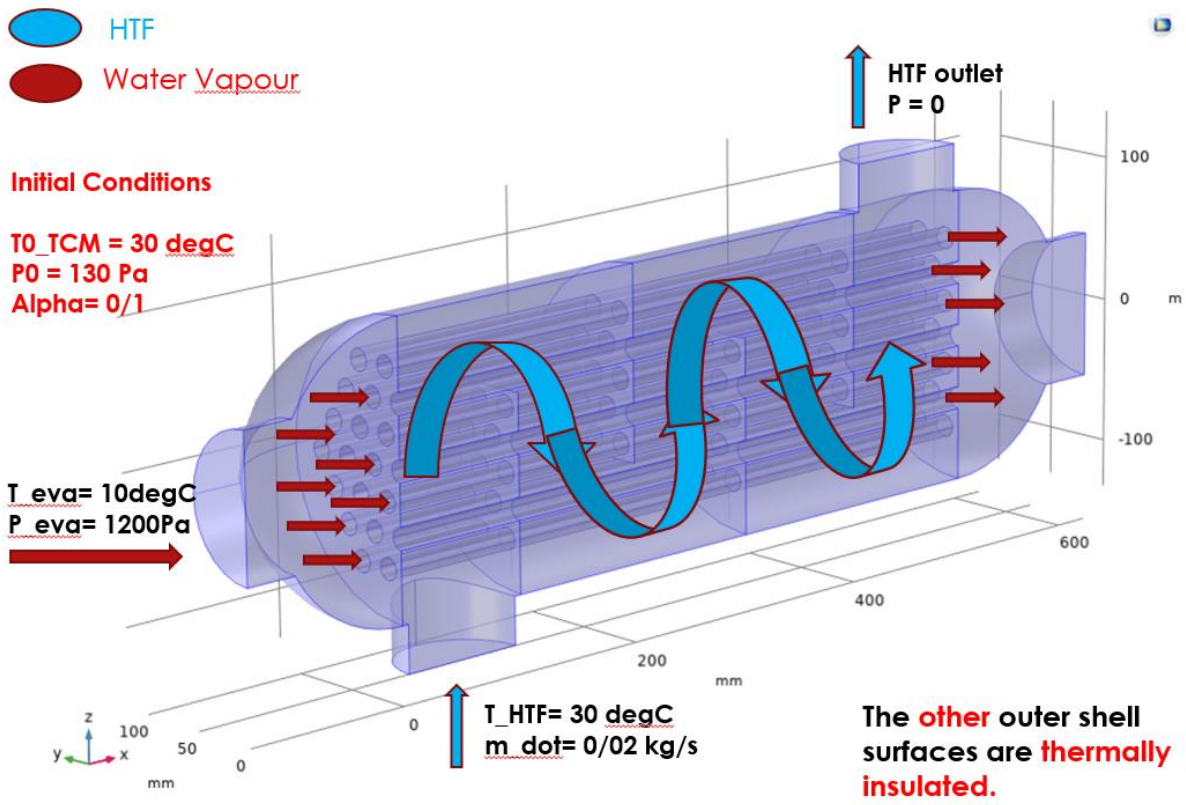

Fig 33. Schematic, B.C.s and I.C.s of the base shell and tube design

Generally, the values for the temperatures and pressures in boundary and initial conditions have been kept the same as the 2D Model. Reaction kinetics and all governing equations are completely the same as the base model and based on the numerical investigations in Chapter 4.

5.3.1. Temperature Surface Plots

To have a better visual understanding of how the heat transfer happens through the reactor and the temperature distribution, for each design, surface plots for some different times have been proposed using COMSOL. Usually, a zero-second plot has been generated to confirm the initial condition of the temperature for the bed and heat transfer fluid. The other plots include a time before the temperature of the heat transfer fluid reaches to the peak value and a time after the peak value. Figures 34 are the temperature surface plots for initial multi-tube design.

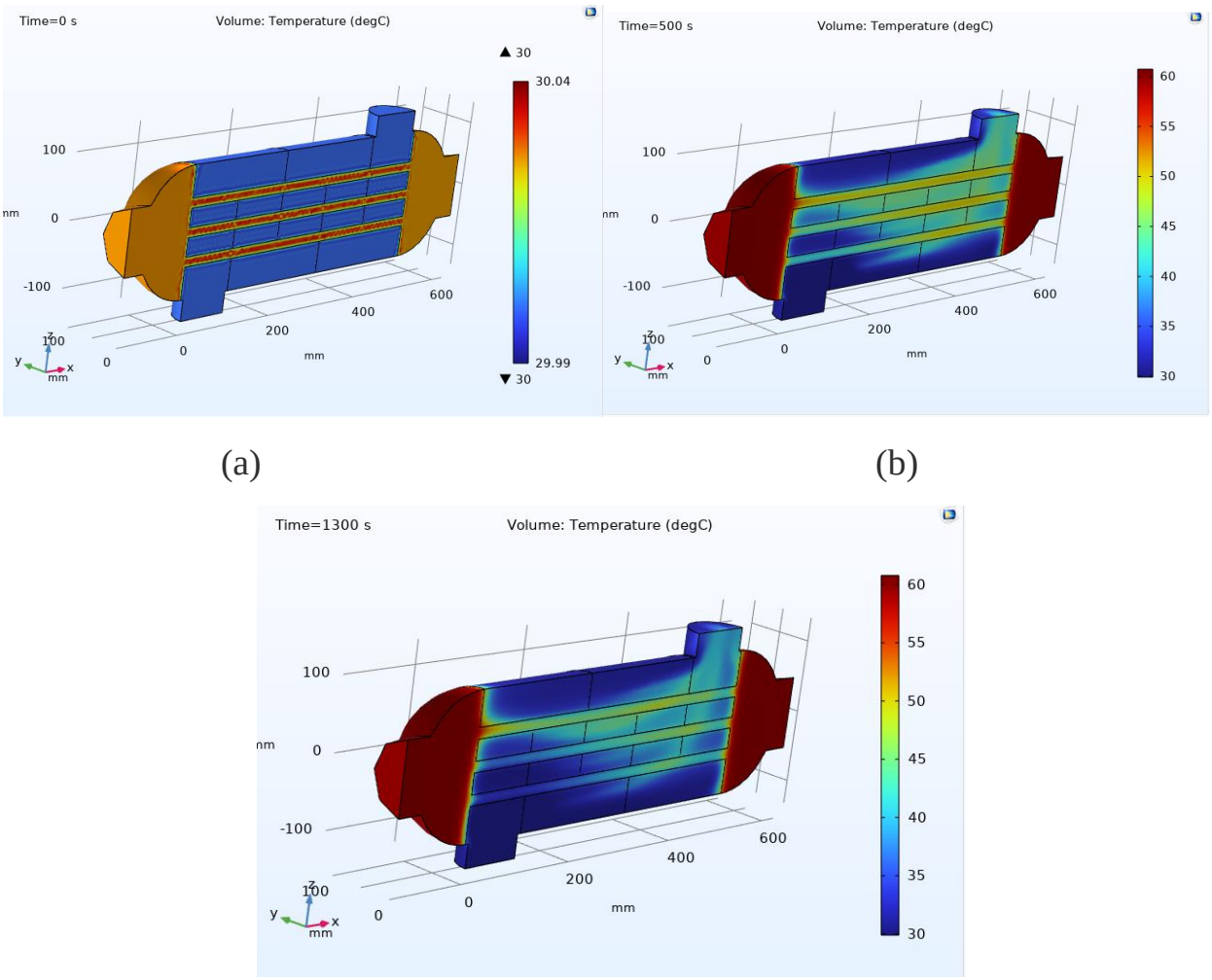

(a) (b)

(c)

Fig 34. Surface Temperature Plots for the initial multi-tube design

Fig 34a shows that in t=0s, the minimum and the maximum values of the whole geometry is 30 °C, which is the defined initial temperature for both bed and HTF in the model. As hydration reaction happens, the reactor bed heats up, reaching to a maximum of 60 °C in the two caps, which is evident in Fig 34b for t=500s. The heat is transferred to the HTF and heats it up too and after a certain peak (which will be shown by line graphs), temperature of the HTF drops as the whole TCM material in the tubes have been consumed and the status of conversion has approached to 1. Fig 34c at t=1300s is one of the after-peak moments.

5.3.2. Average HTF Outlet Temperature – Line Graph

The temperature surface plots in the previous section were used to show the temperature distribution in the whole reactor in different times. Also, the heat transfer fluid outlet temperature variation, which is one of the main results of this study, can be found out approximately by checking the corresponding colors in the outlet surface. However, those plots cannot give a more accurate value and the peak time. To this aim, line graphs (like figure 35) are used to demonstrate the average HTF outlet temperature.

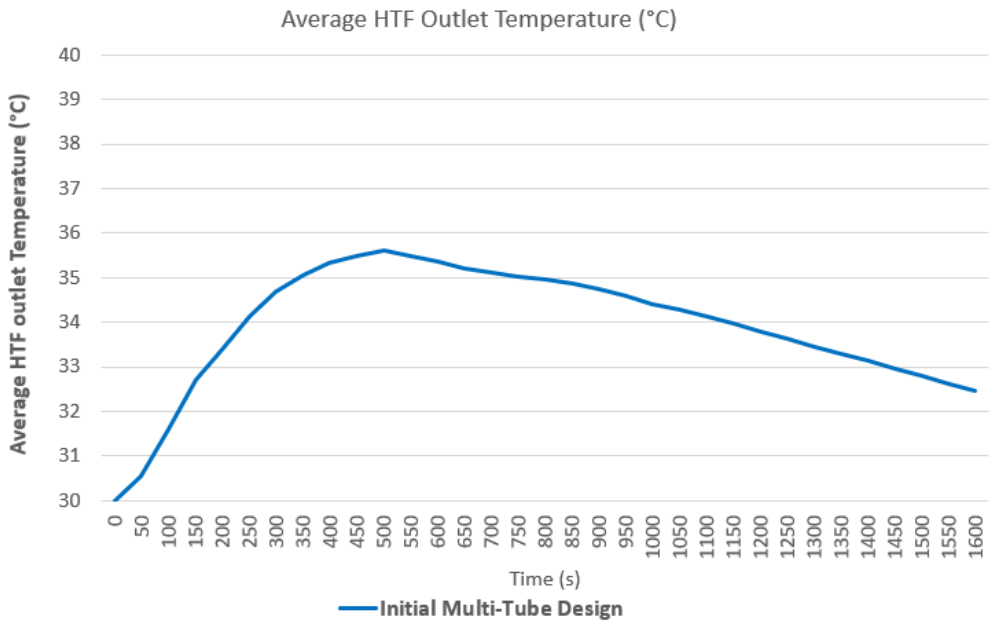

Fig 35. The Average HTF outlet Temperature for the initial multi-Tube design

Fig 35 shows that during this heat exchange process, the heat transfer fluid has reached to a maximum temperature of 35.5°C in t=500s It is clear that this temperature range is low for the required district heating applications (temperatures above 45°C are desired). So, there is the need to improve this reactor based on the knowledge from chapter 2 to get temperatures above 45 °C.

5.3.3. Status of Conversion – Surface Plots

To have a better visual overview of the process of TCM conversion and progress of the reaction, surface plots for the status of conversion (α), have also been generated (figure 36) with the same approach for some different times.

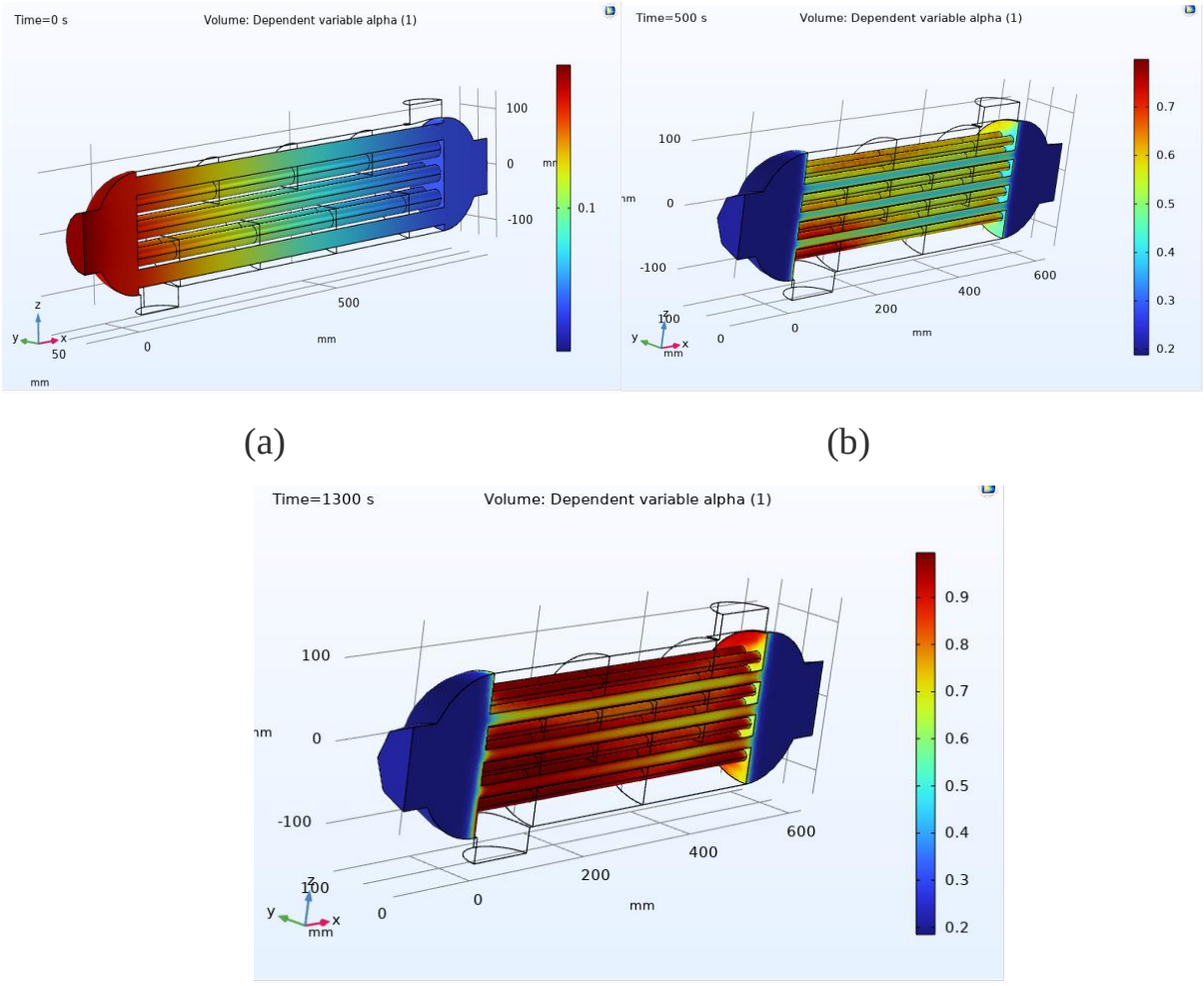

(a) (b)

(c)

Fig 36. Status of Conversion Surface Plots for the initial multi-tube design

Fig 36 clearly shows the α=0.1 at t=0s for the whole bed, which is actually the initial condition defined for the model. As the hydration reaction has progressed and more TCM Material has been converted, the status of conversion has reached to maximum values above 0.7 at t=500s in the tubes and above 0.9 at t=1300s. It has also been

observed that the TCM material which is in the two left and right caps of this design, has witnessed a lower conversion compared to the one in the tubes. The reason for this is simply because the tubes have more contact surface and thus heat exchange with the heat transfer fluid.

5.3.4. Average Status of Conversion – Line Graphs

Like the HTF outlet temperature, the average status of conversion for the reactor bed can also be plotted as a line graph in figure 37 to see the trend more clearly:

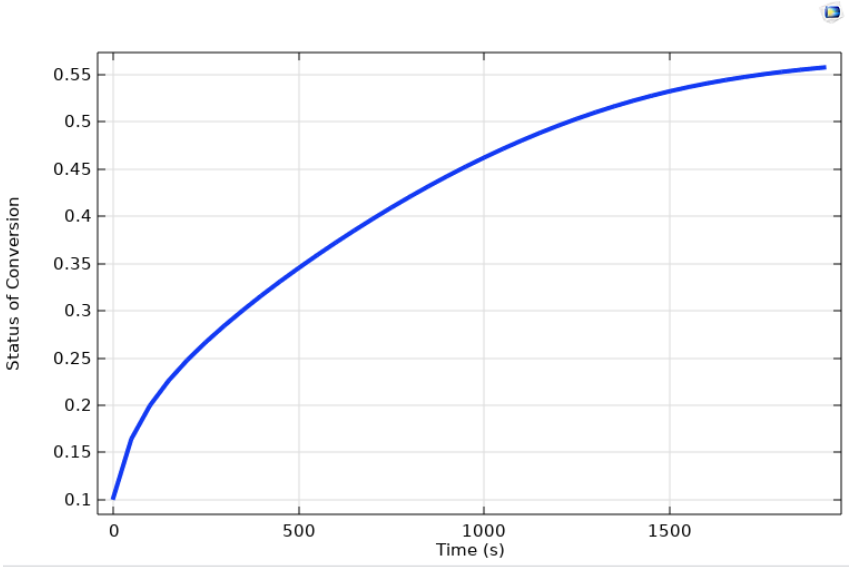

Fig 37. Average Status of Conversion for the reactor bed in initial multi-Tube design

Unlike the basic 2D Model, the average status of conversion may never approach to 1, and this is exactly due to two left and right caps in this design which have a lower heat exchange surface with the heat transfer fluid and thus have a lower status of conversion. Therefore, an important conclusion should be made.

It can be concluded that for this design, the average status of conversion line graph cannot be a good indicator to evaluate the performance of the reactor. The status of conversion should be monitored by the surface plots in the whole reactor. Finally, for better evaluation of this reactor setup, more focus should be on parameters like the average HTF outlet temperature, Energy Density and the hydration power.

5.3.5. Hydration Power

The Hydration Power plot for this setup is as figure 38:

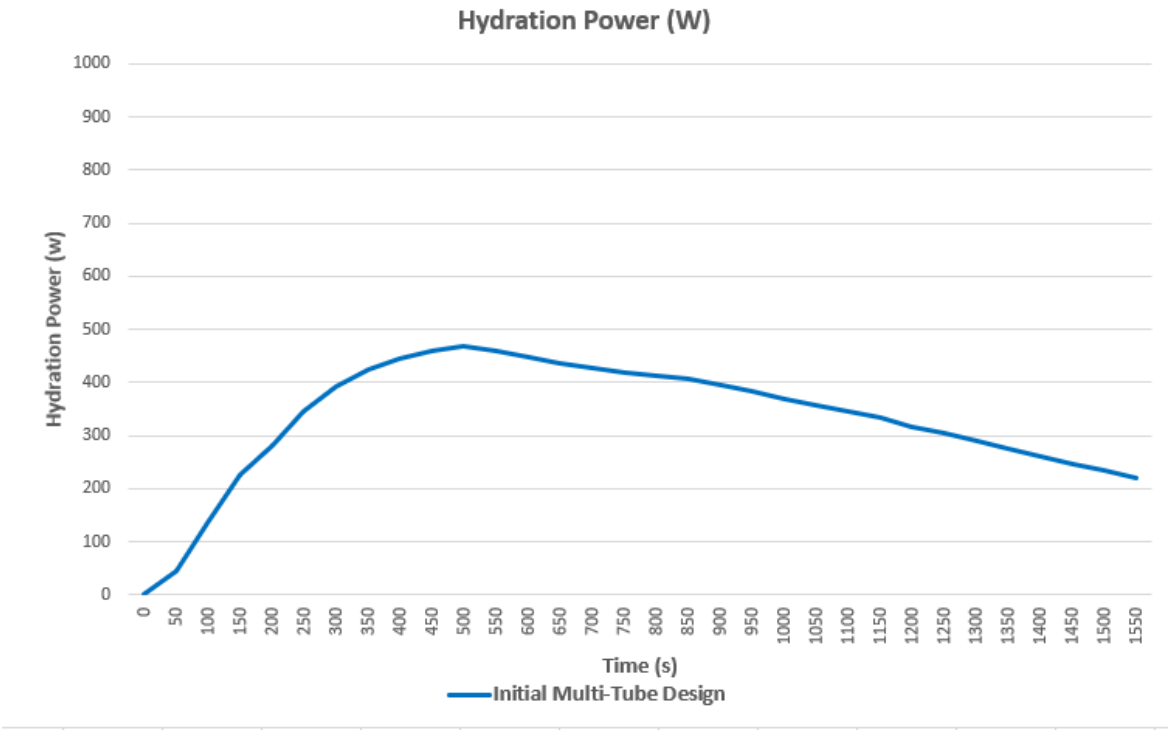

Fig 38. Hydration Power for the initial multi-Tube design

The Power diagram is compatible with HTF temperature diagram. The better the heat transfer and higher the HTF temperature, the higher the hydration power is.

5.3.6. Other Parameters

TCM Mass: Amount of TCM in kg which can be utilized in the reactor bed, depending on the bed volume, porosity and the density of the salt, derivable from the equation

Energy Density: Amount of TCM reaction energy that can be stored in one m^3 of the total reactor volume (in kJ/m^3), (equation ….).

Ideal Energy density: The maximum possible energy density, if the whole reactor volume contains TCM.

Table 9 shows these results for the initial multi-Tube design.

Table 9. Other results for the initial multi-Tube design

Total Reactor Volume (m^3)	0.01
Bed Volume (m^3)	0.0039
$\frac{Bed\ Volume}{Total\ Volume}$	40 %
TCM Mass (kg)	2.67
Energy Density (kJ/m^3)	169698
Ideal Energy density (kJ/m^3)	445651
$\frac{Energy\ Density}{Ideal\ Energy\ Density}$	0.38

The low Energy density compared to the ideal energy density is the second indicator along with the low outlet temperature which shows this reactor needs improvement. The low energy density is because only 40 percent of the volume (which corresponds to the 2.67 kg of TCM material) is designed for the reactor bed.

5.4. Improved Multi-Tube Design

The first multi-tube setup was implemented successfully, the working mechanism was verified, but some results like the low HTF outlet temperature and also low Energy density proved that the design should be improved. By having the experience of the first setup and also the basic model sensitivity analysis, it has finally been decided to perform the improvement procedure for the model as below:

- **Increasing Total reactor Length**: Reactor length has been increased by 300mm, aiming to increase the heat transfer surface. This will also lead to an increase in Reactor Volume.
- **Increasing Tubes Diameters**: Tubes containing the TCM material have been doubled in diameters (from initial 15mm to 30mm). The aim was to increase the $\frac{Bed\ Volume}{Total\ Volume}$, which was distinguished to be a main reason for the low energy density of the initial design.
- **Decreasing Mass flow Rate:** An operational parameter has also been improved. HTF mass flow rate has been decreased from 0.02 to 0.01 kg/s to have better temperatures because as already discussed, less mass flow rate leads to lower HTF velocity and thus more heat exchange time.

5.4.1. Improved Multi-Tube Design – Concept

Figure 39 shows the schematics of the new multi-tube design. All the boundary and initial conditions are the same with the previous design except for the mass flow rate of HTF.

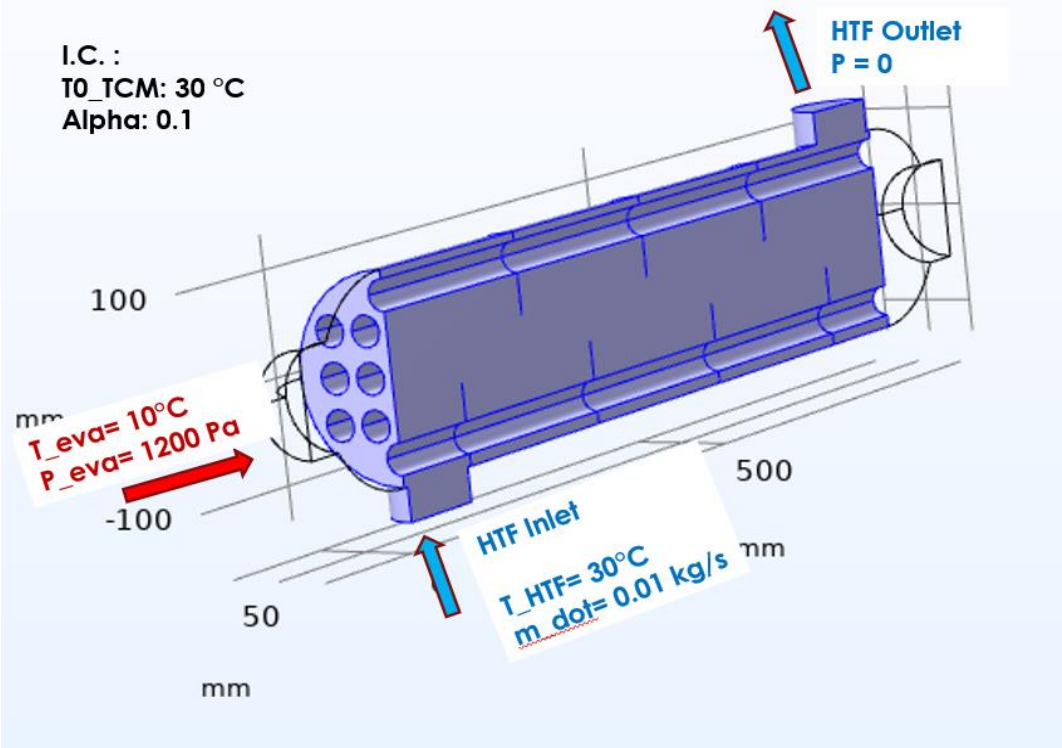

Fig 39. Schematic, boundary and initial conditions of the improved multitube model

The heat transfer mechanism is exactly like the previous model, so temperature surface plots have been skipped. In the next section, the main results including the HTF average outlet temperature, hydration power, TCM mass and the energy density of the reactor have been reported in comparison with the base multi-tube design to better illustrate the extent of the improvement.

5.4.2. Results Comparison: Improved vs Base Multi-Tube

Some important plots and results have been generated for the improved design and a comparison with the initial design can be made. Figures 40 and 41 and Table 10 clarify this comparison.

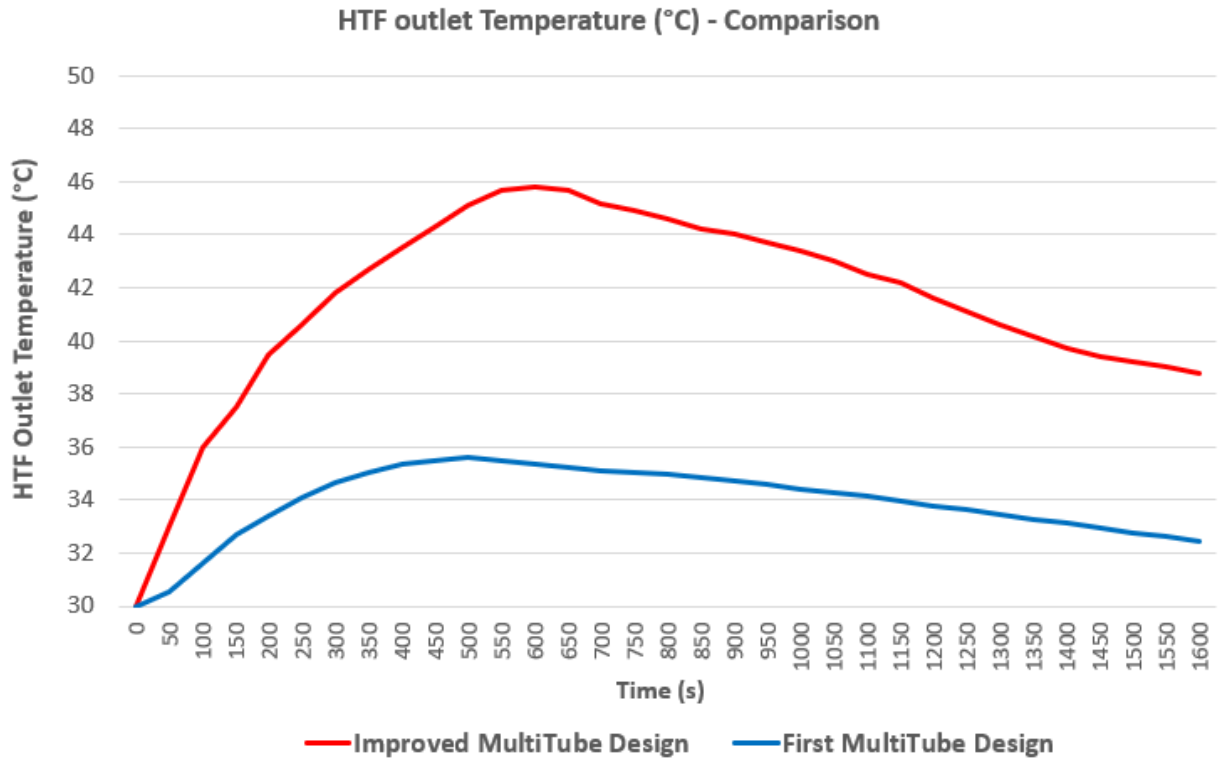

Fig 40. Average HTF outlet temperature for two multi-tube designs

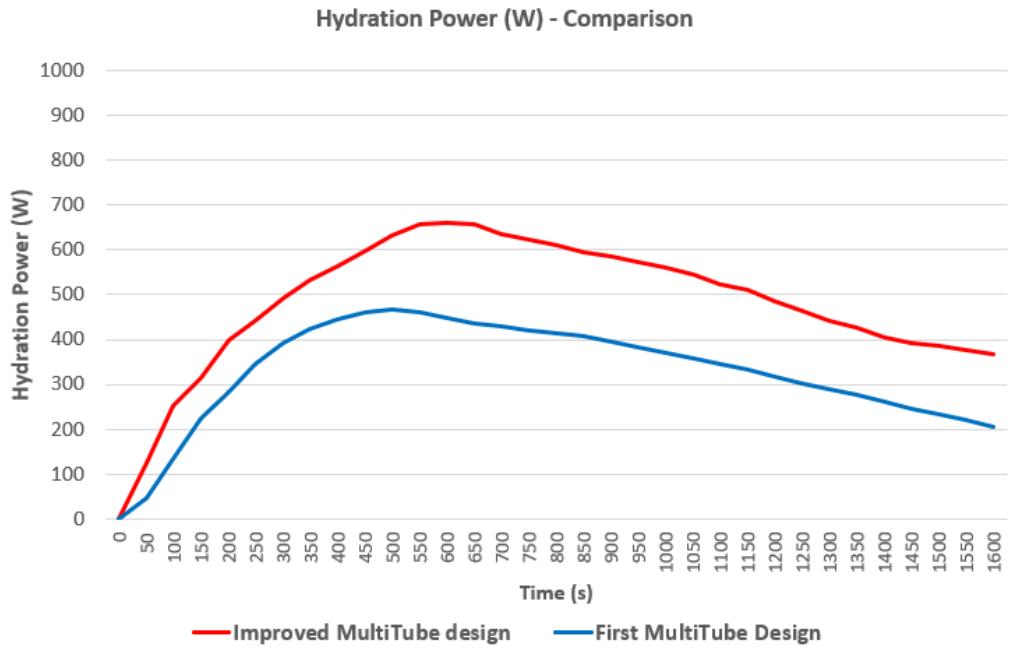

Fig 41. Hydration Power for two multi-tube designs

Table 10. Volume, TCM Mass and Energy density for two multi-tube models

	Initial Multi-Tube	**Improved Multi-Tube**
Total Reactor Volume (m^3)	0.01	0.02
Bed Volume (m^3)	0.0039	0.012
$\frac{Bed\ Volume}{Total\ Volume}$	40 %	60 %
TCM Mass (kg)	2.67	8.24
Energy Density (kJ/m^3)	169698	272464
Ideal Energy density (kJ/m^3)	445651	454107
$\frac{Energy\ Density}{Ideal\ Energy\ Density}$	40 %	60 %

5.4.3. Comparison Observations and Conclusions

As expected, the improved reactor has higher average temperature in the outlet of heat transfer fluid, as a result of increasing the heat transfer surface by geometric improvements. The improved reactor has experienced a peak average HTF outlet temperature close to 46 °C after about 600 seconds of reactor operation, which meets the goal for space heating (T>45°C), considering the fact that a fixed bed reactor is being used. But of course, some other suggestions for improving this design will be proposed in the next chapter.

There has been an increase in the hydration power for the new reactor as a result of the increase in TCM material and energy density of the reactor and thus the increase in HTF average temperature in the reactor.

Furthermore, it could be clearly concluded that a main drawback of the initial design has been solved. In other words, in this bigger reactor, the portion of the volume related to the TCM bed has been increased from 40% in the initial design to 60%. Bigger bed has higher TCM and higher energy density.

One may think of increasing bed portion and TCM mass even more, which can have more energy density in the same volume. However, a good improvement should be done and evaluated based on a trade-off between the HTF outlet temperature and the energy density. A reactor may have a high HTF outlet temperature but has a lower energy density. This point will be further discussed in the next chapter.

In the next part, a second possible design will be proposed which is expected to have better performance than multi-tube design. After a first design to check whether it is an applicable idea, improvements will be made in a way that the final setup has equal volume and TCM mass with the improved multi-tube design, enabling the designer to have a fair comparison between the two concepts.

5.5. Helical Design - Introduction

The advantages of using a helical coil heat exchanger (HCHE) have been completely explained in Chapter 2. It was expected that moving through a helical coil heat exchanger can lead to a more effective design with higher HTF outlet temperatures than the multi-tube design as there is usually larger heat exchange surface in this type of reactor compared to reactors with shell and tube configurations.

The procedure will be started with proposing an initial and small design of a HCHE in order to verify the working mechanism of the reactor and to see whether it has the potential to fit into the requirements of this application.

Later on, the reactor will be improved to have the same volume and the same TCM mass with the final multi-tube heat exchanger setup. This way, the comparison between the temperature plots of the two reactors will have a relatively fair comparison and enable the designer to draw some conclusions. Further conclusions and suggestions for the future studies depending on the results will be proposed in the next Chapter.

5.5.1. First Helical Design – Concept

The reactor consists of a helical coil inserted inside a cylinder shell. The cylinder is the reactor bed, containing the TCM material. Water vapor coming from the evaporator enters this bed at the evaporation pressure and temperature and hydrates the TCM. The heat released from this exothermic hydration reaction is transferred to the heat transfer fluid which is flowing through the helical coils. Figures 42 and 43 demonstrate the schematic of the reactor, with the corresponding boundary conditions. It must be again emphasized that all these B.C.s and I.C.s are the same as the initial multi-tube design.

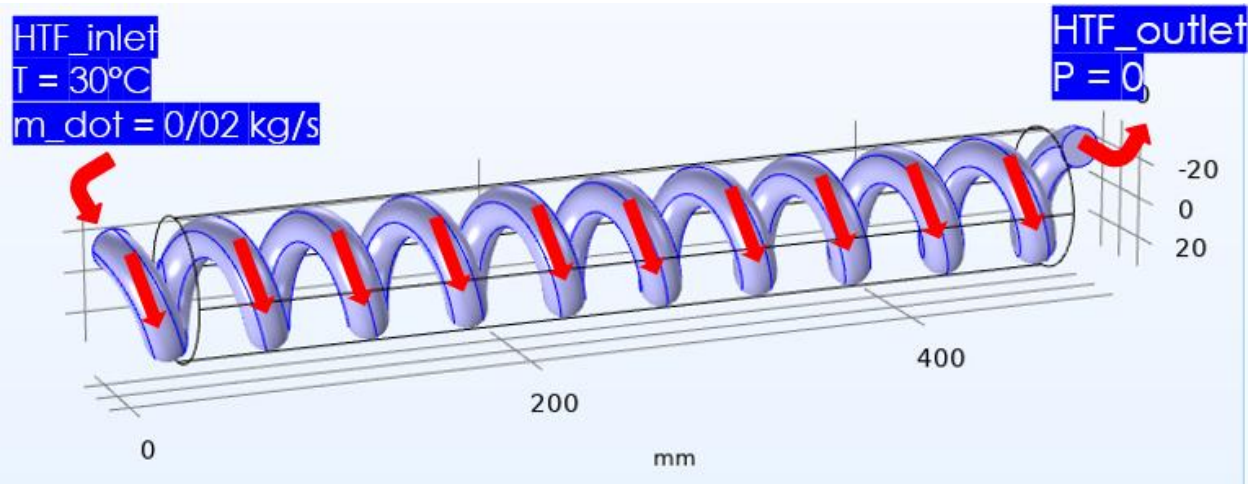

Fig 42. The Helical Coils containing the heat transfer fluid in initial Helical design

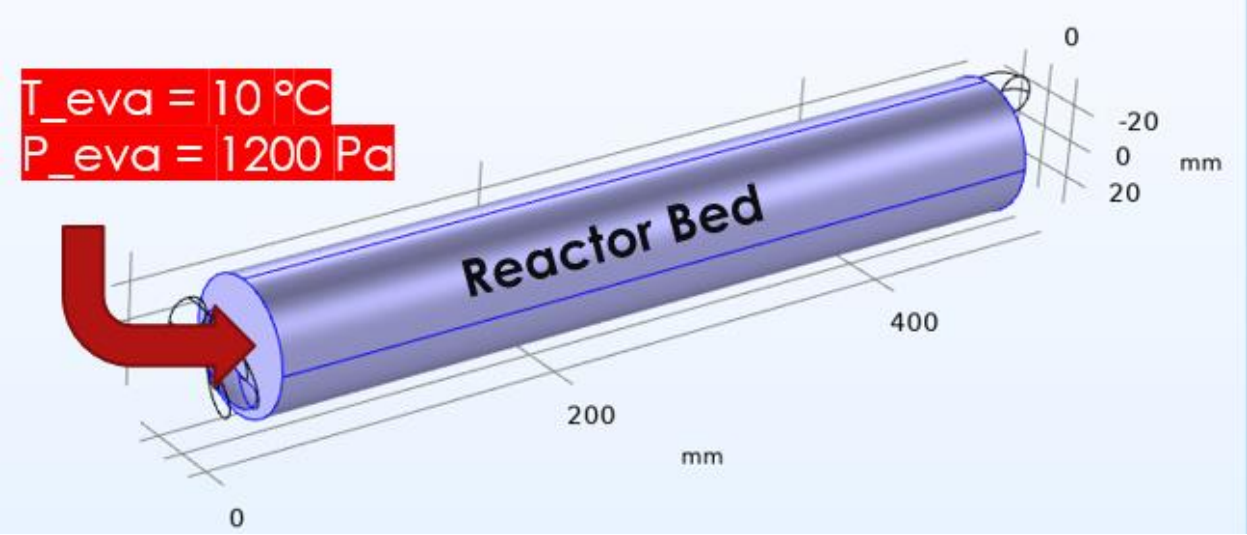

Fig 43. The Cylindrical Reactor Bed in the initial helical design

The initial conditions include: Initial TCM bed temperature = 30°C, Initial HTF temperature= 30°C, Initial Status of Conversion = 0.1.

5.5.2. Temperature Surface Plots

As performed for the multi-tube design, to have a better visual understanding of how the heat transfer happens through the reactor and the temperature distribution, surface plots for some different times have been proposed using COMSOL (figures 44). Once again, a zero-second plot has been generated to confirm the initial

condition of the temperature for the bed and heat transfer fluid. The other plots include a time before the temperature of the heat transfer fluid reaches to the peak value and a time after the peak value.

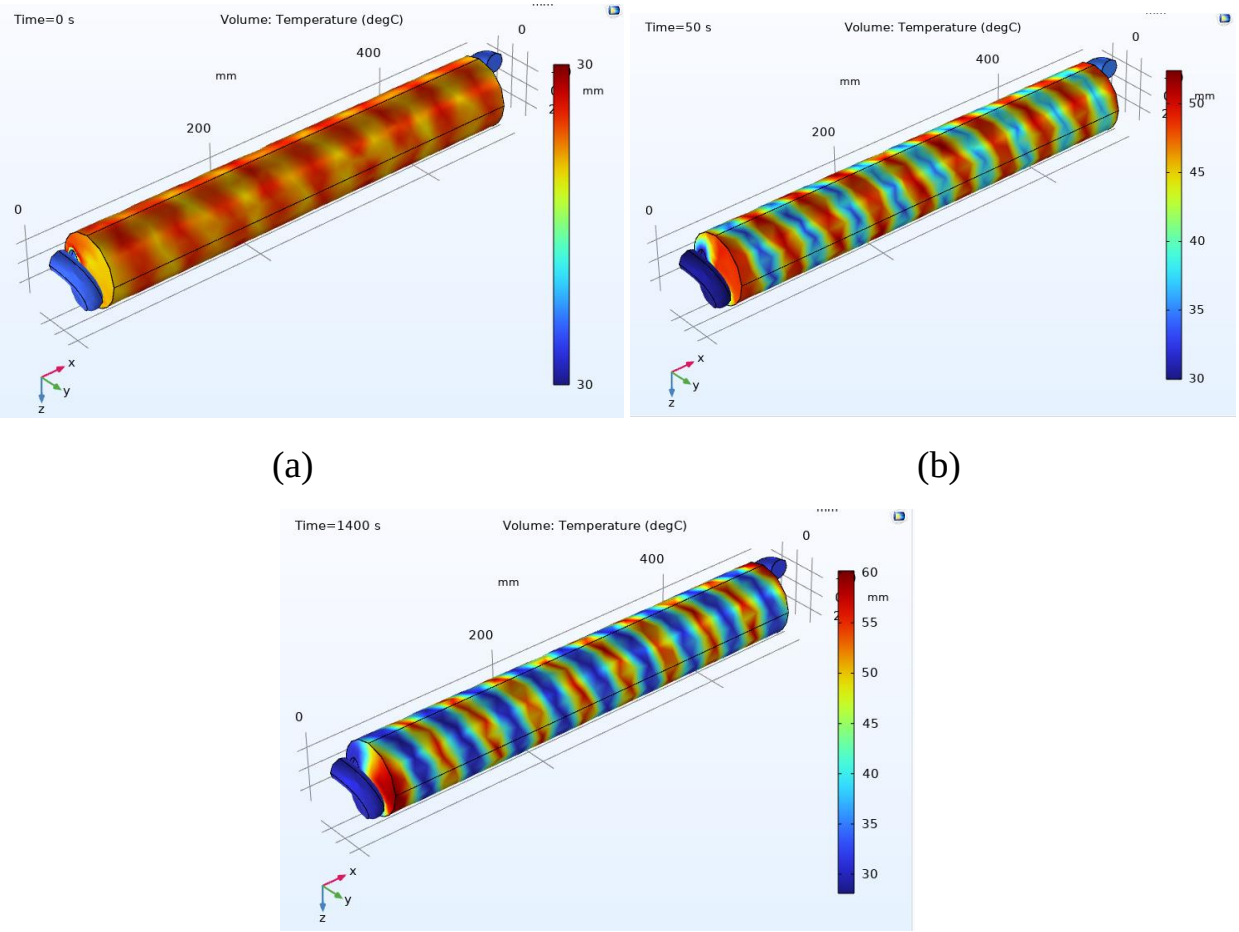

Fig 44. Temperature Surface Plots for the initial Helical Design

Figure 44a shows that in t=0s, the minimum and the maximum values of the whole geometry is 30 °C, which is the defined initial temperature for both bed and HTF in the model. As hydration reaction happens, the reactor bed heats up, reaching to a maximum of 60 °C, which is evident in Fig 44b for t=50s. The heat is transferred to the HTF and heats it up too and after a certain peak (which will be shown by line graphs), temperature of the HTF drops as the whole TCM material in the tubes have been consumed and the status of conversion has approached to 1. Fig 44c at t=1400s is one of the after-peak moments.

5.5.3. Average HTF Outlet Temperature – Line Graph

The temperature surface plots in the previous section were used to show the temperature distribution in the whole reactor in different times. Also, the heat transfer fluid outlet temperature variation, which is one of the main results of this study, can be found out approximately by checking the corresponding colors in the outlet surface. However, those plots cannot give a more accurate value and the peak time. To this aim, line graphs are used to demonstrate the average HTF outlet temperature like figure 45.

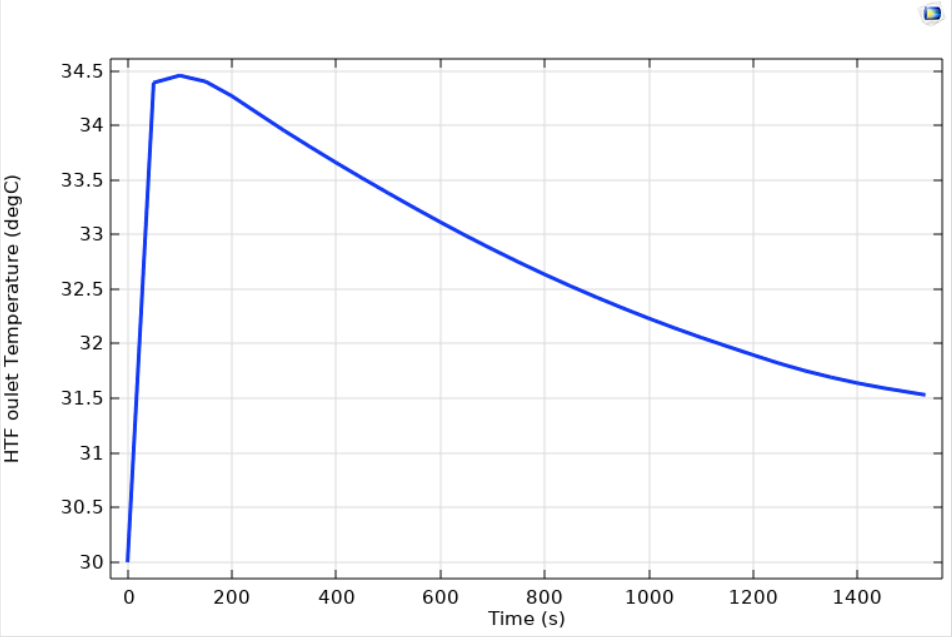

Fig 45. Average HTF outlet temperature for the initial helical design

Figure 45 shows that during this heat exchange process, the heat transfer fluid has reached to a maximum temperature of 34.4°C in t=100s It is clear that this temperature range is low for the required district heating applications. So, there is the need to improve this reactor based on the knowledge from previous chapters to get temperatures above 45 °C.

5.5.4. Status of Conversion – Surface Plots

To have a better visual overview of the process of TCM conversion and progress of the reaction, surface plots for the status of conversion (α), have also been generated (figures 46) with the same approach for some different times.

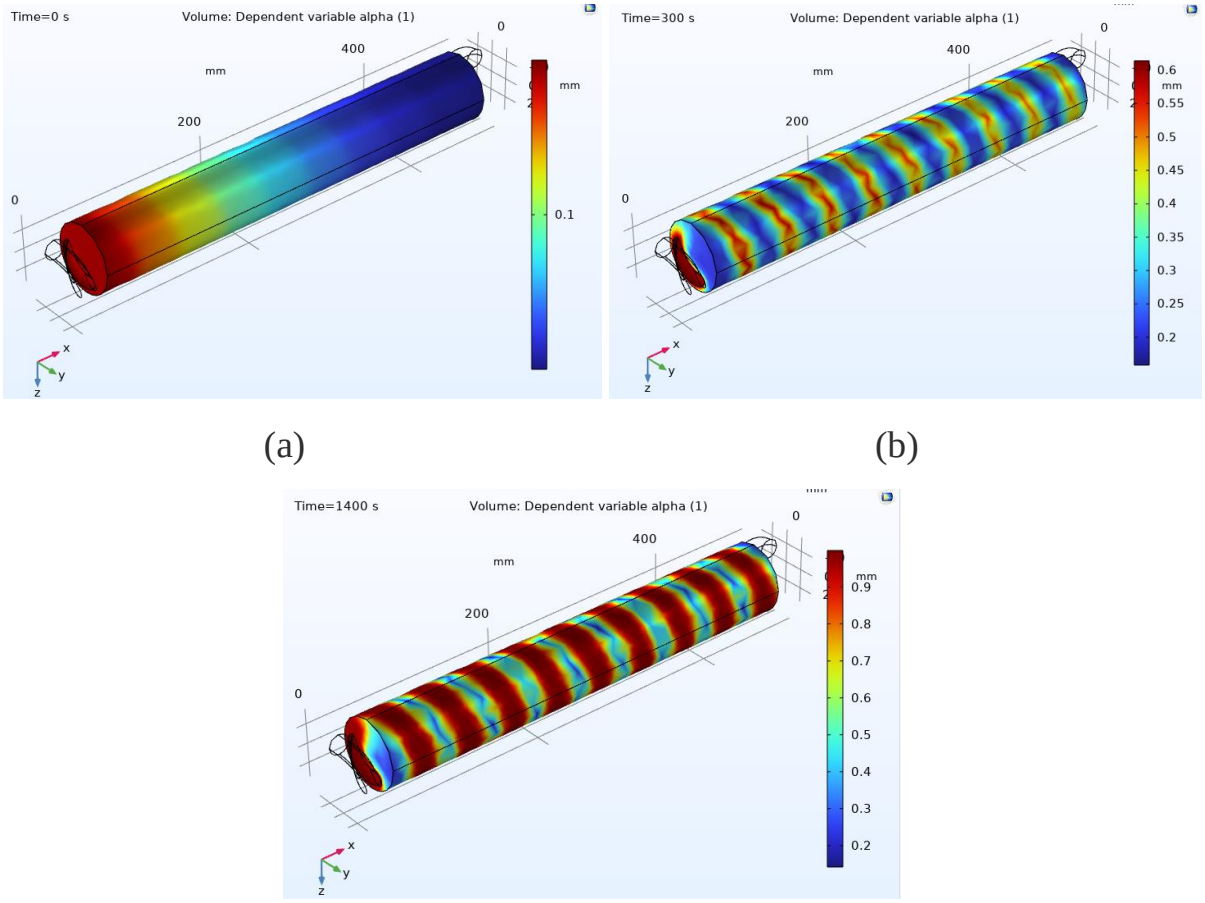

Fig 46. Status of Conversion (α) surface plots for the initial helical design

Fig 46a clearly shows the α=0.1 at t=0s for the whole bed, which is actually the initial condition defined for the model. As the hydration reaction has progressed and more TCM Material has been converted, the status of conversion has reached to maximum values above 0.6 at t=300s in the bed and above 0.9 at t=1400s.

However, this surface plots demonstrates one big problem of this initial design. From Figure 46c, it can be observed that areas closer to the HTF tubes are red (higher conversion) while areas in between are yellow, green or even blue (lower

conversion). This means that in this setup, heat transfer has not been done perfectly. Therefore, parts of the bed which have a bit of distance from the HTF coils, have witnessed lower conversion of material. This fact has actually provided the main improvement target for this setup.

Like the previous model, the average status of conversion line graph will be plotted only to verify its ascending trend, but keep in mind that, also for this setup, this plot cannot be a very good indicator due to very unequal values for the status of conversion through the whole geometry. Plots showing the maximum values will prove that in any case, there will be a time which part of the bed material has had complete conversion.

5.5.5. Average Status of Conversion – Line Graph

Like the HTF outlet temperature, the average status of conversion for the reactor bed can also be plotted as a line graph like figure 47 to see the trend more clearly:

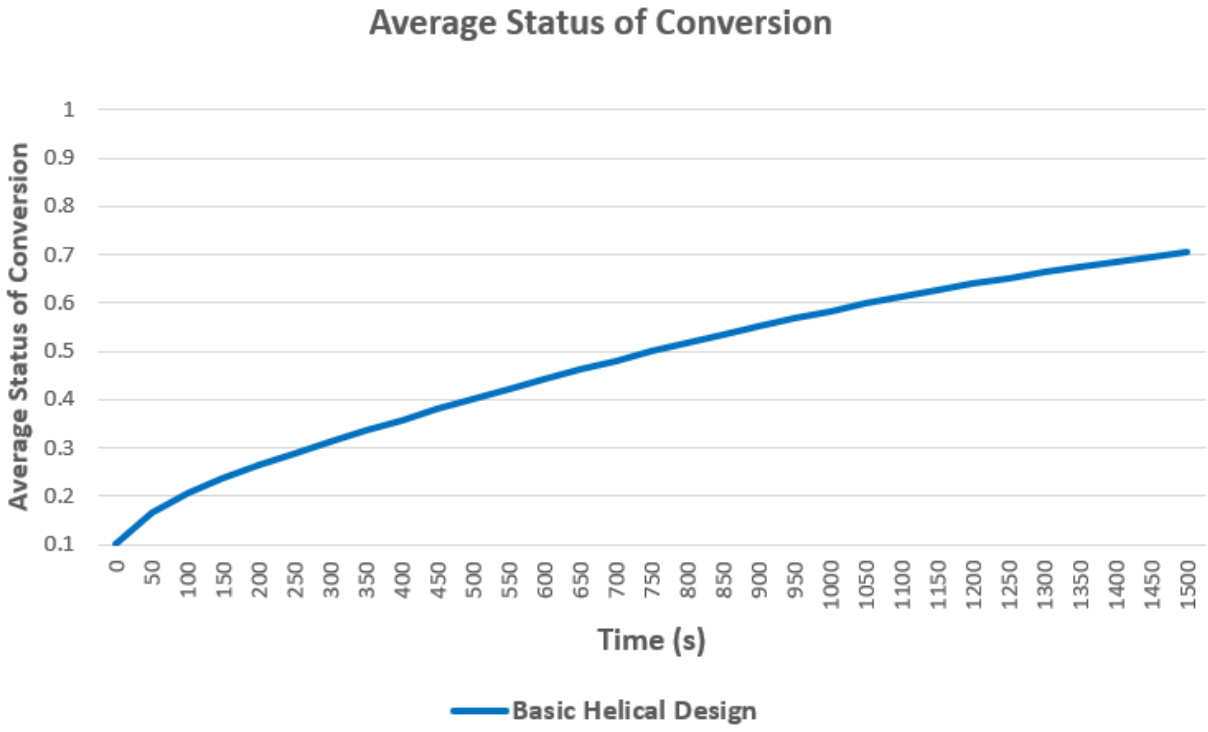

Fig 47. The Average Status of Conversion Line Graph for the initial Helical Design

Figure 47 verifies the expectations one may have by looking at the surface plots in the previous sections. Definitely, the unequal values of status of conversion through the bed which is completely related to the geometric characteristics of the design, is an improvement target. Later, more details for this reactor will be provided in a table which will clarify the problem even more.

5.5.6. Hydration Power

The Hydration Power plot for this setup is as figure 48:

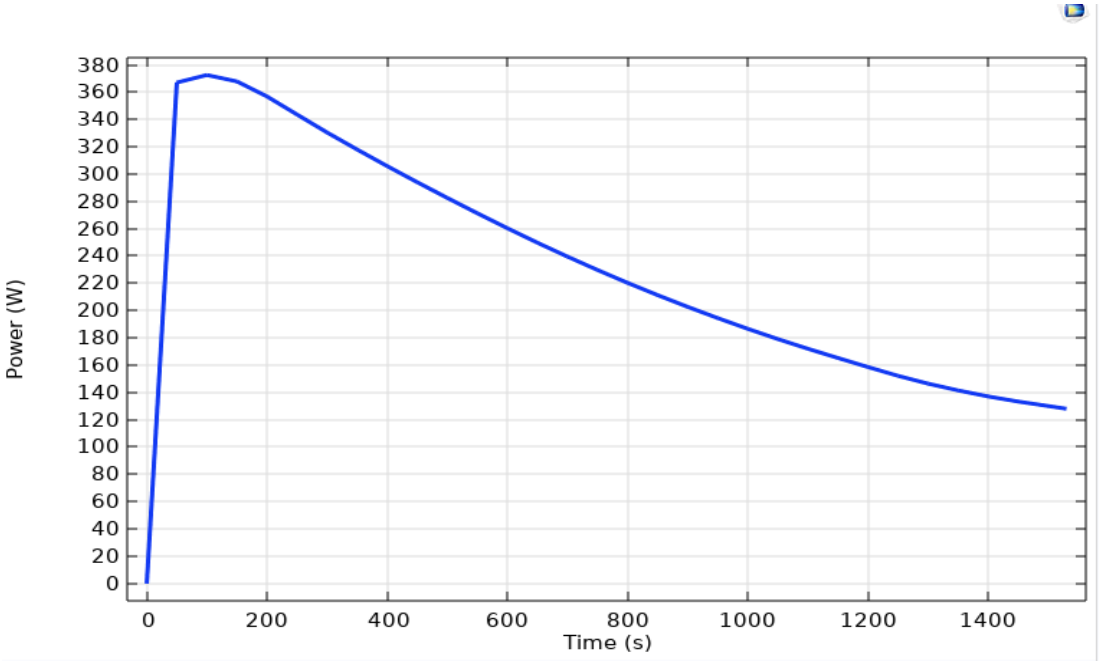

Fig 48. Hydration Power plot for the initial helical design

For this small reactor, power has been reached to 370 W as the hydration reaction and the heat transfer has progressed and then has descended as the conversion has completed and the temperatures have been reduced.

5.5.7. Other Parameters

Other useful characteristics and results for the reactor are listed in Table 11.

Table 11. Volumetric Characteristics, TCM mass and Energy density of the initial helical design

Total Reactor Volume (m^3)	0.0022
Bed Volume (m^3)	0.0017
$\frac{Bed\ Volume}{Total\ Volume}$	78 %
TCM Mass (kg)	1.17
Energy Density (kJ/m^3)	350900
Ideal Energy density (kJ/m^3)	454107
$\frac{Energy\ Density}{Ideal\ Energy\ Density}$	78 %

Interesting point about this initial setup is that, as table 11 also suggests, it has a very high energy density which is actually an advantage. The reason is that 78% of the reactor total volume is dedicated to TCM. However, on the other hand, this reactor has a very low HTF outlet temperature range which was because of the unsuitable heat transfer and incomplete conversion of material in a huge portion of the bed.

Although, this reactor was only an initial, small sample, but it was an interesting example to show that a very high bed volume portion and high energy density does not necessarily mean that the reactor will have better results in terms of HTF outlet temperature. It is concluded again that a nice design should have a trade-off between Energy density, HTF average outlet temperature, status of conversion and TCM mass.

In the next section, an improved helical coil design will be proposed based on all the experiences and results obtained until now.

The Helical coil setup will be rescaled in a way that the total reactor volume becomes equal to the total reactor volume of the multi-tube design, so that after comparing it with the initial helical design, it could be also compared with the improved multi-tube design.

5.6. Improved Helical Design

The initial helical setup was implemented successfully, the working mechanism was verified, but the low HTF outlet temperature, the very unequal values of status of conversion through the bed and bad quality of heat transfer were the main drawbacks which should be subjected to improvement. By having the experience of the first setup and also the basic model sensitivity analysis, it has finally been decided to perform the improvement procedure for the model as below:

- **Increasing Total Bed Length**: Bed length has been increased by 42mm, aiming to increase the heat transfer surface. This will also lead to an increase in Reactor Volume.

- **Decreasing Axial Pitch**: A very important design parameter is the axial pitch. It was reduced from 50mm in the initial design to the 34.75mm in the improved design. This way, the coils have been closer to each other, expecting to solve the bad heat transfer of the initial design.

- **Increasing diameter of helical coils**: Coils containing the HTF have been increased in diameters (from initial 313mm^2 to 1805mm^2). The aim was to increase the HTF volume in the setup which was too low in the initial design

and above that, reduce the distance between coils to improve the status of conversion by better heat transfer.

- **Increasing Number of Turns**: By increasing the length and the volume of the bed, number of turns have been increased by 10 to 16 to be compatible with the lower axial pitch so that the coils become closer compared to the initial design.

- **Decreasing Mass flow Rate:** An operational parameter has also been improved. HTF mass flow rate has been decreased from 0.02 to 0.01 kg/s to have better temperatures. As already explained, lower mass flow rate leads to lower HTF Velocity and thus higher heat exchange time.

5.6.1. Improved Helical Design – Concept

Figure 49 shows the schematics of the new multi-tube design. All the boundary and initial conditions are the same with the initial design except for the mass flow rate of HTF.

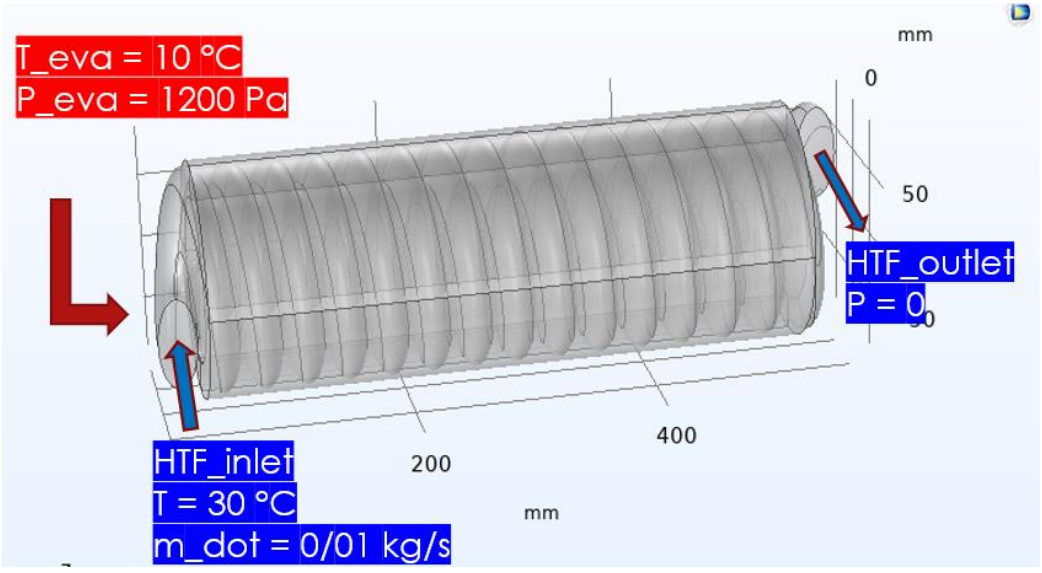

Fig 49. Schematics and Boundary conditions of the Improved Helical Design

The initial conditions include: Initial TCM bed temperature = 30°C, Initial HTF temperature= 30°C, Initial Status of Conversion = 0.1.

The heat transfer mechanism is exactly like the initial model, so temperature surface plots have been skipped but status of conversion surface plots will be checked.

In the next section, the main results including the HTF average outlet temperature, hydration power, TCM mass and the energy density of the reactor have been reported in comparison with the base helical design to better illustrate the extent of the improvement.

5.6.2. Results Comparison: Improved vs. Base Helical Design

Figure 50 compares the average status of conversion for two helical designs.

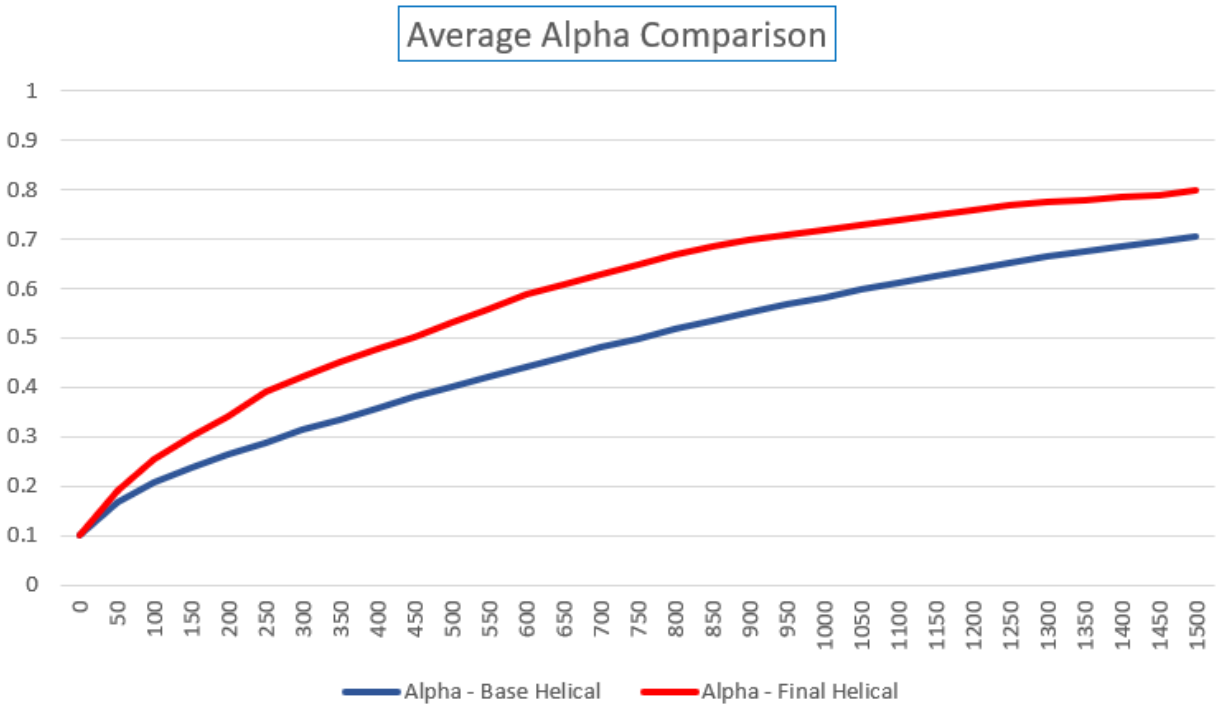

Fig 50. The Average Status of Conversion for the bed in two helical designs

During the analysis of average status of conversion for the bed, it was found out that despite the huge geometric improvements, there were still some parts of the bed volume which had lower status of conversion. However, these parts were mostly in the center line of the cylinder and not on the walls due to the closer and more compact helical design which led to better heat transfer. Thanks to these

changes, the average status of conversion for the whole bed improved. Figures 51 and 52 and Table 12 show other comparisons.

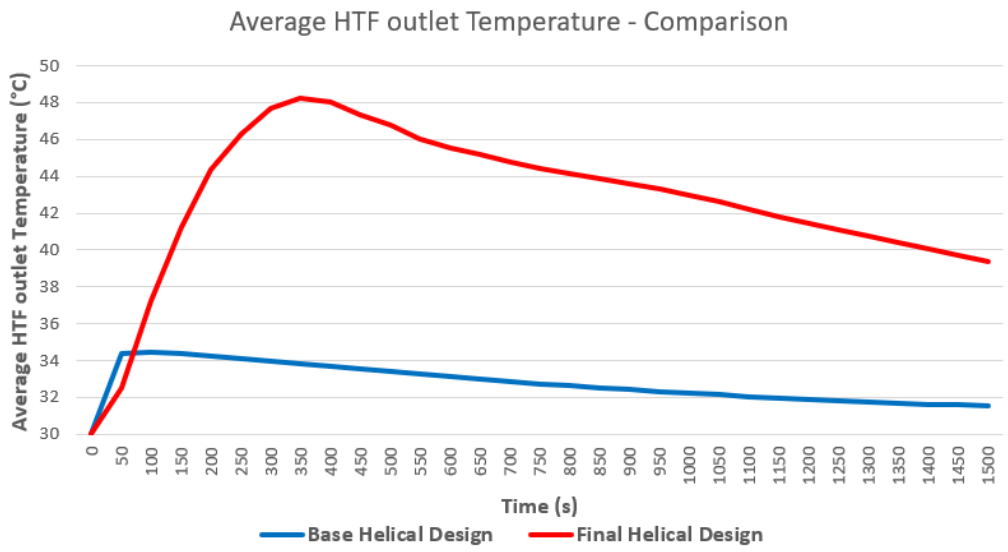

Fig 51. Average HTF outlet temperature comparison for two helical designs

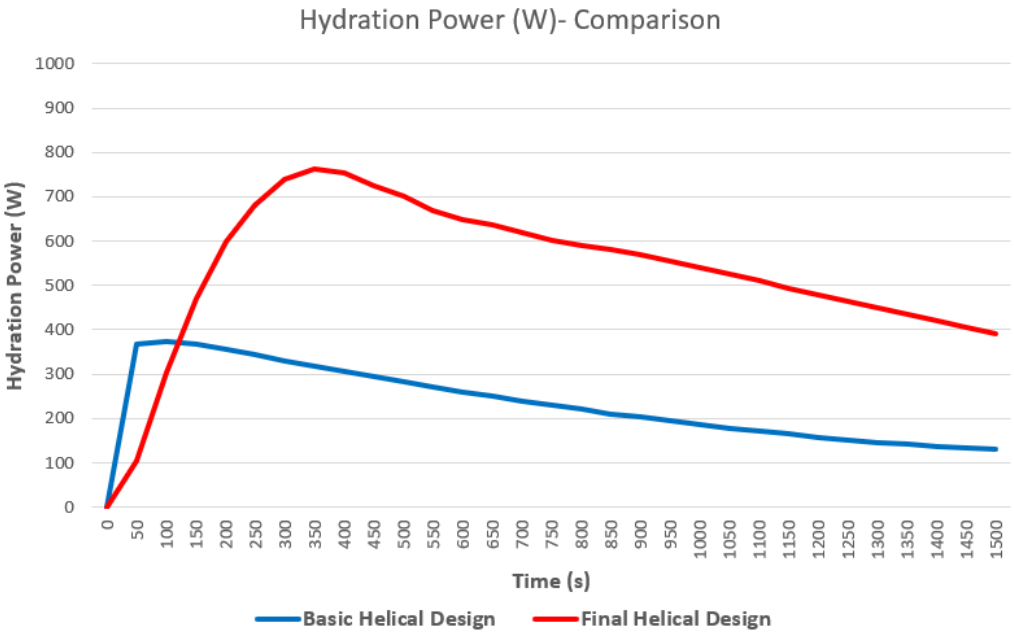

Fig 52. Hydration Power comparison for two helical designs

Table 12. Volume, TCM Mass and Energy density for two helical models

	Initial Helical Design	**Improved Helical Design**
Total Reactor Volume (m^3)	0.0022	0.020
Bed Volume (m^3)	0.0017	0.012
$\frac{Bed\ Volume}{Total\ Volume}$	78 %	60 %
TCM Mass (kg)	1.17	8.245
Energy Density (kJ/m^3)	350900	272497
Ideal Energy density (kJ/m^3)	445651	454107
$\frac{Energy\ Density}{Ideal\ Energy\ Density}$	78 %	60 %

5.6.3. Comparison Observations and Conclusions

As expected, the improved reactor has higher average temperature in the outlet of heat transfer fluid, as a result of increasing the heat transfer surface by geometric improvements. The improved reactor has experienced a peak average HTF outlet temperature close to 48.5 °C after about 350 seconds of reactor operation, which is a suitable value for space heating goal (T>45°C), considering the fact that a fixed bed reactor is being used. But of course, some other suggestions for improving this design will be proposed in the next chapter.

There has been an increase in the hydration power for the new reactor as a result of the increase in TCM material and energy density of the reactor and thus the increase in HTF average temperature in the reactor.

Furthermore, it could be seen that the new reactor has a lower energy density than the initial setup which is a negative factor. This is because of the lower bed portion in the new reactor (60%) than the initial one (78%).

However, although decreasing TCM bed volume portion has decreased the energy density of the improved case, but the resulting HTF portion increase has helped the helical reactor to achieve better conversion, heat transfer and high Average HTF outlet temperature, as demonstrated in the previous results.

It is concluded that the new setup is overall an improved reactor compared to the initial design thanks to the geometric and operational improvements. However, this may not be necessarily the best possible design and the improvement process can always be continued with other ideas. Some suggestions for future designs will be proposed in the next chapter.

5.7. Final Comparison: Helical Design vs. multi-Tube Design

The Helical model was improved such that it also has the same total volume, bed volume, TCM mass and thus energy density with the improved multi-tube design. In this section, the two final designs will be compared. As the above-mentioned parameters have been kept the same, the average HTF outlet temperature and the hydration power have been chosen to be the indicators for comparison.

The equal parameters for the two designs are as follows:

- Total Reactor Volume = 0.02 m^3
- Bed Volume = 0.012 m^3 ($\frac{Bed\ Volume}{Total\ volume} = 60\%$)
- TCM Mass: 8.245 kg
- Energy Density = 272497 kJ/m^3 (which is 60% of the ideal energy density)

Figures 53 and 54 demonstrate the final comparison between the two improved designs.

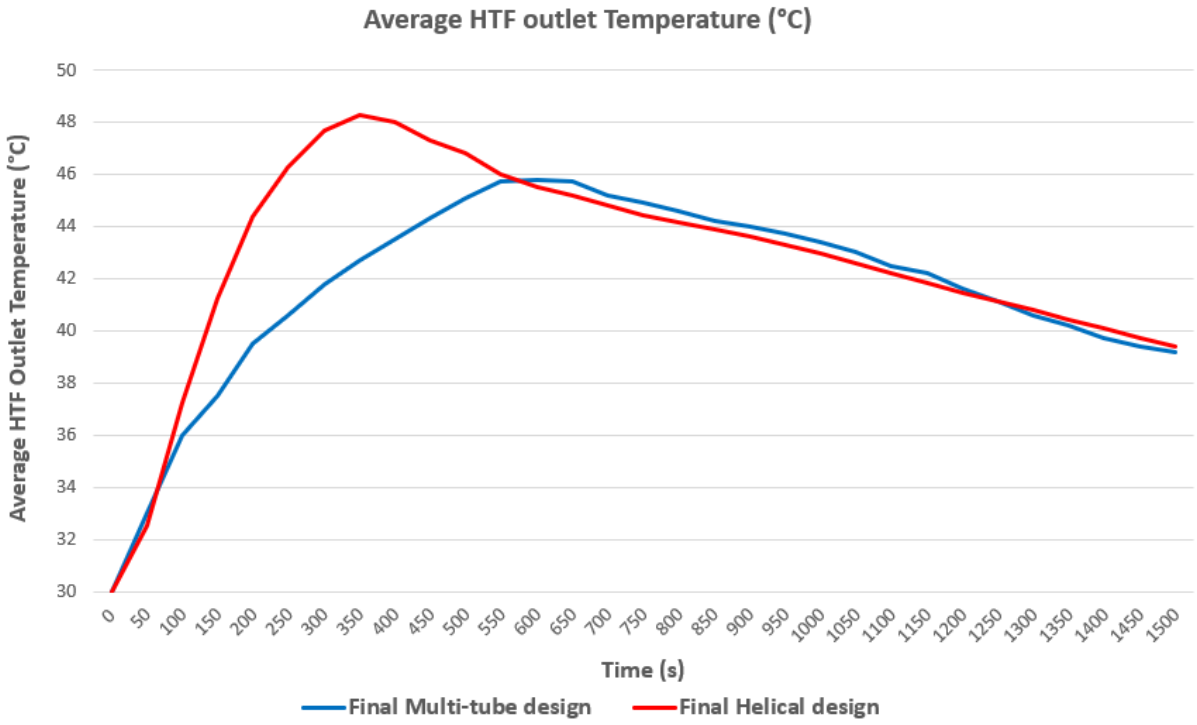

Fig 53. Average HTF outlet temperature for final multi-tube and Helical Designs

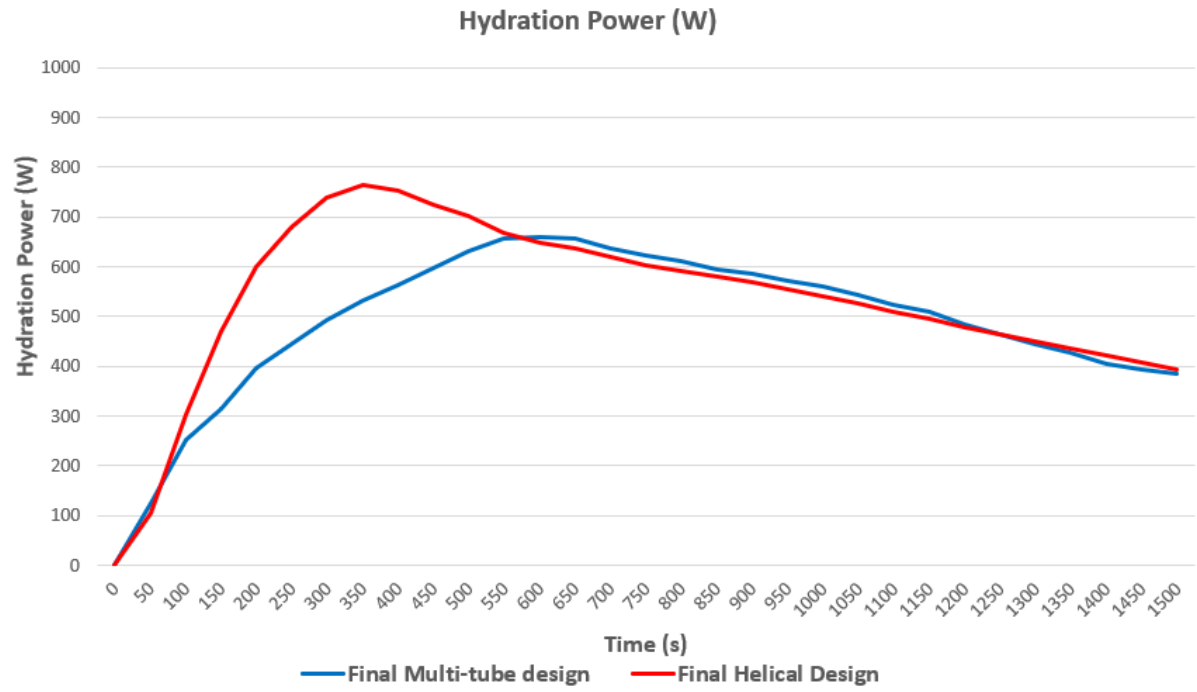

Fig 54. Hydration Power for final multi-tube and Helical Designs

5.7.1. Final Comparison: Conclusions

1. First of all, considering using fixed bed reactors, both reactors have presented good potential to provide acceptable HTF outlet temperature and power output for the specific application of this study. Specifically, they can fit into space heating purposes, but for hot water usage, they need more improvement or should be upgraded to moving bed reactors.

2. The Helical Coil Heat Exchanger has had a slightly better performance. This can be seen as a result of larger heat transfer surface which is actually the main benefit of helical coil design compared to the shell and tube designs.

3. From literature review, it was found out that both these designs may have difficulty while cleaning, and clogging can be an issue. However, Helical heat exchangers need cleaning less often. Also, for the helical design of this study, the cleaning may be easier because of the simpler and more accessible tubes.

Therefore, it is concluded that, the helical coil design is a preferred option in this study.

Definitely, these designs cannot be the most optimized designs for each type and one may be able to improve them in the future by different approaches. The two small reactors designed in this study were only for the research purposes. However, based on all the experiences obtained by designing these two small reactors, some more suggestions for the future relevant studies including improvement ideas will be proposed in the next chapter.

Chapter 6

Conclusions and Recommendations

This chapter consists of two main parts. In the first parts, a brief summary of the steps done in this study and the main conclusions will be made. In the second part, some recommendations will be proposed. These recommendations may be related to the two reactor designs of this study and their possible improvement ideas but also there many any other suggestion which can be useful for the future works and researches.

6.1. Conclusions: Literature Review

The aim of this study has been to design a novel peak-shaving reactor for seasonal heat storage based on thermochemical materials for district heating application.

During the first phase of this study, an extensive literature review was conducted about the thermochemical heat storage technology.

By comparing three methods of thermal energy storage, including Sensible Heat Storage (SHS), Latent Heat Storage (LHS) and Thermochemical Heat Storage (TCHS), it was concluded that the TCHS is a better technology due to advantages like higher storage density, lower heat losses, compact designs and the possibility of heat storage in summer.

After investigating the different system types, on the system level, a closed system with an integrated storage system was developed and on the reactor level, a fixed bed reactor was chosen mainly due to the simplicity of the design.

Later, several possible choices for TCM material were investigated with their different characteristics. It was concluded that Potassium Carbonate could be a good choice as it is highly available, chemically robust, safe, cheap and not so much corrosive.

Finally, liquid water was chosen as the heat transfer fluid for the heat exchangers used in this study because it is cheap, available and safe and also compared to air, another suitable option, it has better heat transfer properties.

6.2. Conclusions: Design

During the second phase of the study, a basic 2D model was modelled in COMSOL, aiming to implement the governing equations on a simple design, better understand the physics of the model and finally, perform a sensitivity analysis to find some of the main design parameters of the model which could also help coming up with ideas how to design the final propose models of the study. Study was done on two groups of parameters, some of them were geometric and some others related to the operations of the reactor. Logical expectations of the designer were compared with the results in the software and the plots to find out some design parameters for the reactor. Indicator plots included the HTF outlet temperature together with the status of the conversion. The aim is to increase this temperature to at least above 45°C to be used in space heating and approach to full conversion of material (α=1) in a short time period (e.g. t<2000s).

In the first phases of the modelling, especially during the basic 2D model and the sensitivity analysis studies, one question was always in the designer's mind:

"Which is the best indicator to evaluate the performance results of a reactor model?"

It has been concluded that focus should be on higher HTF outlet temperature (at least higher than 45°C), higher average status of conversion but also higher energy density on the system level. However, later on, in the improved 3D models of this study, the HTF outlet temperature had desired values despite the low average status of conversion for the bed, and this was because of lower status of conversion in some parts of the bed. This fact emphasized the importance of considering energy density of the reactor which was a factor closely related to the amount of TCM volume compared to total volume of the reactor and TCM mass.

Therefore, it was concluded that:

"A suitable reactor design requires a trade-off optimization among the HTF outlet temperature, average status of conversion and energy density."

During the design phase of the study, two different fixed bed reactors were proposed, one based on a multi-tube heat exchanger and one with helical coil heat exchanger. Firstly, an initial design from each type were modelled, then based on the knowledge obtained from second phase, some geometric and operational improvements were made to produce the final multi-tube and helical designs. Finally, two final designs of each type with the same volume (0.02 m^3), TCM mass (8.2 kg) and energy density (60% of the ideal energy density) were compared in terms of average HTF outlet temperature and power output. By comparing the results, the helical coil design was introduced as a better design for the desired application mainly because of the higher HTF temperatures (48.5°C compared to 46°C in multi-tube) due to larger heat transfer surface.

6.3. Recommendations

Last but not least, it has been tried to provide some useful suggestions in this section to help the future researchers and designers who will work on designing reactors for the same application. Firstly, some design recommendations will be made based on the results from the two setups in this study. Then, some other suggestions related to design and simulations will be provided.

1- During the improvement procedure of both multi-tube and helical coil model, it was clearly seen that the HTF average outlet temperature reached to average values relatively suitable for space heating and energy density was acceptable compared to the maximum energy density for that volume. However, average status of conversion remains as an improvement goal.
   One possible suggestion for multi-tube design, according to Figure 55, is to design this configuration again such that the two caps in the left and right side of the setup are reduced in volume (or even removed) as these two sections do not have good heat transfer with HTF and have low conversion status.

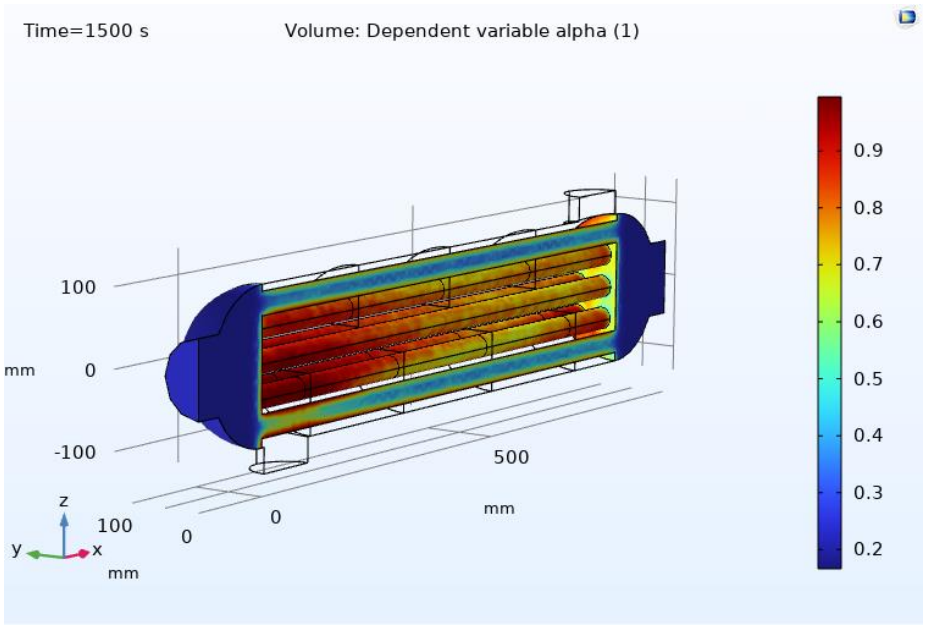

Fig 55. Status of Conversion for the multi-tube design after 1500 seconds

This change will definitely improve the average status of conversion for the whole reactor, but reducing the two caps will reduce the TCM mass and energy density, so the middle part of the reactor should be readjusted such that the Energy density does not reduces and the trade-off is conserved.

For helical coil design, parts of this improvement were done in the study by doing major geometric improvements. According to Figure 56, the central line of the bed (cylinder) has low status of conversion, as this area has more distance with HTF. It is recommended to improve the design of the reactor such that the central area has a lower volume. This way, heat transfer is expected to be a bit better.

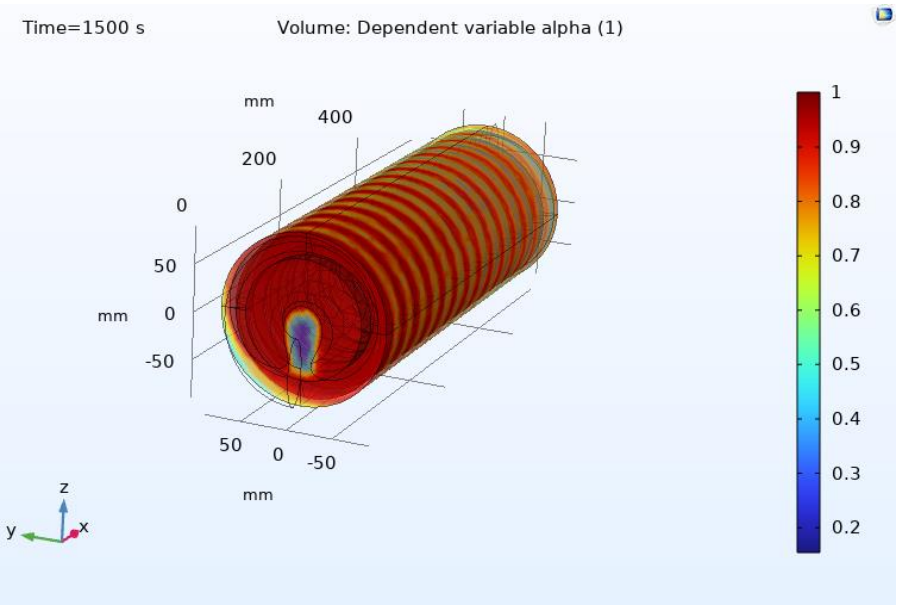

Fig 56. Status of Conversion for the Helical Coil Design after 1500 seconds

2- It must be mentioned that the modelled reactors had a very small size and volume and they were only for the research purpose. A final design for the industry may have volume in a scale of 10 – 15 m^3 (scale factor 1:500 – 1:750). Definitely, the TCM mass and energy density can grow in bigger reactors. However, energy density should always be compared with the ideal energy density to evaluate better the amount of storage in any volume.

3- Cost and Economic evaluations were not a part of the work package and the scope of this study. For any final design, cost will be also an important indicator which should be considered together with the three aforementioned indicators. Also, in the research group of this project, economic analysis of thermochemical heat storage technologies is supposed to be assigned to some other researches in the future.

4- To be able to use the large heat transfer surface of a helical coil design but also improve issue of low conversion in some parts of the volume, going through “Spiral” design with a countercurrent HTF and water vapor flow can also be suggested. This configuration is expected to have a better heat exchange between HTF and TCM. A sample configuration can be seen as figure 57.

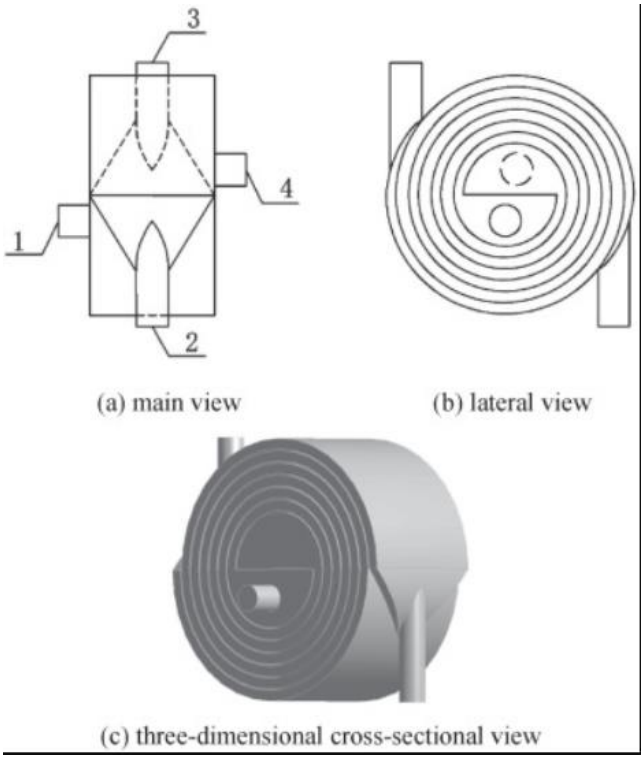

Fig 57. Spiral Heat Exchanger with countercurrent fluids flow [34]

5- This study was done using a fixed bed reactor and it was concluded that a fixed bed reactor using potassium carbonate as TCM is expected to fulfill the space heating temperature demand. By performing the improvements mentioned in the previous section, maybe reaching to average HTF outlet temperature close to 50°C is feasible. But generally, this is not the best desired temperature range. If the reactor is supposed to be used also for hot water

usage of the buildings, the desired temperatures will be higher than 55°C. To this aim, it is recommended to put effort on designing reactors based on a moving bed reactor. Also, closed system design can be substituted with the open system. Modelling an open system moving bed reactor is much more complex than a closed system fixed bed design, but it is expected to have higher outlet temperatures and higher heat transfer between HTF and TCM.

In all CFD modelling and computations, setting up a correct solver based on a correct PDE equation [54] and also a correct mesh is essential.

For this study, the main PDE equation used in COMSOL Multiphysics was equation 7, which was completely described in Chapter 2. The constant values of this equation have been taken from an experimental literature conducted by University of Twente [40]. However, while designing the helical coil reactor, several convergence errors by the software were being observed. As a result:

1- It is recommended to continue similar experimental studies to figure out whether the current PDE equation can be improved even more, e.g., developing a form of PDE equation that is also applicable to curved surfaces. (Of course, this is only a raw idea of the designer.)

2- For every different reactor setup, it is recommended to perform a mesh independency test to figure out whether the results of the model are independent of the underlying mesh. In this study, a short similar test was done for the 2D Model. There are lots of relevant articles about this test in CFD simulations which can be useful [55][56].

3- For having more accurate results and avoid the problem of converging, it is suggested to spend some time in each design for the mesh settings and also mesh refinement techniques in COMSOL may be useful [57].

Bibliography

[1] "Net Zero by 2050 – A Global Roadmap for the Global Energy Sector", IEA, May 2021, Net Zero by 2050 – Analysis - IEA

[2] "Natural Gas Statistics" , IEA, April 2022 update, Gas - Fuels & Technologies - IEA

[3] "National Climate Agreement – The Netherlands", Klimaatakkoord, Published on 28 June 2019, National Climate Agreement - The Netherlands | Publicatie | Klimaatakkoord

[4] "Transitievisie Warmte en Wijkuitvoeringsplan", Rijksdienst voor ondernemend Nederland, 24 February 2022, Transition vision Heat and District Implementation Plan (rvo.nl) (In dutch)

[5] "The Netherlands Energy Statistics", IEA, April 2022 update, The Netherlands - Countries & Regions - IEA

[6] "Less Gas from Russia", Government of the Netherlands, March 2022, Reducing dependence on Russia | Less gas from Russia | Government.nl

[7] "Dutch aim to stop using Russian fossil fuels by year-end", Reuters, 22 April 2022, Dutch aim to stop using Russian fossil fuels by year-end | Reuters

[8] "NVDE: options for less fossil energy and less energy dependency", NVDE (Dutch Sustainable Energy Association), 2 March 2022, 20220302-NVDE-options-for-less-fossil-energy-and-less-energy-dependency.pdf

[9] Dincer, I.; Rosen, M.A. "Thermal Energy Storage: Systems and Applications, 2nd ed.; Wiley: UK, 2011

[10] Ali H. Abedin, Rosen, M.A, "A Critical Review of Thermochemical Energy Storage Systems", The Open Renewable Energy Journal, 2011, Microsoft Word - Rosen_MS.doc (benthamopen.com)

[11] J.Yan, Z.H.Pan, C.Y.Zhao, "Experimental study of $MgO/Mg(OH)_2$ thermochemical heat storage with direct heat transfer mode",

Elsevier, 2020, Experimental study of MgO/Mg(OH)2 thermochemical heat storage with direct heat transfer mode - ScienceDirect

[12] Devrim Aydin, Sean P.Casey, Xiangjie Chen, Saffa Riffat, "Novel "open-sorption pipe" reactor for solar thermal energy storage", Elsevier, 2016, Novel "open-sorption pipe" reactor for solar thermal energy storage - ScienceDirect

[13] J.Xu, R.Z.Wang, Y.Li, "A review of available technologies for seasonal thermal energy storage", Elsevier, 2014, A review of available technologies for seasonal thermal energy storage - ScienceDirect

[14] L.F. Cabeza, I.Martorell, L.Miro, A.I.Fernandez, C.Barreneche, "1 - Introduction to thermal energy storage (TES) systems", Woodhead Publishing Series in Energy, 2015, Introduction to thermal energy storage (TES) systems - ScienceDirect

[15] Ruby-Jean Clark, Abbas Mehrabadi, Mohammed Farid, "State of the art on salt hydrate thermochemical energy storage systems for use in building applications", Elsevier, 2020, State of the art on salt hydrate thermochemical energy storage systems for use in building applications - ScienceDirect

[16] H.Kerskes, B.Mette, F.Bertsch, S.Asenbeck, H.Drück, "Development of a Thermo-Chemical Energy Storage for Solar Thermal Applications", ISES, Solar World Congress, 2011, Microsoft Word - ISES11_CWS-V06.doc (researchgate.net)

[17] Benoit Michel, Pierre Neveu, Nathalie Mazet, "Comparison of closed and open thermochemical processes, for long-term thermal energy storage applications", Elsevier, 2014, Comparison of closed and open thermochemical processes, for long-term thermal energy storage applications - ScienceDirect

[18] Luca Scapino, Herbert A.Zondag, Johan Van Bael, Jan Diriken, Camilo C.M.Rindt, "Sorption heat storage for long-term low-temperature applications: A review on the advancements at material and prototype scale", Elsevier, 2017, Sorption heat storage for long-term low-temperature applications: A review on the advancements at material and prototype scale - ScienceDirect

[19] Andreas Hauer, Eberhardt L.avemann, "Open Absorption Systems For Air Conditioning And Thermal Energy Storage", Springer, OPEN ABSORPTION SYSTEMS FOR AIR CONDITIONING AND THERMAL ENERGY STORAGE | SpringerLink

[20] Aran Sole, Ingrid Martorell, Luisa F.Cabeza, "State of the art on gas–solid thermochemical energy storage systems and reactors for building applications", Elsevier, 2015, State of the art on gas–solid thermochemical energy storage systems and reactors for building applications - ScienceDirect

[21] H.A. Zondag, Alex Kalbasenka , Martijn van Essen , Lucas Bleijendaal, Roelof Schuitema , Wim van Helden , Lucienne Krosse, "First studies in reactor concepts for Thermochemical Storage", 2015, 236 paper Zondag Eurosun2008 final2 (researchgate.net)

[22] N'Tsoukpoe, K.Edem, Liu,Hui, Le Pierres,Nolwenn, Luo,Lingai, "A Review on long-term sorption solar energy storage, 2009, Scopus - Document details - A review on long-term sorption solar energy storage | Signed in

[23] S.Mauran, H.Lahmidi, V.Goetz, "Solar heating and cooling by a thermochemical process. First experiments of a prototype storing 60 kW h by a solid/gas reaction", Elsevier, 2008, Solar heating and cooling by a thermochemical process. First experiments of a prototype storing 60 kW h by a solid/gas reaction - ScienceDirect

[24] Ard-Jan de Jong, Fanny Trausel, Christian Finck, Laurens van Vliet, Ruud Cuypers, "Thermochemical Heat Storage – System Design Issues", Elsevier, 2014, Thermochemical Heat Storage – System Design Issues - ScienceDirect

[25] D. Kunii, Octave Levenspiel, "Fluidization engineering – Second edition", 1991, Fluidization Engineering - D. Kunii, Octave Levenspiel - Google Books

[26] Armand Fopah-Lele, Frederic Kuznik, Thomas Osterland, Wolfgang K.L. Ruck, "Thermal synthesis of a thermochemical heat storage with heat exchanger optimization", Elsevier, 2016, Thermal synthesis of a thermochemical heat storage with heat exchanger optimization - ScienceDirect

[27] Aldo Cosquillo Mejia, Sandra Afflerbach, Marc Linder, Matthias Schmidt, "Experimental analysis of encapsulated $CaO/Ca(OH)_2$ granules as thermochemical storage in a novel moving bed reactor", Elsevier, 2020, Experimental analysis of encapsulated CaO/Ca(OH)2 granules as thermochemical storage in a novel moving bed reactor - ScienceDirect

[28] H.A. Zondag, V.M. van Essen, R. Schuitema, L.P.J. Bleijendaal, A. Kalbasenka, W.G.J. van Helden, M. Bakker, "Engieering Assessment of Reactor

Designs For Thermochemical storage of Solar Heat", 2009, Zondag: Engineering assessment of reactor designs... - Google Scholar

[29] Herbert Zondag, Martijn van Essen, Lucas Bleijendaal, Jaume Cot, Roelof Schuitema, Wim van Helden, Wilko Planje, Tjerk Epema, Henk Oversloot, "Comparison of Reactor Concepts for Thermochemical Storage of Solar Heat", 2008, Zondag, H, van Essen, M, Bleijendaal, L, Cot, J,... - Google Scholar

[30] P.A.J. Donkers, L.C. Sogutoglu, H.P.Huinink, H.R.Fischer, O.C.G. Adan, "A review of salt hydrates for seasonal heat storage in domestic applications", Elsevier, 2017, A review of salt hydrates for seasonal heat storage in domestic applications - ScienceDirect

[31] Kevin J.Albrecht, Clifford K. Ho, "Design and operating considerations for a shell-and-plate, moving packed-bed, particle-to-sCO_2 heat exchanger", Elsevier, 2019, Design and operating considerations for a shell-and-plate, moving packed-bed, particle-to-sCO2 heat exchanger - ScienceDirect

[32] Mazen M. Abu-Khader, "Plate heat exchangers: Recent advances", Elsevier, 2012, Plate heat exchangers: Recent advances - ScienceDirect

[33] Ali Abbas, Howard Lee, Akash Sengupta, Chi-Chuan Wang, "Numerical investigation of thermal and hydraulic performance of shell and plate heat exchanger", Elsevier, 2020, Numerical investigation of thermal and hydraulic performance of shell and plate heat exchanger - ScienceDirect

[34] Feng Jiang, Xinhua Dong, Guopeng Qi, Piaocai Mao, Jinjin Wang, Xiulun Li, "Heat-transfer performance and pressure drop in a gas-solid circulating fluidized bed spiral-plate heat exchanger", Elsevier, 2020, Heat-transfer performance and pressure drop in a gas-solid circulating fluidized bed spiral-plate heat exchanger - ScienceDirect

[35] Muhammad Usman Sikandar, "Design of Helical Coil heat exchanger for a mini powerplant", International Journal of Scientific and Engineering Reseaech, 2019, Design of Helical Coil Heat Exchanger for a mini powerplant (ijser.org)

[36] Jung-Yang San, Chih-Hsiang Hsu, Shih-Hao Chen, "Heat transfer Characteristics of a helical heat exchanger, Elsevier, 2012, Heat transfer characteristics of a helical heat exchanger - ScienceDirect

[37] Patil, Ramachandra K.; Shende, B.W.; Ghosh, Prasanfa K. , "Designing a helical-coil heat exchanger". Chemical Engineering. 92 (24): 85–88. Retrieved 14 July 2015, https://www.researchgate.net/publictopics.PublicPostFileLoader.html?id=54daea37d5a3f295028b45be&key=cd7c7059-0d79-41f2-9d51-56d00af44bad

[38] Haraburda, Scott S. (July 1995). "Three-Phase Flow? Consider Helical-Coil Heat Exchanger", Chemical Engineering. 102 (7): 149–151. Retrieved 14 July 2015, http://www.chemengonline.com/articles.php?file=1985-1999/Vol102/chevol102_num7_68.html

[39] Zhifeng Wang, "Design of the receiver System" in "Design of Solar Thermal Power Plants", Elsevier , 2019, Design of the Receiver System - ScienceDirect

[40] Amirhoushang Mahmoudi, Pim A.J. Donkers, Khuram Walayat, Bernhard Peters, Mina Shahi, "A thorough investigation of thermochemical heat storage system from particle to bed scale", Elsevier, 2021, https://www.sciencedirect.com/science/article/pii/S0009250921004425

[41] M.Gaeini, S.A. Shaik, C.C.M. Rindt, "Characterization of potassium carbonate salt hydrate for thermochemical energy storage in buildings", Elsevier, 2019, https://www.sciencedirect.com/science/article/pii/S0378778818319315#bib0023

[42] M.Gaeini, A.L.Rouws, J.W.O. Salari, H.A.Zondag, C.C.M. Rindt, "Characterization of microencapsulated and impregnated porous host materials based on calcium chloride for thermochemical energy storage", Elsevier, 2018, https://www.sciencedirect.com/science/article/pii/S0306261917318548

[43] Daniel M. Tartakovsky, Marco Dentz, "Diffusion in Porous Media: Phenomena and Mechanisms", Springer, 2019, Diffusion in Porous Media: Phenomena and Mechanisms | SpringerLink

[44] A.A. Mohamad, "Combustion in Porous Media: Fundamentals and Applications", 2005, Porous Medium - an overview | ScienceDirect Topics

[45] Liang Xue, Xiaozhe Guo, Hao Chen, "Fluid Flow in Porous Media : Chapter 2: basic Theory", Book Published in 2020, available online:https://www.worldscientific.com/doi/pdf/10.1142/9789811219535_0002#:~:text=Fluid%20flow%20in%20the%20porous,flow%20mechanics%20through%20porous%20media

[46] J. Bear, “Hydraulics of Groundwater”, McGraw-Hill, 1979

[47] S.E. Ingebritsen and W.E. Sanford, “Groundwater in Geologic Processes”, Cambridge University Press, 1998

[48] J. Bear, “Dynamics of Fluids in Porous Media”, Elsevier Scientific Publishing, 1972

[49] “CFD Module User’s Guide”, Comsol Documents, https://doc.comsol.com/5.3/doc/com.comsol.help.cfd/CFDModuleUsersGuide.pdf

[50] A. Golnik and G. Elert. ,“Energy Density of Gasoline” [Online]. Available: http://hypertextbook.com/facts/2003/ArthurGolnik.shtml

[51] “Comsol Multiphysics Reference Manual”, Comsol Documents, COMSOL Multiphysics Reference Manual

[52] “NIST-JANAF Thermochemical Tables”, NIST-JANAF Thermochemical Tables

[53] “The Engineering ToolBox”, The Engineering ToolBox

[54] “Physics, PDEs, Mathematical and Numerical Modeling”, Comsol Cyclopedia, Comprehensive Introduction to Physics, PDEs, and Numerical Modeling (comsol.com)

[55] Siddharth Suhas Kulkarni, Craig Chapman, Hanifa Shah, “Computational Fluids Dynamics (CFD) Mesh Independency Study of a straight blade Horizontal Axis Tidal Turbine, 2016, file:///C:/Users/Windows/Downloads/preprints201608.0008.v1.pdf

[56] Dan Zhao, ... Arne Reinecke, in Wind Turbines and Aerodynamics Energy Harvesters, 2019, Independence Study - an overview | ScienceDirect Topics

[57] “Performing a Mesh Refinement Study”, COMSOL Documents, Independence Study - an overview | ScienceDirect Topics